

# **Design of an Implantable Reparative Device for Ulnar Collateral Ligament in Overhead Throwing Athletes**

GXP-2021

A Major Qualifying Project Report Submitted to the faculty  
of Worcester Polytechnic Institute

in partial fulfillment of the requirements for the degree of Bachelor of Science

Submitted by:

Maria Decelles<sup>1</sup>  
Evan Hallberg<sup>1,2</sup>  
Brooklynn Paris<sup>1</sup>  
Meagan Smith<sup>1</sup>

Approved by:

George Pins, Ph.D., Advisor<sup>1</sup>  
Karen Troy, Ph.D., Advisor<sup>1,2</sup>  
Dr. David Magit, M.D., Advisor<sup>3</sup>

<sup>1</sup>Biomedical Engineering Department, Worcester Polytechnic Institute, Worcester, MA

<sup>2</sup>Mechanical Engineering Department, Worcester Polytechnic Institute, Worcester, MA

<sup>3</sup>Beth Israel Deaconess Medical Center, Boston, MA

April 28<sup>th</sup>, 2022

# Table of Contents

Table of Contents .....	2
Authorship .....	7
Acknowledgements .....	8
Abstract .....	9
Table of Figures .....	10
Table of Tables .....	12
1. Introduction.....	13
2. Literature Review.....	17
2.1 Clinical Need.....	17
2.1.1 Biomechanics of the Baseball Pitch.....	18
2.1.2 Anatomy of the Ulnar Collateral Ligament.....	19
2.1.3 Mechanical Properties of the UCL .....	20
2.1.4 Ligament Structure and Tears .....	21
2.2 Natural Ligament Healing Process .....	22
2.2.1 Ligament Wound Healing .....	22
2.2.2 Growth Factors' Role in Ligament Healing.....	25
2.3 Current Clinical Practices .....	26
2.3.1 Nonoperative Treatments .....	27
2.3.2 Platelet Rich Plasma .....	28
2.3.3 Internal Brace by Arthrex.....	28
2.3.4 Tommy John Surgery.....	29
2.3.4 Engineering Need and Criteria. ....	30
2.4 Scaffolds for Ligament and Tendon Reparation .....	30
2.5 Prior Art .....	32
2.5.1 Bridge-enhanced ACL Repair (BEAR) .....	34
2.5.2 Zimmer Collagen Repair Patch for Rotator Cuff Repair .....	35
2.5.3 Dermal Allografts .....	36
2.5.4 Unmet Need.....	37
3.0 Project Strategy .....	38
3.1 Initial Client Statement .....	38
3.2 Stakeholders .....	38

3.3 Initial Objectives and Constraints.....	39
3.3.1 Initial Objectives.....	39
3.3.2 Constraints.....	40
3.4 Revised Client Statement.....	41
3.5 Final Objectives.....	41
3.6 Project Approach.....	46
3.6.1 Management Approach.....	46
3.6.2 Design Approach.....	47
3.6.3 Financial Approach.....	47
4.0 Design Process.....	48
4.1 Needs Analysis.....	48
4.1.1 Design Needs.....	48
4.1.2 Design Wants.....	49
4.1.3 Needs and Wants Design Matrix.....	50
4.2 Functions and Specifications.....	51
4.2.1 Mechanical Testing Results.....	53
4.3 Conceptual Designs.....	55
4.3.1 Crimped Vessel Design.....	56
4.3.2 Thread Based Designs.....	56
4.3.3 Layered Designs.....	57
4.3.4 Yule Log Design.....	58
4.3.5 Sponge Based Designs.....	59
4.4 Design Considerations.....	61
4.4.1 Healing promotion.....	61
4.4.2 Delivers a Therapeutic Agent.....	67
4.4.3. Mechanically Sound.....	73
4.4.4 Reproducibility.....	77
4.4.5 Surgically Compatible.....	80
4.5 Alternative Designs.....	82
4.5.1 Layer-by-Layer Filaments.....	83
4.5.2 Encased Porous Scaffold.....	84
4.6 Mathematical Modeling.....	85

5.0 Verification of Final Design .....	87
5.1 Fabrication of Designs .....	87
5.1.1 PETG Inverse Mold .....	87
5.1.2 PDMS Mold .....	88
5.1.3 Silk Hydrogels Preparation .....	88
5.1.4 Collagen Sponges .....	89
5.1.5 Acellular Dermal Matrix Casing .....	89
5.1.6 Sterilization of Scaffold .....	89
5.2 Design Verification.....	89
5.2.1 Effect of Various PDGF-BB Concentrations on Cell Proliferation .....	90
5.2.2 BSA Diffusivity through Acellular Dermal Matrix Casing .....	91
5.2.3 Uniaxial Tensile Testing of Acellular Dermal Matrix .....	94
6.0 Final Design and Validation .....	97
6.1 Final Design .....	97
6.2 Design Validation .....	97
6.2.1 Initial BSA Drug Elution on Various Scaffold Designs .....	98
6.2.2 PDGF-BB Elution Testing .....	100
6.2.3 Effect of Eluted PDGF-BB on Cell Proliferation.....	101
6.2.4 PDGF-BB Diffusion through Acellular Dermal Matrix Casing .....	103
6.3 Client Feedback .....	104
7.0 Discussion.....	106
7.1 Drug Elution Studies.....	106
7.1.2 Final PDGF-BB Drug Elution from Collagen Sponge Reinforced Hydrogels .....	107
7.2 Cell Studies .....	108
7.2.1 Effect of Various PDGF-BB Concentrations on Cell Proliferation .....	108
7.2.2 Effect of Eluted PDGF-BB on Cell Proliferation.....	108
7.3 Diffusion Studies .....	109
7.4 Tensile Testing Study .....	110
7.5 Impact Analysis .....	110
7.5.1 Economics .....	110
7.5.2 Environmental Impact.....	111
7.5.3 Societal Impact .....	111

7.5.4 Political Ramifications .....	112
7.5.5 Ethical Concerns .....	112
7.5.6 Health and Safety .....	113
7.5.7 Manufacturability .....	113
7.5.8 Sustainability .....	113
8.0 Conclusions and Recommendations.....	114
8.1 Recommendations and Next Steps .....	114
8.1.1 Test Different Silk Hydrogel Fabrication Solutions .....	114
8.1.2 Test Collagen-PDGF-BB Composite Sponge .....	114
8.1.3 Use a Portfolio of Growth Factors.....	114
8.1.4 Research and Test how to Seal the Casing.....	115
8.1.5 Develop Method to Fixate the Scaffold to the Ligament.....	115
8.1.6 Animal Testing .....	115
8.1.7 Apply the Scaffold to Other Ligaments .....	115
8.2 Conclusion.....	115
References .....	117
Appendices .....	127
Appendix A: Images of the Anterior Bundle of the UCL Coated in Silver Particles .....	127
Appendix B: Pairwise Comparison Charts of the Primary Objectives from Each Individual ....	128
Appendix C: Pairwise Comparison Charts of the Secondary Objectives from Each Individual	131
Appendix D: Design Team Gantt Chart.....	140
Appendix E: Pugh Analysis Weighting Criteria.....	142
Appendix F: Materials with Growth Factors Research.....	143
Appendix G: Material Properties .....	144
Appendix H: MATLAB Code for Mathematically Modeling Diffusion Across a Semi-Permeable .....	146
Appendix I: Bill of Materials.....	150
Appendix J: Silk Hydrogel Fabrication Protocol.....	151
Appendix K: Sterilization Protocols for Final Design .....	152
Appendix L: Cell Proliferation Testing and Bioactivity Testing.....	155
Appendix M: Acellular Dermal Matrix (ADM) Tensile Testing Protocol .....	159
Appendix N: Drug Elution Testing.....	161
Appendix O: Diffusivity Across Casing Material Protocol .....	164



# Authorship

Section Title	Author(s)	Reviewer(s)
<b>1.0 Introduction</b>	Maria, Meagan	Brooklynn
<b>2.0 Literature Review</b>		
2.1 Clinical Need	Meagan, Maria	Brooklynn
2.2 Natural Ligament Healing Process	Brooklynn, Maria	All
2.3 Current Clinical Practices	Meagan, Evan	All
2.4 Scaffold for Ligament and Tendon Reparation	All	All
2.5 Prior Art	Meagan Smith	All
<b>3.0 Project Strategy</b>		
3.1 Initial Client Statement	All	All
3.2 Stakeholders	Maria	Brooklynn
3.3 Initial Objectives and Constraints	Brooklynn, Evan, Maria	All
3.4 Revised Client Statement	All	All
3.5 Final Objectives	Brooklynn, Maria	Meagan
3.6 Project Approach	Evan	Maria
<b>4.0 Alternative Designs</b>		
4.1 Needs Analysis	All	All
4.2 Functions and Specifications	All	All
4.3 Conceptual Design	All	All
4.4 Design Considerations	All	All
4.5 Alternative Designs	Brooklynn	All
4.6 Mathematical Modeling	Evan	All
<b>5.0 Design Verification</b>		
5.1 Fabrication of Designs	All	All
5.2 Design Verification	All	All
<b>6.0 Final Design and Validation</b>	TBD	TBD
6.1 Final Design	All	All
6.2 Design Verification	All	All
6.3 Client Feedback	All	All
<b>7.0 Discussion</b>		
7.1 Drug Elution Studies	Meagan	All
7.2 Cell Studies	Brooklynn	All
7.3 Diffusion Studies	Maria	All
7.4 Tensile Testing Study	Evan	All
7.5 Impact Analysis	All	All
<b>8.0 Conclusions and Recommendations</b>	All	All
8.1 Recommendations and Next Steps	Meagan	All
8.2 Conclusion	Maria	All
<b>References</b>	All	All

## **Acknowledgements**

We would like to acknowledge the following individuals for their contributions, expertise, and guidance throughout this project:

Professor Karen Troy, PhD

Professor George Pins, PhD

David Magit, MD

Kevin Cornwell, PhD

Professor Jeannine Coburn, PhD

Professor Sakthikumar Ambady, PhD

Lisa Wall

Robert Kirch

## **Abstract**

Overhead throwing athletes experience tears in their ulnar collateral ligament (UCL) due to excessive forces the elbow joint experiences. Current treatment methods reconstruct the existing anatomy using an autografted tendon. This study aims to design an implantable reparative device for partial UCL tears. A collagen sponge reinforced silk hydrogel was designed to encapsulate and release 300 ng platelet derived growth factor-BB (PDGF-BB) a two-week period. This design was encased in an acellular dermal matrix (ADM). The design was validated through cell proliferation, tensile, and drug elution testing. Preliminary results showed that the scaffold would release PDGF-BB over a two week period, have a diffusion coefficient of PDGF-BB out of the scaffold through the acellular dermal matrix to be  $9.14 \times 10^{-8} \pm 1.1 \times 10^{-7}$  cm<sup>2</sup>/s, and would be easily implanted in the operating room. Further assessment of the healing promotion of our design is needed. We anticipate that this scaffold will provide a transformative new approach for treating partial UCL tears in overhead throwing athletes.

## Table of Figures

Figure 1. The Six Phases of a Baseball Pitch (Fleisig et al., 1999). .....	18
Figure 2. Diagram of the Anatomy of Ulnar Collateral Ligament .....	20
Figure 3. Comparison of the Grades of Ligament Tears .....	22
Figure 4. Wound Healing Repair Timeline .....	24
Figure 5. Comparison of the Side Effects of BEAR versus ACLR surgery (Murray et al., 2016). .....	35
Figure 6. Primary, Secondary and Tertiary Objective Tree .....	42
Figure 7. The Force-Displacement Curves for Chicken Skin. ....	54
Figure 8. The Force-Displacement Curves for Band-Aids.....	55
Figure 9. Autograft Blood Vessel Capsule Sketch. ....	56
Figure 10. Sketches of Woven Threads, Woven Threads Through Sponge, Layered Woven Threads. ....	57
Figure 11. Layer-by-Layer Filaments Sketch, Thread Supported Layer-by-Layer Filaments Sketch, and Layer-by-Layer Filaments with Sponge Sketch. ....	58
Figure 12: <i>Multi-Layered Membrane Sketch</i> . ....	58
Figure 13. Sketch Yule Log Design.....	59
Figure 14. Sketch of Fiber Supported Sponge Design and Supported Sponge Design. ....	60
Figure 15. Sketch of Skirt Supported and Encased Sponge Design. ....	60
Figure 16. Netting Method for Fixation. ....	82
Figure 17. Drawing of the Layer-by-Layer Filament Design.....	83
Figure 18. Drawing of the Encased Porous Scaffold Design. ....	84
Figure 19. Diffusion Mathematical Model of Protein through Acellular Dermal Matrix.....	86
Figure 20. Image of Inverse PETG Mold used to Make PDMS Mold .....	88
Figure 21. Images of NIH 3T3 cells A) After 3 days in culture with 1.0 ug/mL PDGF-BB. B) After 3 days in culture with 0.0 ug/mL PDGF-BB. C) After 5 days in culture with 1.0 ug/mL PDGF-BB. D) After 5 days in culture with 0.0 ug/mL PDGF-BB.....	90
Figure 22. Cell Count versus Time in Culture of Different Concentrations of PDGF-BB in Culture.....	91
Figure 23. Casing Diffusion System including Ussing Chamber and Magnetic Shaker Plate.....	92
Figure 24. Graph of BSA Diffusion through Acellular Dermal Matrix Over Seven Days. ....	93
Figure 25. Diffusion of BSA through Acellular Dermal Matrix Fitted to Diffusion Mathematical Model. ....	94
Figure 26. ADM in Instron before Tensile Testing .....	94
Figure 27. Stress vs Strain Curve for Acellular Dermal Matrix .....	95
Figure 28. An Image of the Final Design Components .....	97
Figure 29. Graph of the Raw Cumulative Release Data of BSA from the Three Tested Conditions .....	99
Figure 30. Graph of the Cumulative Release of BSA from the Silk Hydrogel Design and the Calculated Sponge Reinforced Hydrogel.....	100

Figure 31. Graph of the Cumulative Release of PDGF-BB from the Collagen Sponge Reinforced Silk Hydrogel.....	101
Figure 32. Representative Images from BrdU Assay five days after adding supernatant. A) Combined image of DAPI and BrdU positive cells. B) Image of DAPI positive cells. C) Image of BrdU positive cells.....	102
Figure 33. BrdU/DAPI Positive Cells After Three and Five Days with Supernatant. Error bars represent standard deviation between the four scaffolds for each time point .....	103
Figure 34: <i>Casing Diffusion System including Ussing Chamber and Magnetic Shaker Plate.</i> ..	103
Figure 35. Diffusion of PDGF-BB through Acellular Dermal Matrix Fitted to Diffusion Mathematical Model. ....	104

## Table of Tables

Table 1: <i>Summary of Failure Rates to Nonoperative Treatment of the UCL Depending on Location and Grade of the Tear</i> .....	27
Table 2: <i>Product Name, Distributors, Product Description, and Patent Numbers of Different Scaffolds for Ligament and Tendon Repair</i> .....	32
Table 3: <i>Design Initial Design Objectives and their Descriptions</i> .....	39
Table 4: <i>Design Constraints and their Descriptions</i> .....	40
Table 5: <i>Summary of the Stakeholder’s Pairwise Comparison Charts of the Primary Objectives</i> .....	43
Table 6: <i>Healing Promotion Secondary Objective Definitions</i> .....	44
Table 7: <i>Mechanically Sound Secondary Objective Definitions</i> .....	44
Table 8: <i>Delivers a Therapeutic Agent Secondary Objective Definitions</i> .....	44
Table 9: <i>Surgically Compatible Secondary Objective Definitions</i> .....	44
Table 10: <i>Reproducible Secondary Objective Definitions</i> .....	45
Table 11: <i>Cost-Effective Secondary Objective Definitions</i> .....	45
Table 12: <i>Summary of the Stakeholder’s Pairwise Comparison Charts of the Secondary Objectives</i> .....	45
Table 13: <i>Design Needs</i> .....	48
Table 14: <i>Design Wants</i> .....	49
Table 15: <i>Design Needs Matix</i> .....	50
Table 16: <i>Design Wants Matix</i> .....	50
Table 17: <i>Functions and Specifications</i> .....	51
Table 18: <i>Mass and Volumes Needed of Each Growth Factor</i> .....	63
Table 19: <i>Therapeutic Agent Pugh Analysis</i> .....	64
Table 20: <i>Summary of Growth Factors Present in Natural Ligament Healing Process</i> .....	65
Table 21: <i>Growth Factor Pugh Analysis</i> .....	66
Table 22: <i>Benefits and Limitations of Natural Materials</i> .....	67
Table 23: <i>Material for Drug Loading Pugh Analysis</i> .....	70
Table 24: <i>Benefits and Limitations of Synthetic Materials and Dermal Matrices</i> .....	74
Table 25: <i>Material Property Ranges for the Materials being Further Investigated</i> .....	75
Table 26: <i>Degradation Rate Ranges for the Materials being Further Investigated</i> .....	76
Table 27: <i>Support Material Pugh Analysis</i> .....	76
Table 28: <i>Final Cell Count Averages and Percent Increase Compared to Controls</i> .....	90
Table 29: <i>Values obtained from dermal matrix testing</i> .....	95

# 1. Introduction

Overhead throwing athletes experience near failure torques every time they throw an object, causing injuries to this area very frequently. The only way overhead throwing athletes can reduce the torque that UCL experiences is to either reduce the force the elbow experiences or minimize the arm radius of the torque. For most overhead throwing athletes, the goal is to achieve high accelerations, thus the force cannot be logically reduced. Another way a player can reduce the overall torque by shortening the radius of the torque arm. To do this, the player would have to avoid elbow flexion near 90°, which is challenging considering the motion and muscles involved in the overhead throw (*Biomechanics: Ulnar Collateral Ligament - Dec 18, 2008 - Blog - TexasLeaguers.Com, 2008*). There is a need for a treatment method that will assist in the repair of the native UCL to reduce return to play time and restore function.

Currently, there are both nonoperative and operative treatments for UCL tears. The treatment method depends on the patient's specific injury, needs, and response to the treatment. Nonoperative methods, such as rest and physical therapy, are the first treatment attempt. When nonoperative treatments are ineffective, more intensive treatment is needed. Tommy John Surgery is the most common reconstructive procedure that replaces the UCL with a harvested autologous or allogeneic tendon to function as the new UCL (*The Benefits and Risks of Tommy John Surgery, 2017*). Tommy John Surgery is an intense recovery process and usually takes nine to twelve months for a player to recover fully. A less invasive surgical UCL repair technique, known as Primary Repair Surgery, uses an implant called the internal brace to try to heal the damaged UCL (*New Tommy John Surgery Alternative Has Potential to Cut Rehab Time in Half, 2017*). The implant is a fibrous tape that is coated in collagen and fastened to the UCL (Roth et al., 2021). A limitation of this repair method is that the internal brace is only intended for low grade tears of the UCL, thus, it is not suitable for a UCL that has high wear-and-tear (*New Tommy John Surgery Alternative Has Potential to Cut Rehab Time in Half, 2017*).

Tommy John surgery has become an epidemic among overhand throwing athletes such as baseball players to treat tears of the ulnar collateral ligament (UCL). A study in the American Journal of Sports Medicine found that athletes between the ages of fifteen and nineteen accounted for 56.8% of all Tommy John Surgeries (Bush-Joseph et al., 2015). The prevalence of these surgeries in major and minor leagues is increasing. Twenty-five percent of MLB pitchers

undergo reconstruction surgery, according to the results of a survey of 5088 professional players (Meldau et al., 2020).

Ligaments and tendons can take a significant amount of time to heal on their own, which has sparked an interest in finding ways to increase healing time through implants like collagen scaffolds. Many medical companies have developed ligament and tendon healing scaffolds for other areas of the body like the anterior cruciate ligament (ACL) and rotator cuff. An orthopedic surgeon developed a collagen scaffold derived from bovine tissue that assists in the repair of the ACL. This repair technique is known as the Bridge-Enhanced ACL Repair (BEAR) method and has shown proven success in clinical trials. The BEAR method is of interest to us because it is a natural material that can hold a significant amount of substrate containing therapeutic agents (Murray et al., 2016). The Zimmer Collagen Repair Patch (ZCR) is another reparative scaffold and is of interest due to its success as a rotator cuff repair method. The rotator cuff, which is a tendon in the shoulder, experiences many injuries in overhead throwing athletes. This makes it a good model for the UCL repair technology that we are interested in developing. The ZCR is a nondegradable collagen scaffold that helps reinforce a torn or strained rotator cuff. This technique has been shown to reduce pain and allow a person to return to their normal activity (*Zimmer® Collagen Repair Patch Surgical Technique, 2012*). The knowledge of these existing ligament and tendon repair techniques allowed us to develop a technique that meets the need of UCL injuries.

There was an unmet need for a healing technique that restores the UCL back to its natural state for all grades of tears. Tommy John surgery replaces the UCL all together, while the Internal Brace<sup>TM</sup> method only repairs the ligament for a select number of patients. Thus, there was a demand for a method that heals the damaged ligament such that the original UCL performs its job and allows overhead throwing athletes to achieve the same throwing ability they had prior to injury. The recovery time for the surgery needed to be less than or equal to that of the current surgical methods, which is nine to twelve months.

The goal of this project was to develop a physiologically relevant drug delivery scaffold to serve as an implantable regeneration treatment system. The device needed to be suitable for implantation, and its efficacy was evaluated through testing. Once created, the feasibility of scaling up and commercializing the device was evaluated. Following discussions of these goals

with our advisors and surgeon client, Dr. David Magit, the objectives to meet these goals were identified as delivering a therapeutic agent, promotes healing, reproducible, mechanically sound, surgically compatible, and cost effective. We also defined constraints of timeline, budget, sterilization, biocompatibility, surgical limitations, and size.

To develop alternative designs for this project, we completed a thorough design process. Following refining the client statement, we identified ranked objectives using a Pairwise comparison chart, and defined design wants and needs. We then defined functions and specifications through values found in literature as well as preliminary testing. We assessed the ability of our design to meet our objectives which were healing promotion, controlled of a therapeutic agent, surgically compatible, and mechanically sound. In addition, we considered cost effectiveness and reproducibility but were unable to test these objectives due to time and budget constraints.

After consideration of many conceptual designs, two alternative designs were chosen for further consideration. These were i) the layer-by-layer (LbL) filaments design and ii) the encased sponge design. The LbL design was composed of layers of films that are made with a growth factor solution and stacked to improve loading capacity and mechanical properties. It was advantageous for its ability to elute a therapeutic agent, favorable mechanical properties, biocompatibility, and surgical compatibility. The encased sponge was composed of a porous scaffold which would be made with growth factors incorporated, and then a hydrogel with more growth factor was inserted into the sponge before finally encasing the sponge in filaments. It was beneficial for its ability to load a large volume of therapeutic agents, and favorable mechanical properties.

After evaluating the feasibility and accessibility to various materials and manufacturing of these designs, we moved forward with the collagen sponge reinforced silk hydrogel loaded with PDGF-BB and encased in an acellular dermal matrix (ADM). We modeled this design with and without the collagen sponge. The results showed that the collagen sponge reinforced silk albumin hydrogel sustained a more controlled release of therapeutic agents compared to the silk albumin hydrogel alone. To create the final design, we sonicated silk fibroin solution at 5 wt% in 1.5mL batches for 90 seconds. Then, we added 1.00  $\mu\text{g}/\text{mL}$  of PDGF-BB to the silk pre-gel solution. Using a positive displacement pipet, we injected 150  $\mu\text{L}$  of pre-gel into the

polydimethylsiloxane (PDMS) mold, placed a collagen sponge on top, and then injected another 150  $\mu\text{L}$  of pre-gel solution into the mold. We placed the collagen sponge reinforced hydrogels into a vacuum chamber for 20 minutes to release air bubbles. The scaffolds gelled at 20°C in a dark box for 48 hours to gel. The dimensions of the final hydrogel were 20 mm x 7.5 mm x 2 mm and the dimensions of the ADM were 24 mm x 10 mm x 0.4 mm.

To validate our design, we conducted uniaxial tensile testing, cell proliferation testing, drug elution testing, and diffusivity testing. Prior to fabricating the final design, drug elution testing was done with BSA loaded devices to model PDGF-BB. We found that the concentration of PDGF-BB that promoted the highest cell proliferation was 1.00  $\mu\text{g/mL}$ , which was statistically significant ( $p = 0.00015$ ) when compared to the control. Preliminary testing showed that the ADM casing should slowdown the release of PDGF-BB from the sponge reinforced hydrogel scaffold, as less than 10% of BSA diffused the ADM after 7 days.

Finally, after fabricating the final design, we performed validation testing with PDGF-BB and collected client feedback. Since drug elution testing showed significant burst release, it was concluded that to extend the release period of PDGF-BB to 14 days and provide the proper mechanical properties, the scaffold should be encased in ADM. Additionally, there was not a statistically significant effect of eluted PDGF-BB on cell proliferation testing, thus a higher concentration should be evaluated. Diffusion testing of PDGF-BB from the scaffold through the ADM showed that the ADM was an appropriate material to reduce burst release. Using the experimentally derived diffusion coefficient, the diffusion of PDGF-BB was modelled and determined to be in the ideal range to release of PDGF-BB over two weeks, a critical role in the repair of the UCL. Finally, we presented the final design to the client who deemed that it would be easily implantable in the operating room, with this new device, it is anticipated that the patients' native ligament may heal much quicker due to the presence of PDGF-BB. In addition, the risk of post-operative injuries will be reduced.

Future recommendations for this technology are to test crosslinked collagen, to experiment with different concentrations of silk hydrogels to improve the release profile and to perform studies in small and large animal models. With the successful completion of these trials, the device could begin to be tested for the treatment of UCL tears in overhead throwing athletes.

## **2. Literature Review**

In this chapter, we discuss the clinical need and background on topics related to the treatment of ulnar collateral ligament tears. To better understand the scope of this project we extensively researched the clinical need, natural ligament wound healing, current clinical practices, and prior research. To address the clinical need of this project we outline the anatomy of the UCL, its mechanical properties, and diagnosis of different types of UCL tears. It is pertinent that we understand the natural ligament healing processes as our device must mimic and enhance the natural healing process and the growth factors that are associated with ligament wound healing. It is also important that we understand existing clinical practices so that we are aware of the methods that we are trying to deviate from and develop a better product than what is on the market currently. In addition to research regarding existing and known products, methods, and processes we had to conduct the bulk of our research around aspects that will meet the objectives of our project. After conducting research on existing methods, we developed an unmet need which our product will address.

### **2.1 Clinical Need**

The most common treatment for overhand throwing athletes such as baseball pitchers is ulnar collateral ligament (UCL) reconstructive surgery (Camp et al., 2016). In the MLB these procedures cost up to \$1.9 million per player (Meldau et al., 2020). Currently, Tommy John Surgery is the standard for reconstruction of the UCL. Between 1974 and 2016, there were over 1,400 of these types of surgeries performed on pitchers in both the major and minor leagues of baseball. Of these surgeries performed, 84% of players returned to any level of play and 73% of players returned to the former level of play (Camp et al., 2018). This type of surgery has become more prevalent in the youth population, where more players are undergoing these surgeries each year (*Magit, D. CORR LECTURE*, 2018). In fact, 56.8% of all Tommy John Surgeries are done on players aged fifteen to nineteen (Bush-Joseph et al., 2015). For young players, Tommy John Surgery requires a long recovery period for someone who may not advance to the next level of play. According to our client and various other sources, the recovery time of these reconstructive surgeries is typically nine to twelve months (D. Magit, personal communication, September 24, 2021).

There is a need for a UCL repair method to treat partial ulnar collateral ligament tears in youth players that shortens their return to play time and restore function. Young athletes have years of life ahead of them, whether it is playing baseball or not, so it is important to consider the long-term effects and how closely the scaffold heals the native UCL function and anatomy. Restoring the ligament to its natural state through a repair method will help eliminate the incidences of post-traumatic osteoarthritis as seen in ACL and other ankle injuries. Post-traumatic osteoarthritis can follow joint injury causing degeneration of cartilage and bone in addition to pain and stiffness (Thomas et al., 2017). To understand how to best address this need, we conducted research on pitching biomechanics, the structure of the UCL, current clinical practices, and methods currently used to promote ligament healing.

### 2.1.1 Biomechanics of the Baseball Pitch

To better understand why the UCL experiences injuries and failures, we researched the overhead throwing mechanism of a baseball pitch. This information was critical to developing methods on how to best treat UCL ligament tears. A baseball pitching motion is a ballistic motion where a player achieves high velocity pitching speeds in a short time frame of 0.145 seconds. This can cause significant stress to be put on the shoulder and elbow joint, leading to a high risk of injury (Magit, 2018). The UCL specifically, has a high risk of injury among pitching athletes as the ligament provides the greatest resistance to valgus stress (Labott et al., 2018). It is imperative to study the biomechanics of the baseball pitch to understand how injuries arise, how to treat them, and how to define successful recovery. Figure 1 shows each stage of the baseball pitch.

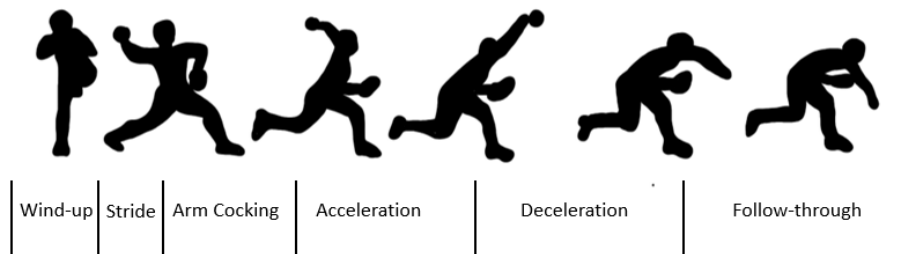


Figure 1. *The Six Phases of a Baseball Pitch (Fleisig et al., 1999).*

The baseball pitch consists of 6 phases: wind-up, stride, arm cocking, arm acceleration, arm deceleration, and follow through. The elbow and shoulder joints experience the greatest

forces and moments during the arm-cocking, acceleration, and deceleration phases (Oyama, 2012). During the pitch, the energy is funneled from a player's legs, pelvis, and torso to their upper extremities (Magit, 2018). In the initial wind-up phase, the player brings their stride (front) foot up to their supporting leg to begin the pitching motion. The player shifts their weight to their supporting leg, which determines the cadence for the pitching motion and thus delivery of the ball. The player then enters the stride phase and drops their stride leg towards the batter, stepping out a distance slightly less than the athlete's height. During arm-cocking phase the player rotates their hips, flexes their elbow, and rotates their shoulder to its maximum external rotation (170-190°) (Oyama, 2012). It is during this phase that the varus moment in the elbow is produced, thus the phase where tears most commonly occur. The player then begins the acceleration phase by internally rotating their shoulder from 120° to 30° and extending the elbow (Magit, 2018). A lag between shoulder rotation and elbow flexion helps create the largest angular velocity in the arm. The ball is then released while the trunk is flexed and the arm is nearly at full extension (Dillman et al., 1993). Once the ball is released, the player begins the arm deceleration phase, where the shoulder internally rotates, and the arm is extended. The arm comes to a complete halt in about 0.05 seconds (Oyama, 2012). The risk for injury in the acceleration and deceleration phases are also high. Finally, the player begins the follow-through phase, the most important phase in injury reduction (Dillman et al., 1993). During this phase, the original supporting leg moves forward, and the player's body is caught up to their arm and leg (Magit, 2018).

### **2.1.2 Anatomy of the Ulnar Collateral Ligament**

Ligaments are composed of nonlinear viscoelastic solids, which make them dynamic to metabolic responses and remodeling. Ligaments do not function alone. The forces of the entire joint play a role in ligament tears and healing. The ulnar collateral ligament (UCL) specifically is composed of type I collagen fibers organized in a helix to create a strong rope-like structure that holds the humerus to the ulna (Ratcliffe et al., 1990).

The UCL is responsible for providing valgus stability to the elbow joint. As shown in Figure 2, the UCL consists of three major parts: the anterior bundle, the posterior bundle, and the transverse ligament. The anterior bundle starts at the medial epicondyle and attaches to the sublime tubercle of the ulna. The anatomy of these connection points can be seen in Figure 2. The anterior bundle is the longest part of the UCL and the primary contributor to resisting valgus

stress. For this reason, overhead throwing athletes most commonly experience injury in this portion of the UCL. An anatomic image from a cadaver section shows this portion of the ligament in Appendix A. The posterior bundle connects the semilunar notch of the ulna and medial epicondyle (Awh, 2010). The ulnar nerve runs adjacent to the posterior bundle. The transverse ligament spans across the coronoid process and the olecranon. The function of this portion of the UCL is still unclear, however, it is known that it contributes little to valgus stability.

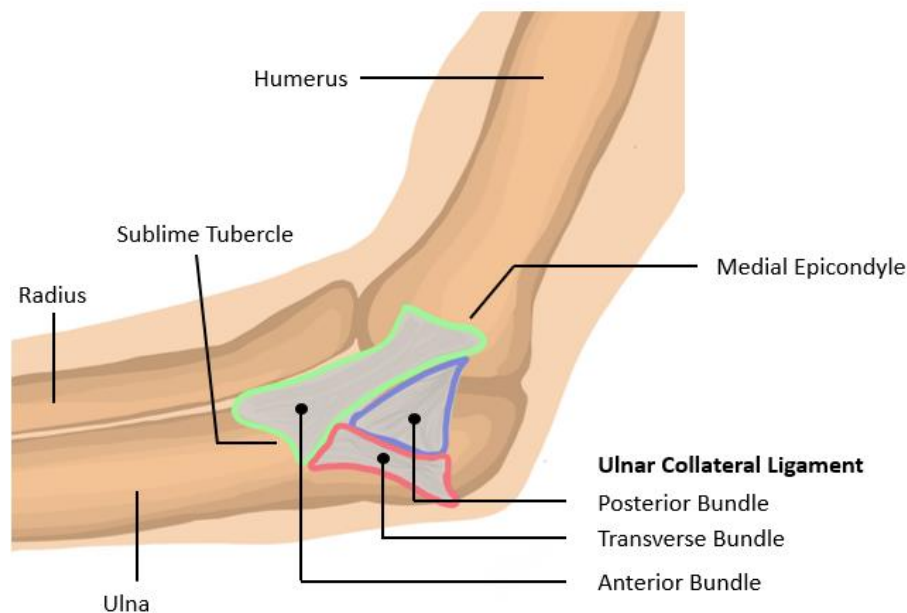


Figure 2. *Diagram of the Anatomy of Ulnar Collateral Ligament*

### 2.1.3 Mechanical Properties of the UCL

Now that an understanding of the baseball pitching motion has been established, we needed to understand how this motion impacts the UCL. The mechanical properties of the UCL need to be known as these determine when the UCL will fail. The failure load of the UCL is reported to be  $294.3 \pm 28.2$  N and the Young's modulus is  $37.3 \pm 5.1$  MPa. Another source reported the failure load of the UCL to be 260 N when being pulled in tension at a rate of 100% per second (Dustin et al., 2015). The maximum torque that occurs within the elbow happens when the elbow is flexed at a  $90^\circ$  angle. The varus torque that the elbow experiences is estimated to be 64-82 N\*m. It is predicted that the UCL is responsible for resisting 54% of the total elbow joint torque (Smith & Bernholt, 2020). According to additional sources, the UCL can withstand

elbow torques of  $32.1 \pm 9.6 \text{ N}\cdot\text{m}$  (Coughlin et al., 2019). At this torque, a pitcher's UCL experiences near failure stresses. The inability to reduce the stress on the ligament leads to ruptures and tears.

#### **2.1.4 Ligament Structure and Tears**

Ligament tears occur when the ligament experiences a greater amount of force than its failure load or torque. These injuries can occur acutely or gradually over time (Deal et al., 2017). The frequency of pitching and duration of play are other factors that contribute to UCL injuries. Players who pitch over 100 innings in a year are three times more likely to experience upper extremity injury that requires surgery. Furthermore, if they play for more than eight months per year, their likelihood of an injury requiring surgery increases fivefold (Fleisig et al., 1999). When material fatigue damage occurs, the ligament can tear or rupture especially if it is not sufficiently restored by hydration and circulation (Ratcliffe et al., 1990). A tear can occur in any part of the ligament. Distal tears tend to be the most problematic and difficult to treat (D. Magit, personal communication, September 24, 2021). In some cases, an avulsion of the ligament can occur (Mckim, 2016).

As shown in Figure 3, there are three distinct levels of tear: grade I, grade II, and grade III (Mckim, 2016). A grade I tear is a low-grade partial tear of the ligament, while a grade II tear is a high-grade partial tear of the ligament, and grade III is a complete rupture of the ligament. Patients with grade I tears are sprains that may still endure some pain, but they can still go about their day-to-day tasks. A grade II tear will cause more pain and discomfort, and the patient is less likely to be able to perform daily tasks. A grade III tear will cause the most pain and is the most difficult to treat (Joyner et al., 2016). This level of tearing will cause the most swelling, joint instability, and disruption to everyday tasks. All three types of tears can pose problems for healing and treatment. Most commonly, the anterior band of the anterior bundle experiences tears due to its fibrous formation. Additionally, tears in the distal portion are more problematic than tears in other locations (D. Magit, personal communication, September 24, 2021).

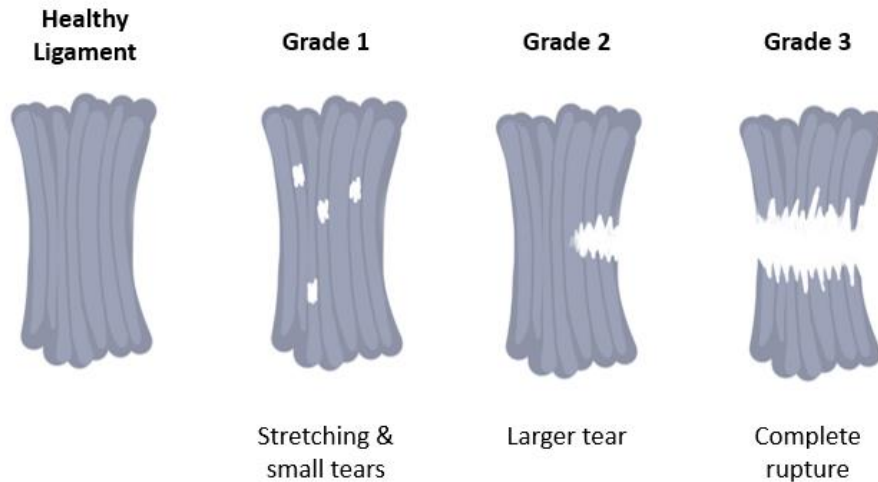


Figure 3. Comparison of the Grades of Ligament Tears

## 2.2 Natural Ligament Healing Process

When designing a repair method for a ligament, it is important to understand the natural healing process and the growth factors that are present in each phase. A stable blood supply is crucial for the ligament to function properly as it provides nutrients and growth factors to cells and tissues that allow for growth and healing. The blood supply in the elbow joint comes from the superior ulnar collateral artery that originates from the brachial artery (Hapugoda, n.d.). The UCL is well vascularized on the proximal end, while on the distal end the ligament is hypovascular (Buckley et al., 2019).

Through inflammation, repair, and remodeling, the ligament can return to its natural function. The main growth factors needed for ligament repair are platelet-derived growth factor (PDGF-BB), transforming growth factor- $\beta$ 1 (TGF- $\beta$ 1), vascular endothelial growth factor (VEGF-2), basic fibroblast growth factor (FGF-2), and insulin-like growth factor- I (IGF-1). The following sections will provide context and detail to the ligament healing process and main growth factors of interest.

### 2.2.1 Ligament Wound Healing

Ligament wound healing occurs over three stages: inflammation, reparation/proliferation, and remodeling. Figure 4 shows the timeline for this wound healing process. Inflammation occurs immediately after injury and lasts for up to a week. Phagocytic cells are recruited to the injury site to clear debris and release chemokines and chemotactic anaphylaxis of inflammatory

cells. The next stage is the repair stage or proliferative stage. The repair stage occurs three or four days after injury and lasts for up to six weeks (“The Ligament Injury-Osteoarthritis Connection,” 2012). During this stage leukocytes release growth factors and cytokines to attract repairing cells, and macrophages release VEGF-2 to support vascular growth in the area (Babensee, 2020; Molloy et al., 2003). Additionally, fibroblasts aid in the formation of new collagen. Platelets and neutrophils release TGF-  $\beta$  to promote the deposition of new extracellular matrix material. Finally, the remodeling stage occurs 42 days until 18 months days after injury (“The Ligament Injury-Osteoarthritis Connection,” 2012). During this phase enzymes such as the matrix metalloproteinases (MMPs) and tissue inhibitor of metalloproteinase (TIMP) remodel tissues (Babensee, 2020). Collagen fibers become denser and increase in diameter (“The Ligament Injury-Osteoarthritis Connection,” 2012). This stage is important because excessive scar tissue formation can be caused by unrestricted fibroblast proliferation. TGF-  $\beta$  and hyaluronic acid can help aid in scar-free wound healing.

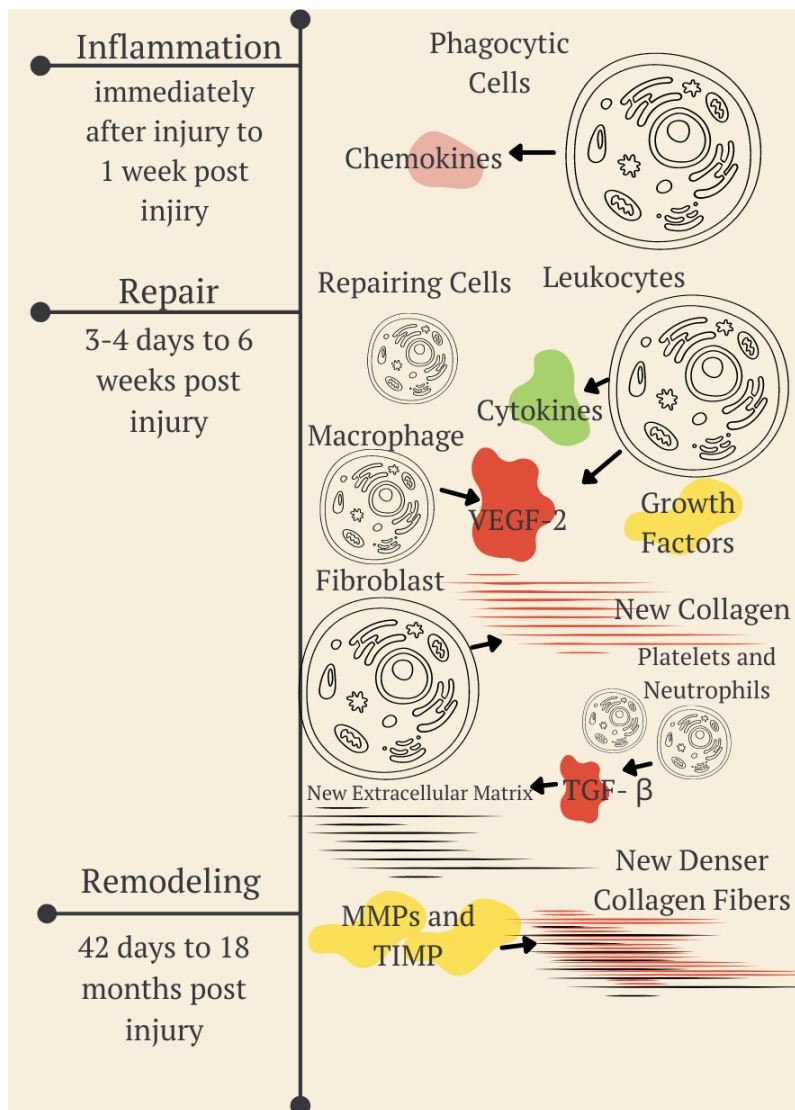


Figure 4. *Wound Healing Repair Timeline*

In a ligament wound healing, restored structure correlates to restored function. Through the natural healing process, fiber orientation rarely heals correctly as scar tissue because scar tissue does not have the same fibril organization of the native tissue which affects mechanical function of the ligament. Usually, connective scar tissue forms and is stronger than the original tissue, however it creates a much denser fiber structure (Ratcliffe et al., 1990).

There are several factors that can affect ligament healing. Passive motion or physical stimuli may be better for healing after some period of immobilization (Ratcliffe et al., 1990). However, increased tension during training and exercise may help with fiber alignment. Growth factors, hormones, nutrients, matrix cell receptors, inflammatory stimuli, and biotech signals

present positive impacts on ligament growth and maturation. During ligament regrowth, the extracellular matrix must prove a balance of synthesis and anabolic activities and degradation and catabolic activity of tissue. Immobilization can cause tissues to stiffen and ligaments to weaken. Hypoxia, corticosteroids, pharmacological agents, diabetes mellitus, and aging also present negative effects on ligament healing (Ratcliffe et al., 1990). The complexities of ligament healing involve the various stimuli that are present during each phase of healing to create the structure needed to restore native mechanical function to the ligament.

### **2.2.2 Growth Factors' Role in Ligament Healing**

As previously indicated, growth factors and mechanical stimuli are important in restoring the fibril organization associated with ligament regeneration and healing. Growth factors can be used for cellular proliferation, migration, and differentiation by attaching themselves to transmembrane receptors on cells. Despite their capabilities, they are limited by a short half-life, poor stability, rapid inactivation by enzymes under physiological conditions (Ma et al., 2018). Currently, growth factors used commercially have limited success because of variables such as the location they are introduced to, the duration of release, the chemical structure of scaffolds, and the combination of multiple growth factors.

During the ligament healing process, specific growth factors are present. These growth factors serve to induce mitosis, extracellular matrix (ECM) production, neovascularization, cell maturation, and differentiation. While there is limited research on which growth factors are present in UCL healing, there is literature available about the healing process of the rotator cuff in animal studies, which is sufficient for the purpose of this study. The main growth factors involved in the tendon healing process are PDGF-BB (platelet derived growth factor-BB), TGF $\beta$ -3 (transforming growth factor beta-3), VEGF-2 (vascular endothelial growth factor 2), FGF-2 (basic fibroblast growth factor also known as FGF-2) and IGF-1 (insulin-like growth factor 1). These growth factors are expressed during the repair phase of the healing process, which is typically during days 5-14. Most growth factors are upregulated after 1 week in rat models, when the healing reaches the repair phase. Because of this, the application of growth factors is much more effective on day 7 than it would be on day 3. It is important to note that the natural healing process is not perfect and can lead to failed healing in up to 12% of patients (Gulotta et. al., 2002).

PDGF-BB has been known to enhance ligament and tendon healing through collagen and non-collagen protein production and DNA synthesis (Molloy et al., 2003). It can be used to speed up healing in various surgical procedures. The clinical efficacy of this growth factor has been indicated safe for use in the body (Andrae et al., 2008). PDGF-BB influences the generation of other growth factors like IGF-1 and TGF $\beta$ -1. TGF $\beta$ -1 is associated with the formation of collagen I and III and is crucial during the inflammatory phase of healing. TGF- $\beta$  can stimulate “extrinsic cell migration, regulation of proteinases, fibronectin binding interactions, termination of cell proliferation via cyclin-dependent-kinase-inhibitors and stimulation of collagen production” (Molloy et al., 2003). Lymphocytes, macrophages, endothelial cells, smooth muscle cells (SMCs), epithelial cells, and fibroblasts, which are all cell types that are crucial for the healing process, all secrete TGF- $\beta$ . TGF- $\beta$ 3 specifically is associated with improved mechanical properties of tissue that has formed (Gulotta & Rodeo, 2009). VEGF-2 has a high angiogenic effect and increases vascularity to aid in ligament healing. VEGF-2 is responsible for the proliferative and mitogenic activities of VEGF. Its expression can be upregulated during osteogenesis through biological and mechanical stimuli. The growth factor FGF-2 is responsible for signaling the production of collagenase in fibroblasts and stimulates the proliferation of capillary endothelial cells to facilitate angiogenesis as well as the formation of granulation tissue. IGF-I has been shown to stimulate protein synthesis, increase cell proliferation, collagen synthesis, and decrease swelling. Following soft tissue surgery, IGF-1 is increased at the mRNA and protein levels when its receptors are up regulated (Molloy et al., 2003). These growth factors and their properties were further considered for use in the final design as discussed in Section 4.4.1.

### **2.3 Current Clinical Practices**

There are several current clinical practices that address UCL tears: repair and reconstruction. Nonoperative treatments focus on repairing the ligament through rest and physical therapy, while operative treatments include internal braces and Tommy John Surgery. Each of these current treatment techniques will be discussed further in the following sections.

### 2.3.1 Nonoperative Treatments

Nonoperative methods are typically the first attempt of treatment for UCL tears. The location, grade of the tear, and the level of activity the player wants to achieve weigh heavily in injury assessment and treatment plan. While there is not an exact set of steps for conservative treatment of UCL tears, physical therapy and strengthening exercises are usually utilized. Some physical therapy techniques include massaging, ultrasound therapy, electrical stimulation, and soft tissue mobilization. Nonoperative methods begin with rest and range-of-motion exercises. Once the player no longer experiences pain and can achieve a full range of motion, they move onto exercises geared towards strengthening the surrounding muscles (Ford et al., 2016).

There have been very few studies on nonoperative treatment methods for UCL. One study conducted by Ford et al. included 35 professional pitchers and field players. Of these players, 4 experienced grade I tears, while the remaining 31 players had grade II tears. Any player with a grade III tear was immediately recommended for surgical treatment. After six to eight weeks of physical therapy, players were reevaluated to determine if their treatment was effective, and if their symptoms were improving. If there was no improvement, the player would stop the program and consider reconstructive surgery. Ninety-one percent of the players in the study returned to play by the next season, and the remaining nine percent of players returned the following season.

Table 1: *Summary of Failure Rates to Nonoperative Treatment of the UCL Depending on Location and Grade of the Tear* (Frangiamore et al., 2017)

Locations of Tear and Percent Failure of Those with Nonoperative Treatments					
Location and Type of Tear	Proximal	Distal	Low Grade	High Grade	High Grade and Distal
Percentage of Failure	11%	69%	17%	57%	88%

Another study investigated 32 pitchers from one major league team and its affiliate minor leagues. All three grades of tear were investigated in this study, which showed only 66% of players returned to play after nonsurgical treatment. The results of a statistical analysis on the location and grade of the tear are shown in Table 1. This study defined failure as a lack of success with nonoperative treatment, leading to a need for surgical intervention (Frangiamore et al., 2017).

It is apparent that higher grade tears and distal tears are much more difficult to treat by nonsurgical intervention. It was found that distal tears are over twelve times more likely to result in reconstructive surgery than proximal tears (Frangiamore et al., 2017).

### **2.3.2 Platelet Rich Plasma**

Platelet rich plasma (PRP) is a biological treatment for tissue healing, which has many applications in tissue regeneration and wound healing. PRP is derived from blood plasma. PRP contains growth factors, cytokines, chemokines and other plasma proteins (Apostolakos et al., 2020). Ultimately, these components make PRP a source for mitogenic, angiogenic and chemotactic properties. PRP is the most common biological agent used in UCL tear treatments (Apostolakos et al., 2020). One survey found that 36.6 % of physicians chose to use PRP in UCL tear treatment (Hurwit et al., 2017). In applications of UCL injuries, the efficacy of PRP injections is unclear with inconsistent clinical uses (Rebolledo et al., 2017). Many reviews articles state that although there are positive effects on healing the UCL, the efficacy of PRP for use in UCL tears is not definitive because it is possible that healing through reconstruction without PRP is comparable (Apostolakos et al., 2020; Hurwit et al., 2017). One study found that in combination with physical therapy, 88% of patients who received a PRP injection to treat a UCL tear had a return to play time of 12 weeks (Rebolledo et al., 2017). Another study looked at 544 professional baseball players who were treated non-operatively for UCL injuries from 2011 to 2015. Out of 544 players, 113 were treated with PRP injections. The research conductors matched the players who received PRP injections with those who did not based on age, position, and throwing style to compare the return to play results. In fact, the study found that patients who received PRP injections had a longer return to play time (Chauhan et al., 2019).

### **2.3.3 Internal Brace by Arthrex**

The internal brace produced by Arthrex® is a less invasive surgical UCL repair technique known as Primary Repair Surgery (*New Tommy John Surgery Alternative Has Potential to Cut Rehab Time in Half*, 2017). The Internal Brace™ is a fibrous tape that is coated in collagen and fastened to the UCL. The stiffness of the Internal Brace™ restricts the elbow joint (Roth et al., 2021). The best candidate for this surgery is someone who has a low-grade UCL tear where the UCL does not have any dead tissues, ligament deficiencies, or is completely torn. It is not

suitable for a UCL that has high wear-and-tear (*New Tommy John Surgery Alternative Has Potential to Cut Rehab Time in Half*, 2017).

The recovery period for the Primary Repair Technique is reported to be significantly less than UCL reconstruction surgery. Ten weeks post-operation, a player may begin their return to throwing, while with Tommy John Surgery they must wait at least 18 weeks before this step (*New Tommy John Surgery Alternative Has Potential to Cut Rehab Time in Half*, 2017). In one study performed on overhead throwing athletes, with the majority being baseball pitcher, 96% of athletes were able to return to play between three and twelve months post-operation. Sixty-five percent of these patients returned to the same or higher level of play in less than six months (Dugas et al., 2018).

### **2.3.4 Tommy John Surgery**

When a UCL is injured beyond the point of being able to heal through rest and physical therapy alone, total reconstruction of the UCL may be an option. Tommy John Surgery consists of harvesting a tendon from the patient's own body or from a donor and constructing it to function as a new UCL. In 1974, it was estimated that Tommy John had a 1% chance of returning to baseball after the surgery but today approximately 85% of pitchers who receive Tommy John surgery return to pitching at their previous level after recovery (*The Benefits and Risks of Tommy John Surgery*, 2017). The success rate of this procedure is 80-90% with regards to complications post-operation (*Tommy John Surgery In-Depth | Boston Children's Hospital*, n.d.). Grafts that have been used before and proven successful for this surgery include the palmaris longus tendon from the forearm, hamstring tendon, and the big toe extensor tendon.

Tommy John Surgery consists of two phases: cleaning out the elbow joint and securing the graft. First, the surgeon will access the elbow by making a three-to-four-inch incision on the inside of the elbow through the skin and flexor muscle. Obstructing tissues are also moved out of the way, and if there are any damaged tissues, they are removed (*Tommy John Surgery (Ulnar Collateral Ligament Reconstruction)*, n.d.). To secure the graft to act as the new UCL, three holes are drilled into the distal epicondyle of the humerus, and two holes are drilled into the proximal epicondyle of the ulna. The graft is then threaded through the holes and secured by either sutures, buttons, or screws. Once the graft is secured, the surgical incision is sutured, and

dressings and wraps are applied. The patient's arm is immobilized in a wrap covered splint and the first of three rehabilitation phases begins (Jensen et al., 2020).

The rehabilitation time varies from patient to patient, but three phases of recovery have been defined that estimate the patient's window recovery time, the elbow is secured in a splint or hard brace prescribed by the surgeon at a 60-90° angle for 1-2 weeks. The goal of this phase is to protect the healing tissue and reduce swelling and inflammation resulting from the operation. To avoid as much muscle atrophy as possible, physical therapy can start promptly with exercises focused on the wrist, fingers, shoulder, and biceps. The second phase begins one to two weeks post-surgery in which the patient can begin moving their elbow joint. The doctor can prescribe a sling to the patient depending on their current level of activity to limit the patient's use of the UCL. Physical therapy focuses on increasing the elbow's range of motion and strength. The final phase of rehabilitation begins at the end of the first month post-op where the patient can fully extend the elbow and gradually work towards not wearing a brace. With routine physical therapy, patients regain their normal range of motion in two to four months (*Tommy John Surgery (Ulnar Collateral Ligament Reconstruction)*, n.d.).

Thus, there is an unmet clinical need for a reparative technique that can heal all types of grade two, partial UCL tears. This will help reduce recovery time as well as risk for post-operative osteoarthritis.

#### **2.3.4 Engineering Need and Criteria.**

Design, develop and test an implantable scaffold model that assists in the healing of a torn ulnar collateral ligament (UCL). The material chosen for the scaffold must be biocompatible, biodegradable, and sustain a controlled release of therapeutic agent over a span of at least two weeks. It must be within the dimensions of 40 mm x 15 mm x 3 mm, so that it does not exceed the dimensions of the native ligament.

#### **2.4 Scaffolds for Ligament and Tendon Reparation**

In the United States, there are over 400,000 shoulder, tendon, and ligament repair surgeries annually (Ratcliffe et al., 2015). These repairs can be done with scaffolds made from natural materials, synthetic materials, or composites. For example, collagen scaffolds, an

inherently natural scaffold, can be manufactured with synthetic materials through electrospinning or 3D printing (Patil & Masters, 2020).

Natural scaffolds can be made of extracellular matrix grafts, which help with rapid cell attachment to form new tissue; however, they have poor mechanical properties and may cause disease transmission. Natural scaffolds that can be used to repair or replace ligaments include autografts, allografts, or xenografts. Human autografts come from the patient's body and typically result in graft site morbidity (Ratcliffe et al., 2015). The most common allograft used for UCL tear treatment is the palmaris longus autograft. Plantaris and toe extensor autograft tendons are also used (Smith, 2013). In contrast, autografts are derived from donor tissue and are limited by the potential risk of infection and failure due to immune rejection (Ratcliffe et al., 2015). One study found that 85% of patients had intact tendon repair using the GraftJacket Matrix, an allograft of acellular human dermal layers (Gillespie et al., 2016). Xenografts are derived from animal tissues for use in the human body, but also have the potential for immune rejection. One example of a xenograft is a collagen scaffold derived from cattle hide containing type I collagen. They are biocompatible, have favorable degradation properties, and provide cellular penetration for wound repair. The disadvantages of all graft collagen scaffolds are high cost and variability in sourcing (Friess, 1998). Overall, collagen presents a tailorable method for creating scaffolds for ligament healing in several modalities, such as meshes, hydrogels, and sponges (Patil & Masters, 2020).

Synthetic scaffolds, on the other hand, can present themselves as aligned fibers or meshes. Features and degradation times can be manipulated in synthetic scaffolds so that they are best suited for their unique application (Ratcliffe et al., 2015). Synthetic scaffolds are typically more mechanically sound and are more easily reproduced than biological scaffolds (Gillespie et al., 2016). However, these types of scaffolds vary in strength and stiffness properties and may have biocompatibility issues (Ratcliffe et al., 2015). Some common synthetic scaffold materials are Dacron, polypropylene, polyester, and polyacrylamide. Poly(lactide-co-glycolide) (PLGA) is another fibrous synthetic scaffold material that is biocompatible and degradable. One study found that when electro-spun and combined with basic fibroblast growth factor, PLGA improved collagen organization compared to control groups, and PLGA alone (Gillespie et al., 2016). However, the efficacy of PLGA is not clear in UCL healing applications.

## 2.5 Prior Art

Table 2: *Product Name, Distributors, Product Description, and Patent Numbers of Different Scaffolds for Ligament and Tendon Repair* (Kaleshian et al., 2021; Karuppaiah & Sinha, 2019; Murray et al., 2016)

Product Name	Distributor	Material	Patent #
Restore Orthobiologic Implant	Depuy	Inner lining of a pig intestine	US781988B2
CuffPatch	Biomet	Inner lining of a pig intestine	US5441508A
SportMesh	Biomet	Inner lining of a pig intestine	US10265159B2
GraftJacket	Wright Medical	Decellularized human skin	US8323352 US8007531 US7476249
Collagen Repair Patch	Zimmer	Pig skin	US4950483A
AlloPatch	MTF	Human fascia	US10881501
Conexa	Tornier	Decellularized pig skin	US20100179591A1
OrthADAPT	Pegasus Biologics	Horse skin	US20080188936A1
BEAR Scaffold	Childrens Medical Center Corporation	Bovine tissue	US10786238B2
Kennedy Ligament Augmentation Device (LAD)	3M Company	Braided Poly(propylene) yarns	WO1993006790A2
Strattice	Allergan Aesthetics	Pig skin	US20130158658A1
BioBrace	BioRez Inc.	Bovine tendon reinforced in PLLA	US11116622 US11058532
CardiaMend	HELIOS CARDIO	Decellularized Bovine Dermis	US8613957B2

There are many patents for scaffolds that aim to heal soft tissues like ligaments and tendons. These scaffolds are used for various ligaments and tendons in the body. These scaffolds may be made of natural, synthetic, or a combination of both materials. Natural materials can be derived from a variety of sources like pigs, bovines, horses, or humans. The material of each ligament repair scaffold, the name of the scaffold, its distributor, and patent number are all listed in Table 2 (Karuppaiah & Sinha, 2019).

The Restore Orthobiologic Implant was recommended to not be used due to a lack of a recognizable benefit as compared to the control group (Walton et al., 2007). For this reason, it would not be sufficient for UCL repairs. Both SportMesh and GraftJacket were made by Biomet,

which has been absorbed by Zimmer. Neither product is currently found on the market. The GraftJacket is a regenerative tissue matrix made of acellular dermis that is used to protect tissue to support it during regeneration. Although it has been used for Achilles augmentation, rotator cuff augmentation, and plantar fat pad augmentation, its function does not provide additional therapeutic agent to the area. This needed for the treatment of UCLs which have poor blood supply (“GRAFTJACKET™ Regenerative Tissue Matrix,” n.d.).

The Kennedy Ligament Augmentation Device (LAD) could not be used to treat partial UCL tears because it is a reconstructive method, which is not ideal for partial tears, it is made of polyester materials which our client would not like to use, and because it has been shown to lead to bone defects and fracture (*Ligament Augmentation Device - an Overview / ScienceDirect Topics*, n.d.).

Strattice is a reconstructive tissue matrix that’s main function is to reinforce soft tissue to aid in repair, however it is merely a physical reinforcement method that does not introduce reparative biologic agents (*510(k) Premarket Notification*, n.d.-a).

BioBrace Implant is an implant to reinforce soft tissues such as tendons without fully supporting the anatomy mechanically. Our client needs a device made of natural materials however this implant is reinforced with PLLA. Additionally, it is only used for physical reinforcement, and does not introduce any agents to aid in the healing of tissue (*BIOREZ – The Future of Tendon and Ligament Healing*, n.d.).

OrthADAPT is a type I collagen implant used for the repair and reinforcement of several tendons through promoting tissue ingrowth and enhancing stability of a reconstruction procedure (*OrthoADAPT™ Biologic Collagen / The Foot and Ankle Online Journal*, n.d.). Although it can help repair tissue, it is not meant as a stand along device because according to the FDA indications of use, it is intended to reinforce a tendon for example after a repair surgery (*510(k) Premarket Notification*, n.d.-b).

Conexa is a reconstructive matrix from porcine tissue with an indication of use for tendons. It contains collagen and proteoglycans to help with cellular migration as well as vascular channels. Conexa is primarily for large tears needed reconstruction which differs from

the clinical need for a UCL repair for partial tears (*Tornier And LifeCell Corporation Initiate Clinical Trial for Conexa(TM) to Repair Rotator Cuff Tears*, n.d.).

The Bridge-enhanced ACL Repair (BEAR) method and the Zimmer Collagen Repair Patch (ZCR) are relevant scaffolds in ligament healing. These two technologies are different from each other but have both shown proven success in relieving pain in ligament and tendon injuries and healing the injury site. The BEAR method has reached phase two of clinical studies and has shown proven success in a repair method for ACL (Murray et al., 2016). ZCR is intended for the repair of the rotator cuff, which experiences similar forces to that of the UCL. It also had a different makeup than that of the BEAR scaffold (*Zimmer® Collagen Repair Patch Surgical Technique*, 2012).

### **2.5.1 Bridge-enhanced ACL Repair (BEAR)**

Dr. Martha Murray is an orthopedic surgeon that specializes in the repair and reconstruction of the anterior cruciate ligament (ACL) and meniscus (*Martha Murray, MD / Boston Children's Hospital*, n.d.). She has co-invented the bridge-enhanced ACL repair (BEAR) technique, which uses a scaffold loaded with the patient's blood to reconnect the torn ligament. The scaffold is bioactive, consisting of collagen from bovine tissue and extracellular matrix proteins. The DNA content present in the scaffold is less than 50 ng/mg, which helps minimize unwanted immune responses from the patient. Additionally, the scaffold was not crosslinked. To be successful, the patient needs to be skeletally mature and have a completely torn ligament that is still attached to the bone. The ligament is first sutured together, and the scaffold is then secured to the sutured area. Next, it is loaded with ten milliliters of blood from the patient. Because the scaffold is highly hydrophilic, it can absorb five times its weight in fluid. After eight weeks, it degrades completely in the body (Murray et al., 2016).

In an initial clinical trial of 20 patients, BEAR surgery was compared to the gold standard ACL reconstruction (ACLR) surgery to prove its effectiveness. The ACLR procedure uses a hamstring allograft to replace the ACL. None of the patients with the BEAR scaffold needed the

implant to be removed. Figure 5 below demonstrates the side effects of both types of surgery. Overall, side effects between the two types of surgeries were quite similar (Murray et al., 2016).

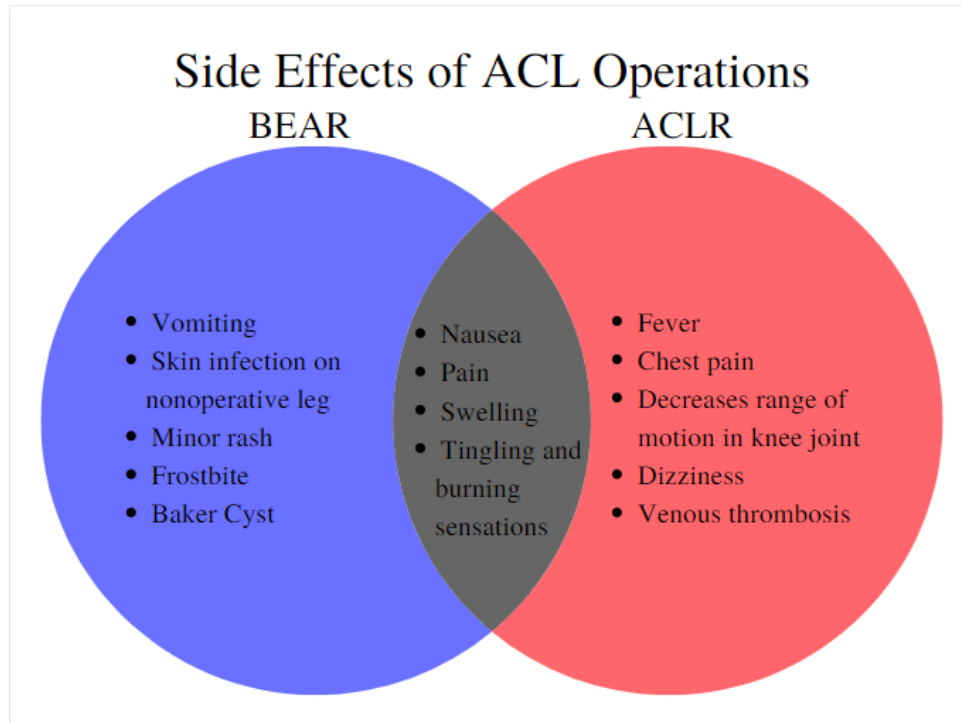


Figure 5. Comparison of the Side Effects of BEAR versus ACLR surgery (Murray et al., 2016).

In a phase II clinical trial study, a population of 100 patients with torn ACLs underwent either BEAR surgery (65 patients) or ACL reconstruction surgery (35 patients). Of this study group, 14% of the BEAR subjects and 6% of the ACLR subjects needed to undergo a second ACL surgery due to reinjury. In addition, 8 out of the 65 BEAR patients converted to ACL reconstruction surgery during the two-year study period. After two years have passed, patients returned for a physical examination to measure the patients' International Knee Documentation Committee (IKDC) Subjective Scores and AP Knee Laxity tests. Overall, there were no significant differences between the BEAR group and ACLR groups when it came to their IKDC scores and AP Knee Laxity tests (Murray et al., 2016). Thus, the BEAR scaffold showed to be as effective as the ACLR surgeries.

### 2.5.2 Zimmer Collagen Repair Patch for Rotator Cuff Repair

Tissue Science Laboratories developed an FDA approved collagen scaffold that aids in the repair of rotator cuffs known as the Zimmer Collagen Repair Patch (ZCR). It is an acellular xenograft derived from porcine skin (Gillespie et al., 2016). Due to the chemical crosslinks that

exist in the scaffold, it is not biodegradable. This first step in implanting the ZCR sheet is to suture the rotator cuff tendon together. The patch is then sized and sutured to the tendon such that none of the material is unsecured or hanging loose. The rotator cuff is to then be in a brace for six weeks (*Zimmer® Collagen Repair Patch Surgical Technique*, 2012). This was followed with a range of motion and strengthening exercises being ten weeks and four months post-operation respectively. The player could then resume any normal activities including sports six months after surgery. In a study performed by UCLA, five patients with massive rotator cuff repairs underwent surgery that used the Zimmer Collagen Repair Patch. They also performed a series of tests outlined by the American Shoulder and Elbow Surgeons (ASES) and were scored preoperatively and postoperatively. The scores following surgery were significantly higher than the patient's original scores, meaning that they were able to perform better after receiving the ZCR scaffold. However, this study lacked a control to compare if this method was better than current practices (Cho et al., 2014).

### **2.5.3 Dermal Allografts**

There are numerous commercially available dermal allografts and xenografts that have orthopedic surgical applications. These grafts include human dermis, porcine dermis, porcine intestinal submucosa, and synthetic materials. Human dermal allografts are primarily extracellular collagen matrices and can be advantageous due to their in vivo revascularization, cellular incorporation, and biomechanical properties. The allograft is designed to be implanted as a bridge between tissues. Host cells can then migrate into the allograft to allow for healing promotion. The graft is subjected to decellularization and sterilization, which can affect the biomechanical strength of the graft. The preparation, storage, and hydration of the implant also impacts the biomechanical properties (Acevedo et al., 2015). However, dermal allografts have been shown to have superior suture pullout strength compared to other materials (Barber et al., 2006).

In patients with irreparable rotator cuff tears, human dermal allografts have been used. The tissue is harvested from human cadavers for the purpose of improving graft consistency and mitigating complications, since rotator cuff repair has a high likelihood of poor healing after surgery (Scarfe, A, 2019).

In elbow surgery, acellular dermal matrix (ADM) is a viable graft for interposition arthroplasty due to its suture retention strength. ADM has also been used in posterolateral rotary instability (PLRI). This is when the elbow capsule is stretched from chronic subluxation of the radial head and causes a deficient lateral ulnar collateral ligament (LUCL). To treat PLRI, a tendon allograft is used to reconstruct the LUCL. ADM can be sutured to the tendon graft and native elbow capsule as a replacement for a damaged elbow capsule. There are additional applications for ADM in the elbow that are still awaiting clinical studies (Acevedo et al., 2015).

#### **2.5.4 Unmet Need**

There is a need for a less traumatic repair technique that enhances the repair of a partially torn UCL to restore it to its normal function. It should allow overhead throwing athletes to achieve the same throwing ability they had prior to injury. The recovery time for the surgery should be less than or equal to that of the current surgical methods, which is nine to twelve months.

## **3.0 Project Strategy**

This section details the project strategy and design approach that was utilized to identify the problem, potential solutions, and develop a design. In addition, this section will discuss the stakeholders involved in the project and any constraints that we have. It will also include the objectives of the project that are ranked by importance.

### **3.1 Initial Client Statement**

We were tasked with creating a device to help heal UCL tears. The device would be responsible for delivering a therapeutic agent to the injury site to stimulate ligament reparation and return the player to their original pitching or throwing capacity. The initial statement provided to us from the client was to:

*“Design, develop, and characterize a physiologically relevant biomechanical model of an implantable ligament regeneration treatment system to improve surgical outcomes for UCL repair procedures.”*

The most common current solutions for UCL healing include Tommy John surgery and nonoperative healing methods such as physical therapy. These methods are not designed to address moderate tears such as grade two tears. Our solution would address the need for less intense operative methods, but more reparative methods than rest and physical therapy. In addition, the device should reduce the surgical recovery period that a patient endures when compared to other methods, like Tommy John surgery.

### **3.2 Stakeholders**

The stakeholders are important people and organizations to consider in the research, design, and implementation of this project. They have the potential to be impacted by this project in a variety of ways, so their consideration and involvement is vital to the project’s success. The stakeholders of this project fall under three main categories: patients, surgeons, and designers.

The most important stakeholders are the patients who have experienced a UCL tear and need medical treatment. The target population for this treatment would be athletes of all ages that are experiencing a partial ligament tear (D. Magit, personal communication, September 24, 2021). The patient has the ultimate say in deciding if the developed product is something they

would like to pursue. Not only will patients consider the safety of the device, but they will also want to be ensured with satisfactory results that reduce their recovery time. Patients and insurance companies are financially responsible for the treatment and going through any associated postoperative physical therapy. The concerns of the patient group are valuable design considerations.

The surgeons are the stakeholders that would implement the treatment to patients. The surgeons' preferences need to be considered during the design process because they make the final decision on whether to offer this treatment to their patients. The surgeons value ease of use and patient satisfaction. According to Dr. Magit, the surgeons use a new device that aligns with standard surgical practices and requires minimal or simple training.

Our group is considered the major contributors to the design of this project. The role of the designers is to understand the problem and develop and test viable solutions that will be beneficial to the other stakeholders. Maria Decelles, Evan Hallberg, Brooklynn Paris, Meagan Smith, Dr. David Magit, Professor George Pins, and Professor Karen Troy are the individuals on the project design team.

### 3.3 Initial Objectives and Constraints

Based on initial meetings with clients, we outlined numerous needs and wants for the implant. These helped identify objectives and constraints for the project, which are outlined in the following sections.

#### 3.3.1 Initial Objectives

Table 3: Initial Design Objectives and their Descriptions

Objective	Description
Delivers a Therapeutic Agent	The scaffold needs to be able to contain a therapeutic agent and release the therapeutic agent to the UCL at a controlled rate over a set period
Healing Promotion	Must augment and support the regeneration of the ligament to stimulate cell proliferation, migration and synthesis of fibroblasts, restore the aligned matrix deposition, form granulation tissue, and stimulate angiogenesis
Reproducible	Must be able to be reproduced such that each device has precise and accurate mechanical properties, therapeutic delivery capabilities, shelf life and degradation rate

Mechanically Sound	Must be flexible enough so that the joint can move once implanted, but be strong enough that it can withstand surgical manipulation and attachment to the ligament
Surgically Compatible	Can be manipulated to fit in the standard surgical window and anchored to the ligament
Cost-Effective	Must cost effective materials and manufacturing to allow the device to be affordable for professional and amateur athletes

We conducted a meeting with the client surgeon, Dr. David Magit, to determine the objectives for the design. From this meeting, we developed five main objectives for the design: *healing promotion, mechanically sound, delivers a therapeutic agent, surgically compatible, reproducible, and cost effective*. After finalizing the primary objectives, they were sent to the client for review and ranking. This would help determine which was the highest priority and ensure that the clients' needs were met in the final design. Table 3 contains a brief description of each of the initial objectives.

### 3.3.2 Constraints

Table 4: *Design Constraints and their Descriptions*

Constraint	Description
Timeline	The MQP team only has nine months to research, develop, and test a design to repair the UCL
Budget	The MQP team only has a \$1,000 budget to develop the product (\$250 per member)
Sterilization	Must be sterilizable since it will be implanted in the body
Biocompatibility	Must not cause an adverse chronic foreign body or cytotoxicity response and must be made of natural materials
Surgical Limitations	Must be completed using standard surgical window and does not require a follow up or secondary injection or incision
Size	Must be smaller than the anchoring ligament (4 cm x 1.5 cm x 2-3 mm)

After determining the primary objectives, we established a set of constraints. Our design constraints are referenced in Table 4. It is pertinent that our team manages ourselves in the most efficient way possible through using the Gantt Chart and holding frequent meetings so that we may have a finished product by the end of the school year. The cost of the materials that will be purchased and processes that will be outsourced will need to be planned and reviewed as we have a tight budget of \$1,000 to develop our product. It is important the product is sterilizable as it will be implanted in the body and cannot cause any health problems for the patient. The product will also need to be biocompatible as to also not cause adverse immune response to the

body. To not create a more complex surgical procedure, the implantation of the device must be completed using the standard surgical incision window and not require post-operative surgery.

### **3.4 Revised Client Statement**

Following the discussions with the client Dr. Magit and our literature review of the design space (Chapter 2), we revised the client statement to detail the client's priorities for the project.

*Design, develop and test an implantable scaffold that assists in the healing of a torn ulnar collateral ligament (UCL). The design should be biocompatible and begin degrading after 4-6 weeks. The scaffold must significantly increase cell proliferation by releasing a total of 600 ng of PDGF-BB over a period of at least 2 weeks. The scaffold should have a stiffness between 3 and 17 N/mm and a failure load of at least 13 N. The scaffold should be implantable in a 10 cm window and within the dimensions of 15 mm by 40mm by 3mm. The design must be reproducible so that it can be used as an alternative gold standard of care for UCL repair treatments.*

### **3.5 Final Objectives**

Through several additional conversations and our research, we devised primary, secondary, and tertiary objectives. In this section, we present these objectives that will guide our design process in identifying functions and specifications. Figure 6 shows the primary objectives and the underlying secondary and tertiary objectives.

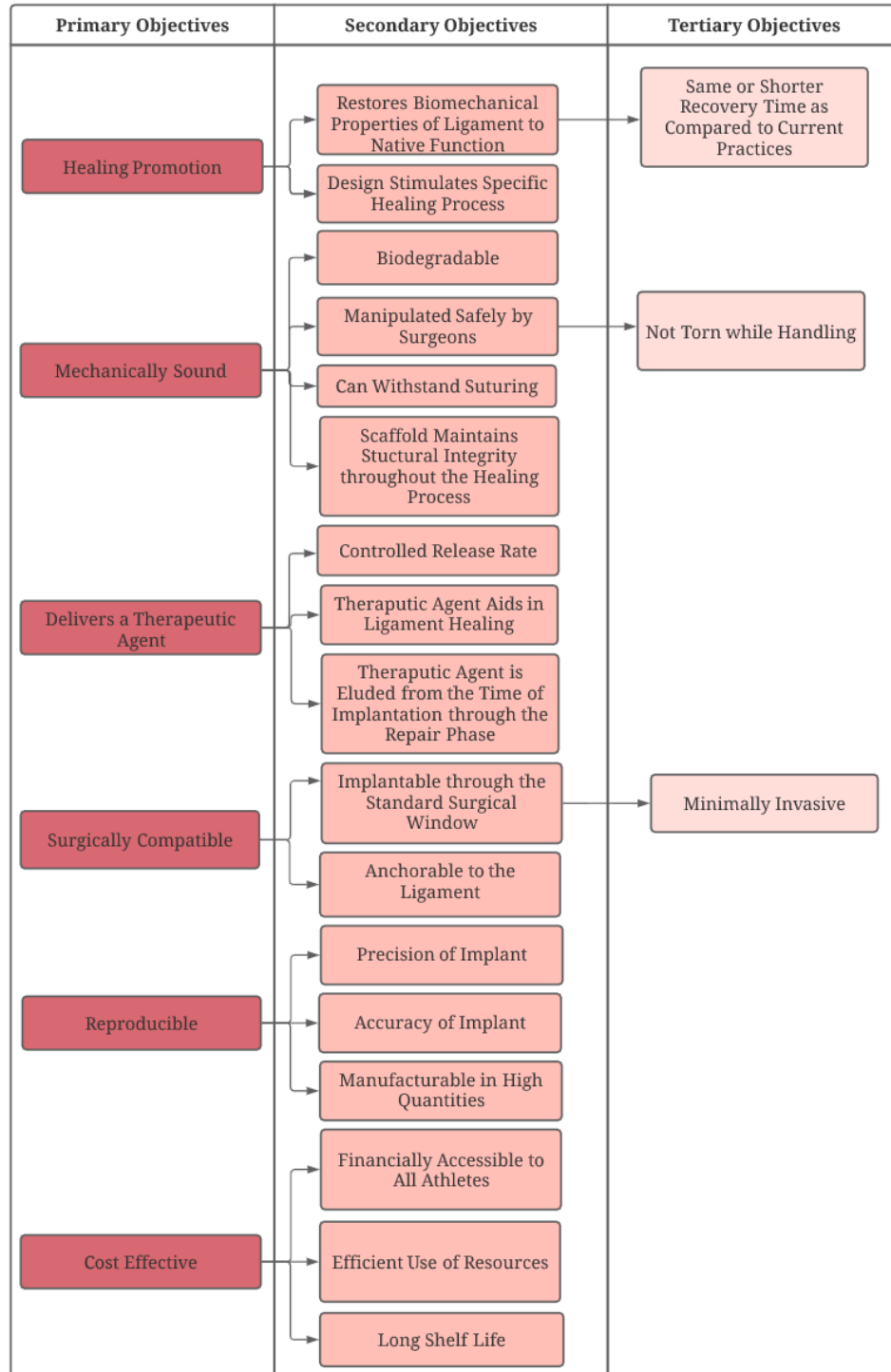


Figure 6. Primary, Secondary and Tertiary Objective Tree

The students, advisors, and the client used a pairwise comparison chart (PCC) to determine the importance of each primary objective. Each objective was ranked either 0, 0.5, or 1 where 0 is less important than the other objective, 0.5 meant they were equally important, and

1 indicated it is more important than the other objective. The scores for each objective were then totaled to help determine the ranking of the primary objectives.

Table 5: *Summary of the Stakeholder's Pairwise Comparison Charts of the Primary Objectives*

Primary Objective	Students	Advisors	Client	Average
Delivers a Therapeutic Agent	3.375	3.25	4	3.54
Healing promotion	4.375	3.5	2.5	3.46
Reproducible	1.125	3.25	3.5	2.63
Mechanically Sound	4	2.75	1	2.58
Surgically Compatible	1.75	2.25	3	2.33
Cost Effective	0.5	0	0	0.17

Table 5 shows the average score from the four students, the average score from the two advisors, the score of the client, and the overall average score of all stakeholders. Everyone's PCC can be found in Appendix B.

Delivering a therapeutic agent is the most important objective because it is considered the defining characteristic that makes this design reparative rather than reconstructive to augment the natural healing process. Healing promotion is the next most important objective because it defines the main function and purpose of the device. Reproducibility is moderately important because the design must be accurate and precise to achieve healing promotion and delivery of therapeutic agent. Mechanically sound is somewhat important because the device can function without achieving this objective although implantation may be difficult. Surgical compatibility is less important because although it is preferred to have minimal procedural differences, physicians would be willing to adjust practices if the design is very effective. Lastly cost effective was deemed the least important primary objective because it is understood that improved healing would save stakeholders and patients time and money and insurance compensation would provide aid.

The following Tables 6-11 outline the definitions of the secondary objectives. These secondary objectives detail the specific parts of the primary objectives.

Table 6: *Healing Promotion Secondary Objective Definitions*

<b>Healing Promotion</b>	
<b>Secondary Objective</b>	<b>Definition</b>
Restores Biomechanical Properties of Ligament to Native Function	Ligament fibril structure must be restored so it is returned to its natural function and mechanical properties in the same or shorter recovery time compared to current practices
Design Stimulates Specific Ligament Healing Process	Stimulates cell regeneration, new collagen formation, production of fibroblasts and granulation tissue, aligned matrix deposition, and angiogenesis

Table 7: *Mechanically Sound Secondary Objective Definitions*

<b>Mechanically Sound</b>	
<b>Secondary Objective</b>	<b>Definition</b>
Biodegradable	The implant should degrade in a biological environment
Manipulated Safely by Surgeons	Must not be torn during handling
Can Withstand Fixation to the Ligament	Must be able to be attached and secured to the ligament
Scaffold Maintains Structural Integrity throughout the Healing Process	Remains mechanically intact and withholds its functionality while undergoing the stresses and strains of elbow during the healing phase

Table 8: *Delivers a Therapeutic Agent Secondary Objective Definitions*

<b>Delivers a Therapeutic Agent</b>	
<b>Secondary Objective</b>	<b>Definition</b>
Controlled Release Rate of Therapeutic Agent	The release of the therapeutic agent, such as or including growth factors, must be at a controlled rate that corresponds to and over the duration of the natural healing process
Therapeutic Agent can be Absorbed or Injected into the Scaffold	Must be an additive to the scaffold that is either injected or absorbed
Therapeutic Agent Eludes from Implantation through the Repair Phase	The timeline of therapeutic elution begins at the time of implantation and lasts through the repair phase of healing

Table 9: *Surgically Compatible Secondary Objective Definitions*

<b>Surgically Compatible</b>	
<b>Secondary Objective</b>	<b>Definition</b>
Implantable through the Standard Surgical Window	Must be able to be implanted in a 10 cm window

Anchorable to Ligament	Must be able to be attached to the ligament so that it does not migrate in the body
------------------------	---

Table 10: *Reproducible Secondary Objective Definitions*

Reproducible	
Secondary Objective	Definition
Precision of Implant	Mechanical properties, therapeutic delivery capabilities, shelf life, and a degradation rate do not differ between each implant produced
Accuracy of Implant	Mechanical properties, therapeutic delivery capabilities, shelf life, and degradation rates meet the specifications for these requirements
Manufacturable in High Quantities	Manufacturing process is repeatable and efficient to produce devices in batches

Table 11: *Cost-Effective Secondary Objective Definitions*

Cost-Effective	
Secondary Objective	Definition
Financially Accessible to All Athletes	The cost of the device, procedure, and recovery should be relatively low so that it is available to amateur and professional athletes
Efficient Use of Resources	Manufacturing, materials, and fabrication resources are used efficiently to minimize excessive costs
Long Shelf Life	Can be stored for long periods of time and still maintain its effectiveness

The students, advisors, and client again used a pairwise comparison chart (PCC) to determine the importance of the top four secondary objectives from each primary objective. Each objective was ranked on the same scale as before (0, 0.5, or 1). The scores for each objective were then totaled to help determine the ranking of the secondary objectives.

Table 12: *Summary of the Stakeholder's Pairwise Comparison Charts of the Secondary Objectives*

Primary Objective	Secondary Objective	Students	Advisors	Client	Average
Healing promotion	Restores Biomechanical Properties of Ligament	8.375	10	2.5	9.1875
Healing promotion	Design Stimulates Ligament Healing Processes	8.5	9.5	4	9
Reproducible	Accurate	7.125	7.5	10	7.3125
Mechanically Sound	Can Withstand Fixation to the Ligament	6	6.25	3	6.125
Reproducible	Precise	5.375	6.5	8.5	5.9375
Delivers Therapeutic Agent	Controlled Release Rate	3.875	6.75	4.5	5.3125

Mechanically Sound	Manipulated Safely by Surgeons	5.25	5.25	4.5	5.25
Delivers Therapeutic Agent	Therapeutic Agent can be Integrated into Scaffold	3.625	5.5	5.5	4.5625
Delivers Therapeutic Agent	Therapeutic Agent Elutes from implantation through repair phase	5.125	4	6.5	4.5625
Healing Promotion	Biodegradable	4.125	2.5	1	3.3125
Mechanically Sound	Scaffold Maintains Structural Integrity throughout the Healing Process	5.125	0.5	4.5	2.8125
Reproducible	Manufacturable in High Quantities	2.75	1.5	3	2.125

Table 12 shows the average score from the four students, the average score from the two advisors, the score of the client, and the overall average score of all stakeholders. Each individual's PCC can be found in Appendix C.

### 3.6 Project Approach

Ground rules were set at the beginning of the project to ensure that the most optimal design would be created. This included holding multiple meetings throughout the year, updating the client and advisors on progress and having an agenda with set deadlines to ensure productivity. Introductory meetings were conducted with the client to ask questions and concentrate background research, as well as develop design specifications and design objectives. It is also important to acknowledge the financial approach that was taken in order to develop the most effective design within budget parameters.

#### 3.6.1 Management Approach

Client and advisor meetings were held weekly to give progress updates and ask questions, as well as clarify objectives and specifications. Team meetings were held three to five times a week to develop weekly objectives and give progress updates. A Gantt Chart was used to ensure that deadlines were met. The Gantt Chart can be seen in Appendix D. It was updated frequently to account for inconsistencies and to complete all stages of the design process effectively.

### **3.6.2 Design Approach**

During A-term, background was obtained on relevant areas. Research was heavily concentrated on scholarly articles that demonstrated successful practices and were concurrent with the latest developments. Project specifications and design objectives were developed based on client input, previous studies, and research that we conducted. The design approach section was updated continuously in order to ensure that the design that best met the objectives was chosen.

### **3.6.3 Financial Approach**

Worcester Polytechnic Institute allotted \$250 to each person to be utilized towards the development and execution of the project. This totals \$1,000 to complete the development and testing of the device. With the limited budget, we will assess all purchases for alternative options or methods and a list of materials and costs for the final design will be developed.

## 4.0 Design Process

To design and test an effective device, we went through several initial steps of the design process. We conducted an analysis of the needs and wants of the device, evaluated design considerations, and identified functions and specifications. We conducted a brainstorming session to identify conceptual designs. Then, we researched the options for design considerations and used a pairwise comparison chart and a Pugh analysis to identify the top two alternative designs.

### 4.1 Needs Analysis

After many meetings with the client and advisors, we finalized their primary objectives and discussed their importance. Then, based on these objectives, a list of requirements of the device was compiled. These requirements were then classified as needs or wants. Things that were required for the design to be successful were classified as needs, and things that were not required were classified as wants. The following sections detail the design needs and wants and their descriptions.

#### 4.1.1 Design Needs

Table 13: *Design Needs*

Needs	Definition
Biodegradable	Capable of degrading in the body so no secondary removal procedure is needed
Elutes Therapeutic Agent	Releases one or more therapeutic agents to augment the natural healing process
Assists in Natural Healing Process	Augments and supports the regeneration of the ligament
Retains Mechanical Properties	Should be able to hold its integrity while being manipulated by the surgeon and during the inflammation phase of healing
Achieves Stable Fixation to the Ligament	Able to be attached to the ligament so that it does not migrate in the body
Reproducible Accurately	Reproducible such that mechanical properties, therapeutic agent delivery method, and degradation rates meet the specifications for these requirements

Reproducible Precisely	Reproducible such that mechanical properties, therapeutic agent delivery, and degradation rate do not differ between each implant produced
------------------------	--

Table 13 shows the design needs that were identified for the scaffold. They are ranked based on importance.

#### 4.1.2 Design Wants

Table 14: *Design Wants*

Wants	Definition
Long Shelf Life	Can be stored for long periods of time and still maintain its effectiveness
Low Cost	Affordable for professional and amateur athletes
Short Return to Play Time	Return to play time is at or shorter than that of the gold standard which is 9 months
Used for Multiple Applications	Provides healing capabilities for ligaments other than the Ulnar Collateral Ligament
Degrades Gradually	Ligament will not degrade until the ligament reaches the remodeling phase of healing
Ease of Use	Easily implantable through use of standard surgical techniques

The design wants, shown in Table 14, were determined from our objectives and interviews with the client. The wants are items that the design does not necessarily need to have but would be desirable for us to achieve. When we completed the PCC for the primary objectives it was determined that cost effectiveness of the scaffold and its surgery was the last priority. Thus, design considerations related to cost were considered wants.

### 4.1.3 Needs and Wants Design Matrix

Table 15: *Design Needs Matrix*

Design Considerations	Biodegradable	Elutes Therapeutic Agent	Assists in Natural Healing Process	Retains Mechanical Properties	Simple Drug Delivery Method	Achieves Fixation to the Ligament	Accurately Reproduced	Precisely Reproduced
Scaffold Size				X		X		X
Scaffold Configuration		X		X	X	X	X	X
Scaffold Material	X	X	X	X	X	X	X	
Scaffold Manufacturing Process	X			X	X		X	X
Amount of Therapeutic Agent		X	X				X	X
Therapeutic Agent Type		X	X		X		X	
Mode of Therapeutic Agent Release	X	X	X		X			
Rate of Therapeutic Agent Release	X	X	X				X	X
Ligament Fixation Method	X			X		X	X	

Table 16: *Design Wants Matrix*

Design Considerations	Long Shelf Life	Used for Multiple Applications	Low Cost	Degrades Gradually	Ease of Surgical Manipulation
Scaffold Size		X			X
Scaffold Configuration		X	X	X	X
Scaffold Material	X		X	X	X
Scaffold Manufacturing Process	X		X	X	
Amount of Therapeutic Agent					
Therapeutic Agent Type	X		X		
Mode of Therapeutic Agent Release	X			X	X
Rate of Therapeutic Agent Release		X			
Ligament Fixation Method		X		X	X

The design matrices in Tables 15 and 16 show the presence of a relationship between each need or want to each scaffold characteristic. An “X” denotes that there is a relationship between the need or want and the scaffold characteristic. While it is important to consider scaffold size, scaffold configuration, and rate of therapeutic agent release, they are not discussed in depth because size is determined by specifications and the amount of therapeutic agent that can be loaded is dependent on the scaffold configuration into our scaffold.

## 4.2 Functions and Specifications

Table 17: *Functions and Specifications*

Functions	Specifications
Contains a Therapeutic Agent	- Contains 300 ng PDGF-BB
Releases a Therapeutic Agent at a Controlled Rate	- Minimum release period of 2 weeks, 4-6 weeks is ideal - Must retain 70% of GFs in the first 5 days
Scaffold Degrades	- Degrades within 4-6 weeks - Retains mechanical strength until replaced by ligament tissue
Increases Cell Proliferation	- Statistically significant increase in cell proliferation with the use of growth factors compared to control
Facilitates Angiogenesis	- Statistically significant increase in endothelial cell proliferation with the use of growth factors compared to control
Withstands Anchoring	- Sutures must be able to withstand 78.3 N so that the ligament or scaffold isn't damaged - Fixation method must degrade slower than the degradation of the scaffold, greater than 4-6 weeks
Withstands Surgical Manipulation	- Implantable in 10 cm incision window and within the dimensions of 15 mm x 40 mm x 3mm - Stiffness is between 3 and 17 N/mm - Failure load is greater than 13 N

In collaboration with the client and advisors the design team identified functions based on the objectives that have been discussed. The functions and corresponding specifications are shown in Table 17.

Based on an analysis of isolated growth factors in Section 4.4.1, PDGF-BB was chosen for the design. The scaffold must contain 300 ng of PDGF-BB. This was determined through calculations based on PDGF-BB content in 10 mL of PRP, which is used in current clinical practices as a non-operative UCL healing method. In addition, this value was confirmed through research from literature values used to heal ligaments (Kieb et al., 2017). These calculations are detailed in Section 4.6.

The scaffold must release the therapeutic agent at a controlled rate over a minimum release period of 2 weeks in order to aid in the healing process over this time period. The release period of at least two weeks with four to six weeks being ideal was determined by client request and corresponds to the timeline for healing as the therapeutic agent should be delivered from implementation and into the repair phase, which takes place until week four (“The Ligament Injury-Osteoarthritis Connection,” 2012). The retention rate of 70% of GFs in the first 5 days was determined by reviewing successful retention from the literature, which ranged from 70-90%, and because the five days is within the timeline of the inflammation period of 7 days and has reported success for other scaffolds in literature (Ji et al., 2011; Tabata et al., 2000).

The scaffold must degrade in four to six weeks as determined by the client and supported by the timeline of ligament healing. The scaffold should degrade when there is no more therapeutic agent being released.

Increasing cell proliferation and angiogenesis, which is characterized by endothelial cell concentration, are necessary functions for a wound healing scaffold as these functions support tissue growth and alignment (Chen et al., 2009). Thus, we define the specification as a statistically significant increase in cell proliferation and endothelial cell proliferation using the scaffold design compared to the control ( $p < 0.05$ ).

The scaffold must be able to withstand anchoring. If the anchoring is achieved by suturing, sutures must be able to withstand a minimum of 78 N so that the ligament or scaffold isn't damaged (Ratcliffe et al., 2015). To ensure that the scaffold is supported in place throughout healing, the anchoring method must degrade slower than the scaffold itself.

Lastly, the scaffold must be able to withstand surgical manipulation and be implantable in the 10 cm incision window. The incision window was determined by client request and current clinical practices. The scaffold dimension specifications of 1.5 cm by 4 cm were determined by typical ligament dimensions found in literature, as well as from measurements taken from a cadaver dissection that was performed under the advisement of the client. One source reports the length of the anterior bundle of the UCL to be in the range of 21 mm, while another says that more recent studies have found it to be closer to 52 mm in length. The same two sources also report slightly different values for the thickness of the anterior bundle of the UCL. One source reports it as  $13.90 \pm 2.37$  mm, while the other states it to be 4.0 to 7.6 mm (Gurbuz et al., 2005;

Labott et al., 2018). Using ImageJ and images from our cadaver dissection shown in Appendix A, the ligament dimensions were determined to be 23.12 mm by 4.16 mm. Thus, from the literature and cadaver dissection, the maximum dimensions were identified to be 15 mm by 40 mm. The thickness of 3 mm was based on the client's request as the anatomy has minimal space for a thicker scaffold.

The scaffold must have a stiffness between 3 and 17 N/mm. This value range was determined through mechanical tensile testing of a Band-Aid and the mechanical tensile testing of chicken skin detailed in Section 4.6. This is because the surgeon mentioned that the scaffold should feel like a Band-Aid, and chicken skin is an acceptable stretchiness for the scaffold. The failure load of at least 13 N was determined by Dr. Magit who stated he will not exhibit more than 3 pounds of force during surgical manipulation.

#### **4.2.1 Mechanical Testing Results**

To understand the desirable material properties of the scaffold, we tested chicken skin and woven gauze wound dressings (Band-Aid brand) as the client had provided these materials as examples for materials that have the correct feel for stiffness and strength that the device would need. We mechanically tested the chicken skin and woven gauze wound dressings on an Instron 5544 at a constant strain rate based on strain percentage per unit time. This would ensure that the strain rate percentage would stay the same regardless of the sample's length.

To determine a physiologically relevant strain rate of a viscoelastic material, in this case skin, we marked Meagan's knee with a dot above and below the kneecap. Then, we measured the distance between the dots when Meagan's knee was extended and then again when it was flexed at the angle that she bends her knee during her toe-off phase of walking. We also measured the time it took for Meagan to reach her toe off phased from the extended position. This resulted in a strain rate of about 30%/minute. This rate was beyond the limitations of the instrument, so we lowered the strain rate to 25%/minute. We then tested our three chicken skin samples with average gage length, width, and thickness of  $66.95 \pm 5.5$  mm,  $13.7 \pm 1.8$  mm, and  $1.0 \pm 0.1$  mm, respectively. The force versus displacement graph can be seen in Figure 7 below.

To calculate stiffness from the reported modulus we used Equation A. To calculate the failure load from the reported fracture strength, we used Equation B. Where A is the cross-

sectional area of the scaffold design, L is the length of the scaffold design, E is the modulus, K is the stiffness, and  $\sigma$  is the failure strength.

$$K = \frac{EA}{L} \quad (A)$$

$$\text{Failure load} = \sigma \cdot A \quad (B)$$

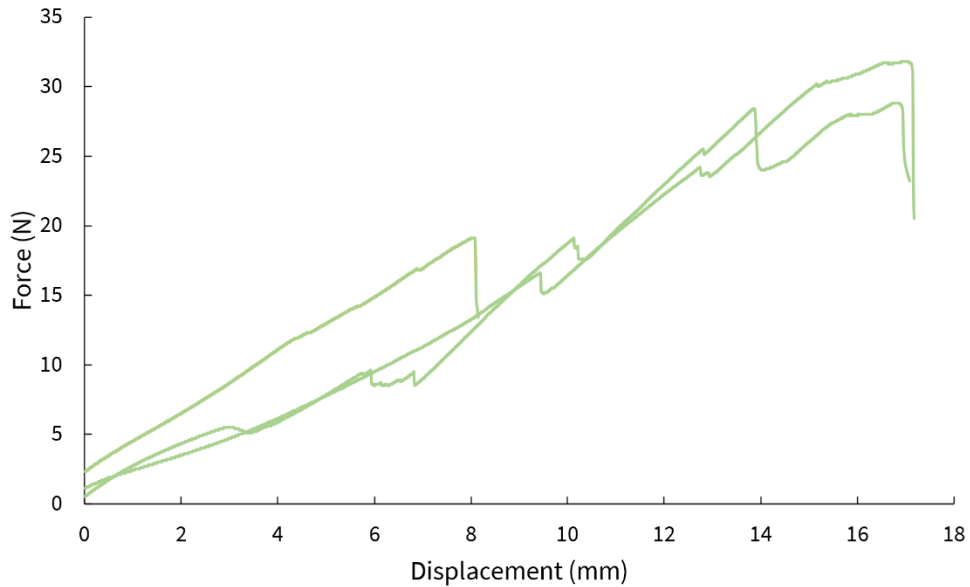


Figure 7. *The Force-Displacement Curves for Chicken Skin.*

We found that the average stiffness and failure load of chicken skin are  $3.1 \pm 1.6$  N/mm and  $31 \pm 13$  N respectively. We could now use this information to evaluate which materials of interest had properties like that of the chicken skin. We then tensile tested three Band-Aids. The force displacement graph can be seen in Figure 8 below.

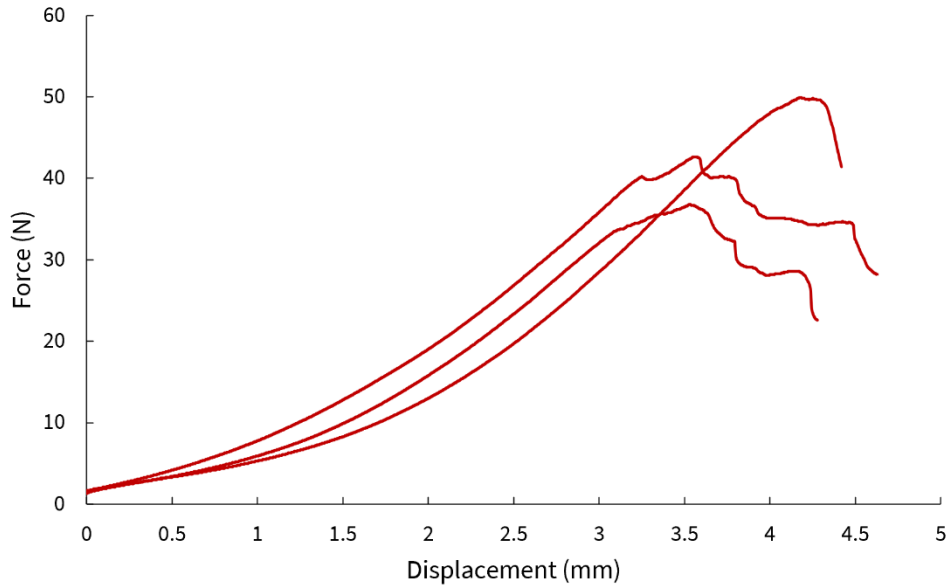


Figure 8. *The Force-Displacement Curves for Band-Aids.*

We found that the average stiffness and failure load of the Band-Aids were  $15.3 \pm 1.1$  N/mm and  $43.3 \pm 4.7$  N respectively. The average gage length, width, and thickness of the samples were determined using calipers to be  $24.52 \pm 2.4$  mm,  $12.73 \pm 1.0$  mm, and  $0.4 \pm 0.0$  mm, respectively. We can now use this information to evaluate which materials of interest had properties like that of the band aids. Now that we have successfully

Our client wanted the design to have the same feel and similar mechanical properties of chicken skin and Band-Aids. So, our stiffness and failure loads of both served as examples of the target values that would render our device easy to manipulate and suture. In conclusion to the tensile testing results we decided that because we want to choose a biomaterial that resembles the stiffness and failure load of chicken skin and Band-Aids our chosen material for our final design must have a failure load greater than 13 N and a stiffness value between 3 and 17 N/mm.

### 4.3 Conceptual Designs

After identifying functions and specifications, we brainstormed conceptual designs to meet the functions and specifications. Then, we detailed the benefits and limitations of each conceptual design and made a design matrix to rank each idea to identify the final design ideas. The benefits and limitations of these conceptual designs are discussed in this section.

### 4.3.1 Crimped Vessel Design

One conceptual design, shown in Figure 9, was to use an autograft blood vessel of optimal size to encapsulate the therapeutic agent. The edges of the blood vessel would then be crimped closed and sutured to the ligament. The main benefits of the autograft blood vessel scaffold are that it is already available in the body, and it will effectively retain therapeutic agents. Additionally, it would naturally reabsorb into the body after some time and if the blood vessel is not decellularized it may retain growth factors that can still be used in the healing process. Some notable limitations of this design include the donor site morbidity, the possibility of the vessel collapsing, and it may bring pathogens into a new part of the body from the donor site. The size and healing rate may also be uncontrollable and the method to crimp the blood vessel to retain growth factors is unknown.

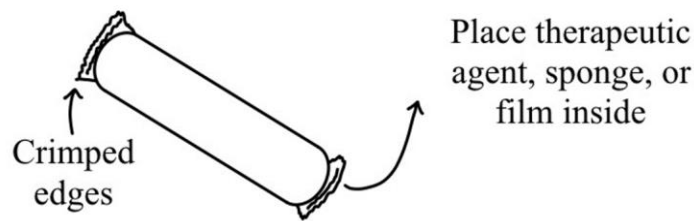


*Figure 9. Autograft Blood Vessel Capsule Sketch.*

### 4.3.2 Thread Based Designs

Another conceptual design, shown in Figure 10, is woven threads or fibers with varying degradation rates to provide sustained structural support during the healing process. This woven mesh could then be soaked in therapeutic agent or growth factors could be attached to the threads. Benefits of this design include that its stiffness can be adjusted by differing the strengths of the threads used, can be electrospun with therapeutic agents, can be used with several biomaterials, and the geometry of the scaffold can be varied. Limitations include that it could be difficult to control the degradation rate of the scaffold, the concentration of therapeutic agents in each thread would have to be carefully determined, and the cost would likely be very high due to its variability which may lead to the accurate and precise reproduction of the scaffold to be difficult. Furthermore, there could be unknown effects from layering different threads with varying degradation rates on top of each other.

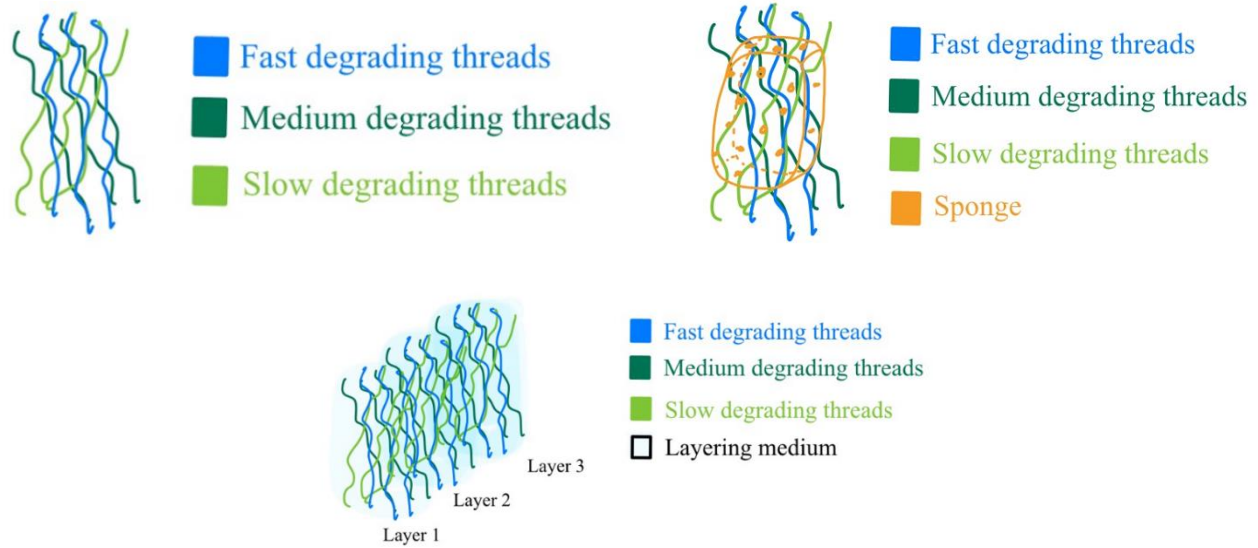


Figure 10. *Sketches of Woven Threads, Woven Threads Through Sponge, Layered Woven Threads.*

### 4.3.3 Layered Designs

Another alternative design is a layer-by-layer approach. Filaments would be manufactured through a means such as electrospinning with growth factors or the films could be soaked in a therapeutic agent such as PRP. These filament layers could also include sponge and thread layers as shown in Figure 11. The benefits of these designs include that the layers add stability and strength to the scaffold, a variety of growth factors can be sequentially released, the filaments can contain the growth factors, the layer-by-layer method proves to retain charged and uncharged molecules depending on the growth factors and biomaterials used, and it allows for a parametric analysis on the number of layers used to test release kinetics of the growth factor loaded scaffold. Some limitations include that the layers may vary in thickness in which precise production may be difficult, the loaded growth factors may not release in the desired order or intended timeframe, the degradation of the scaffold may be complex, the scaffold geometry may be complex, it may come with additional steps that the surgeon would have to follow prior to implantation, and it is unclear how to anchor both the layer-by-layer filaments design as well as the layer-by-layer filaments with sponge design.

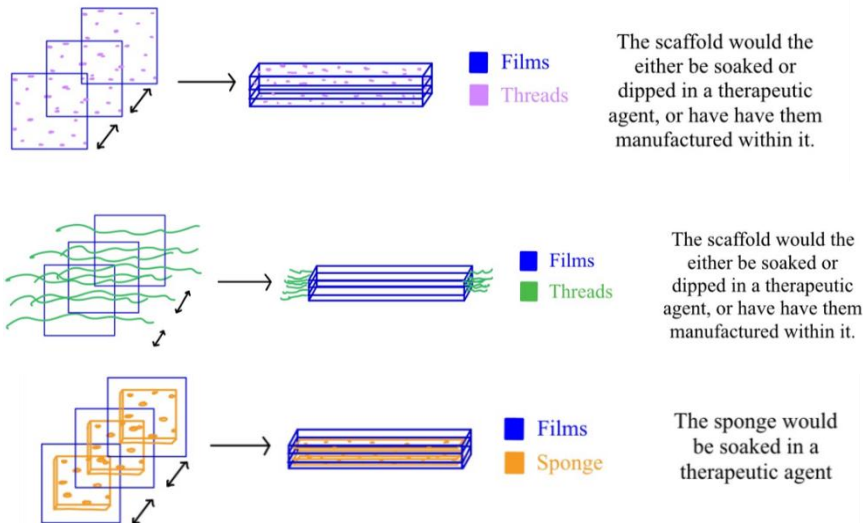


Figure 11. *Layer-by-Layer Filaments Sketch, Thread Supported Layer-by-Layer Filaments Sketch, and Layer-by-Layer Filaments with Sponge Sketch.*

The multi-layered membrane design relies on the presence of three different layered membranes that could degrade at different rates to release growth factors at targeted timepoints during healing. The sketch of this design is shown in Figure 12. The benefits of this design include that it makes the most sense with PRP as the therapeutic agent so there is no need to incorporate several therapeutic agents, it allows for the sustained release of varying membranes filled with PRP, and the membranes can be electrospun with therapeutic agents. Limitations of this design include that the degradation and release of growth factors would be difficult to control, the anchoring method for the scaffold may be complicated, and the accuracy of production may be difficult.

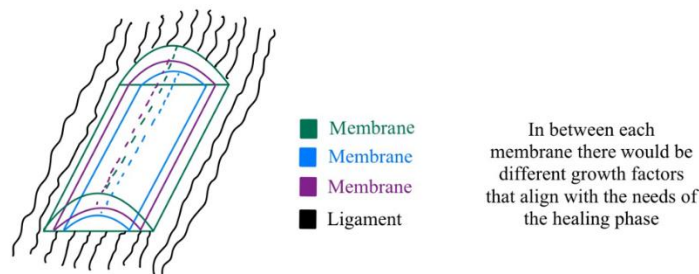


Figure 12: *Multi-Layered Membrane Sketch.*

#### 4.3.4 Yule Log Design

The Yule Log design consists of rolling up electrospun films containing growth factors shown in Figure 13. This benefits to help reduce elution of a large portion of the growth factors

to slow release and target release of certain growth factors at certain degradation times. The benefits of this design include that it is easily reproducible and that it can be used with a wide range of materials and growth factors. Limitations of this design include that it is a complex geometry which may make implantation difficult and the anchoring method for this scaffold is unknown.

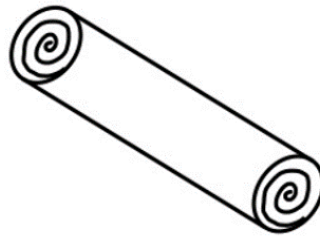


Figure 13. *Sketch Yule Log Design.*

#### **4.3.5 Sponge Based Designs**

The supported sponge design is a sponge or lyophilized scaffold made of a material such as collagen supported with fibers running through or supported with a skirt rim as shown in Figure 14. The sponge could absorb therapeutic agents and the threads would function as mechanical support and means of fixation. The benefits of this design include that the threads add stability to the scaffold while still retaining its absorbent properties, the threads or skirt could act as a means or location of sutures, and the sponge could be filled with any type of therapeutic agent prior to implantation. Limitations of this design include that it is difficult to prevent the elution of growth factors from mechanical force applied to the sponge, the threads or skirt may rip through the fragile sponge, it is difficult to control the rate of growth factor release after implantation, it may be difficult to surgically handle, and even though its production is simple it may not be accurate or precise.

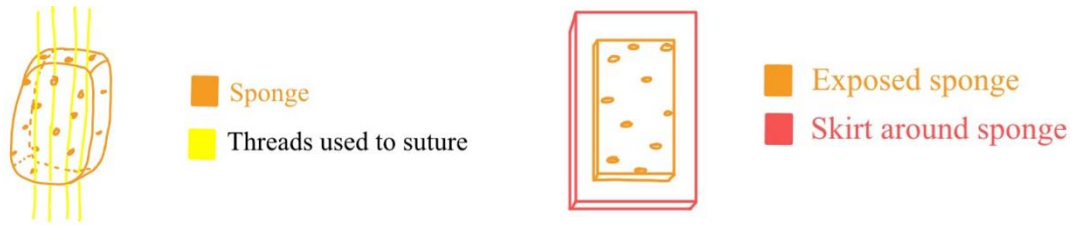


Figure 14. *Sketch of Fiber Supported Sponge Design and Supported Sponge Design.*

The encased scaffold design includes a scaffold, filament or hydrogel scaffold containing therapeutic agent encapsulated by another material film with an outer skirt of supporting material and fiber net shown in Figure 15. The benefits of this design include that it incorporates many means of encapsulating growth factors into the scaffold which makes the sustained release of the growth factors very controllable, the size and dimensions of the scaffold can be varied, it can be anchored easily to the ligament either by fibrin glue or sutures, several growth factors can be used in this design, and it retains its mechanical requirements so the scaffold can be manipulated by the surgeon with being compromised during implantation. Limitations of this design include that it has multiple components so its production may be complicated and the amount of growth factor that is absorbed by the sponge may be inconsistent from scaffold to scaffold.

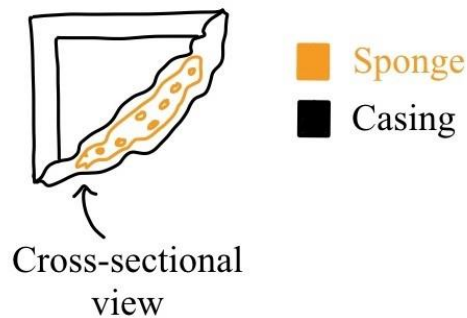


Figure 15. *Sketch of Skirt Supported and Encased Sponge Design.*

After we brainstormed design ideas, we decided to break them down into elements based on our objectives to make decisions for our final design. Many of the components from each design can be combined. The analysis of each design consideration and what we selected from each is discussed in Section 4.4 below.

## **4.4 Design Considerations**

A crucial component of developing the most effective design that aligns with our design needs and wants was to conduct an analysis breakdown of our potential design elements. The analysis breakdown enabled us to rank individual aspects of our design so that our design process was guided in a coherent manner. Our primary design objectives helped us separate our design into the following sections: promotes healing, delivers a therapeutic agent, mechanically sound, accurate and precise reproducibility, and compatibility with current surgical practices. To achieve these objectives, we researched which therapeutic agent would be the best in promoting healing, what material and drug delivery system was best to deliver the therapeutic agent, what material could provide the necessary structural support, and which manufacturing method could be reproduced precisely and accurately.

### **4.4.1 Healing promotion**

In order to have an effective design, healing promotion of the ligament needed to be achieved. This could be accomplished through a variety of therapeutic agents which will be discussed in this section, as well as each agent's role in healing and benefits for our design criteria. It is important that the therapeutic agent chosen for this design are effective to minimize the volume needed and to ensure that the natural ligament healing process is sufficiently augmented to stimulate cell proliferation, cell migration, and synthesis of fibroblasts, restore the aligned matrix deposition, form granulation tissue, and stimulate angiogenesis.

#### **Bone Marrow Aspirate Concentrate and Human Mesenchymal Stem Cells**

Human mesenchymal stem cells (hMSCs) aid in repairing tissues (Rebolledo et al., 2017). However, they are less commonly used and are typically used alongside PRP and BMAC (Hurwit et al., 2017). hMSCs are harvested from bone marrow and can differentiate into fibroblasts, osteoblasts, osteocytes, adipocytes, and chondrocytes and produce growth factors to aid in healing (Yamaguchi et al., 2019). Currently few studies exist on the use of MSCs in UCL injury applications, but they have flexibility to create chosen cell types (Rebolledo et al., 2017). Although they can aid healing by differentiating into ligament cells and fibroblasts, hMSCs would need to be augmented with additional therapeutic agents such as growth factors. They were not able to be used in this design due to lack of availability and high cost.

Bone Marrow Aspirate Stem Cell Concentrate (BMAC) can be used to support ligament healing; however, its use is more recent than PRP. BMAC contains progenitor cells, growth factors, cytokines, chemokines, and anti-inflammatory molecules. Although most studies have been done in bone applications, clinical studies have shown that BMAC can be safe and useful to supplement exercise therapy for tendon applications and can aid in “self-renewal, proliferation, differentiation, and homing effects in order to recruit more cells to the injury site” (*Platelet-Rich Plasma vs Bone Marrow Aspirate Concentrate: An Overview of Mechanisms of Action and Orthobiologic Synergistic Effects*, n.d.). Despite these benefits, the use of BMAC is limited by its invasive collection and a need for a closed system for preparation which is not possible considering the current clinical practice is a single procedure, and for this reason it was unable to be used in this design.

### **Platelet-like Particles (PLP)**

Platelet-like particles (PLP) help hemostasis and clot formation and are made from highly deformable microgel particles with molecular recognition (Brown et al., 2014). Normally, platelets are generated within fibrin networks to stiffen the fibrin matrix, but PLP can be used to enhance healing outcomes, especially in cases of traumatic injury where there can be platelet depletion. PLP increases fibrin stiffness, promotes cell and fibroblast migration, enhances proliferation, enhances collagen synthesis, improves healing outcomes, enhances cell migration and has been shown to increase angiogenesis however higher concentrations can inhibit fibroblast concertation (Nandi et al., 2019). We did not move forward with this therapeutic agent because it would require a high volume of particles that was not compatible with our constraints.

### **Platelet Rich Plasma (PRP)**

Platelet-rich plasma (PRP) contains growth factors, cytokines, chemokines, and other plasma proteins. These components make PRP a source for mitogenic, angiogenic, and chemotactic properties. PRP is low cost, does not require complex equipment, is noninvasive to collect, has minimal risk for immune response, increases vascular ingrowth and mitogenic effects, and increases cell proliferation. More information about PRP can be found in Section 2.3.2. Based on its benefits, PRP has been studied for use in a previous UCL healing scaffold at WPI.

According to the client, Dr. Magit, the current clinical practice is to extract 30-40 mL of blood to create 10 mL of PRP. The 10 mL of PRP is then injected into a patient to support UCL healing. This volume was not possible to include in a design with our dimensions. Since using PRP was not an option, each individual growth factor in PRP was considered for the design. Calculations were performed to identify the amount of growth factor needed for sufficient healing. This value was used as a benchmark for therapeutic agents to aim to load into the design of the scaffold.

Table 18: *Mass and Volumes Needed of Each Growth Factor*

<b>Growth Factor</b>	<b>Growth Factor Concentration Detected (pg/mL)</b>	<b>Mass of Growth Factor Assuming 10 mL volume (ng)</b>	<b>Volume of Growth Factor Needed (µL)</b>
VEGF	528	5.28	0.0528
FGF-2	410	4.10	0.041
PDGF-AB	17,846	178.46	1.7846
TGF-b1	77,533	775.33	7.7533
IGF-1	1,539	15.39	0.1539
Total	97,856	978.56	9.7856

The contents of various growth factors within PRP have been found in various literature sources. The second column of Table 18 shows the concentrations of growth factors present in PRP, prepared using SmartPrep-2 (Kieb et al., 2017). To determine the mass needed, these concentrations were multiplied by the 10 mL of known sufficient volume of PRP as shown in column two. Then, to determine the volume of growth factor needed, the mass of the growth factor was divided by the minimum concentration recommended by the manufacturer (100 µg/ml) (*Growth Factors / ProSpec*, n.d.). Using isolated growth factors will require less volume than PRP and we will be able to include enough healing agent into our final design.

To confirm the mass of PDGF-BB needed from the PRP calculations, research on successful concentrations of isolated PDGF-BB used to heal tendons and ligaments was completed. One study conducted by Wei et al. used 16, 160, 480, 960, and 1600 ng of PDGF-B in an attempt to heal the periodontal ligament (PDL). In this study, 1.6 mg PLGA microspheres delivered the PDGF-BB to the target location (Wei et al., 2006). Another study used PDGF-BB concentrations of 125, 250, and 1,250 ng/mL in a 400 µL fibrin matrix. This system was tested on canine flexor digitorum profundus (FDP) (Thomopoulos et al., 2010). Based on these

concentrations, we set the range of growth factor in our scaffold to be 200-1200  $\mu\text{g}/\text{mL}$ . Due to budgeting, only one growth factor could be considered, and since PDGF-BB ranked the highest, it was further considered for the final design. The 178 ng of PDGF-BB found in PRP is within these ranges found in the literature, which confirms our future testing range.

### PRP Powder

Another method of PRP preparation is as a PRP powder which is a dry substance prepared using pooled PRP by means of lyophilization without the need for centrifugation and can be stored for 12 months. One study created a growth factor preparation (lyophilized PRP powder) and evaluated the concentration of various growth factors. PRP powder had elevated levels of VEGF, FGF-2, PDGF-AB, and TGF-B1 compared to whole blood and other PRP preparations called SmartPrep-2 and platelet concentrates (PC) (Kieb et al., 2017). This powder was not further considered due to hesitation from the client surgeon and lack of availability.

### Isolated Growth Factors

We researched isolated growth factors as they are involved in the natural healing process and do not require large volumes. This is good for our design as we are limited to a small size scaffold. In addition, growth factors have had proven results in promoting the healing of ligaments and tendons. More information about growth factors can be found in Section 2.2.2. Table 19 below shows a pugh analysis for what therapeutic agent we chose to move forward with.

Table 19: *Therapeutic Agent Pugh Analysis*

Evaluation Criteria	Weight	Baseline	PRP	Growth Factors	PRP Powder	BMAC	PLP
Ease of Attainment	3	0	-1	1	1	-1	0
Volume Required Smaller than Total Scaffold Volume	5	0	-1	1	1	0	1
Healing Capability	5	0	1	1	1	1	1
<b>Constraints</b>							
Cost	5	0	1	0	0	0	0
<b>Total</b>	-	-	<b>2</b>	<b>13</b>	<b>13</b>	<b>2</b>	<b>10</b>

Appendix E explains the weighing criteria for the Pugh analyses in this chapter. After analyzing each therapeutic agent for its properties, we evaluated each agent against its ease of attainment, volume required and if it would fit in our dimensions, healing capability, and cost. This is shown in Table 19. Isolated growth factors ranked the highest, so we decided to move forward with isolated growth factors as the therapeutic agent in our design. Now, we needed to determine which specific growth factor to move forward with. We researched VEGF, FGF-2, PDGF-BB, TGF- $\beta$ 1, and IGF-1 as these are the most prevalent growth factors in wound healing. Table 20 shows each growth factor that will be discussed in this section, along with their functions. Each growth factor's role in the ligament healing process is further discussed in Section 2.2.2.

Table 20: *Summary of Growth Factors Present in Natural Ligament Healing Process* (Gulotta & Rodeo, 2009; Molloy et al., 2003).

Growth Factors	Function (s)
Platelet-Derived Growth Factor (PDGF-BB)	Collagen production, protein production, DNA synthesis, increased cell proliferation, generation of other growth factors
Transforming Growth Factor- $\beta$ 1 (TGF- $\beta$ 1)	Increased production of collagen I and III, improved mechanical properties
Vascular Endothelial Growth Factor (VEGF-2)	High angiogenic effect, cell proliferation, vascular growth towards the site of repair, can be upregulated through biological and mechanical stimuli
Basic Fibroblast Growth Factor (FGF-2)	Production of collagenase, proliferation of capillary endothelial cells, angiogenesis, formation of granulation tissue
Insulin-Like Growth Factor- I (IGF-1)	Protein synthesis, cell proliferation, collagen synthesis, decrease swelling, migration of fibroblasts

The success of PDGF-BB is dependent on the dosage, timing, and delivery of the growth factor. In a rabbit knee medial colleterial ligament rupture model, this growth factor improved the load, energy absorbed to failure, and elongation values of the ligament complex in comparison to control. Increased cellular proliferation and angiogenesis were found in a rat model as well (Gulotta & Rodeo, 2009). PDGF-BB influences the generation of other growth factors as well. More specifically, it is involved in the synthesis of IGF-1 and TGF- $\beta$ 1 (Molloy et al., 2003).

Preliminary studies have shown an increase in proliferating cells and the expression of type-III-collagen in the presence of FGF-2, but the results are not compelling enough to make a conclusion about its effectiveness in humans (Gulotta & Rodeo, 2009). *In vivo* and *in vitro*

studies have demonstrated that FGF-2 stimulates angiogenesis as well as cellular migration and proliferation. In a rat patellar tendon, the progression of closure in an *in vitro* wound after the addition of four concentrations of FGF-2 was conducted. The study found that 10 ug/L of FGF-2 accelerated healing the most (Molloy et al., 2003).

TGF- $\beta$ 1 mRNA is believed to be important in the initial inflammatory phase of healing. TGF- $\beta$  is released from degranulating platelets during the wound healing process. TGF- $\beta$ 1 is correlated with an abundance of scar tissue and mechanically weak tissue compared to normal tissue, TGF- $\beta$ 3, on the other hand can result in improved mechanical properties. The inhibition of TGF- $\beta$ 1, or increased expression of TGF- $\beta$ 3, is therefore advantageous in the UCL healing process (Gulotta & Rodeo, 2009).

In a rat model, VEGF was found to improve tensile strength in the Achilles tendon (Gulotta & Rodeo, 2009). All isoforms of VEGF bind to receptor tyrosine kinases called VEGF receptors (VEGFR)-1, -2, and -3. The presence of VEGF is associated with vascular ingrowth from the “epi- and intra-tendinous blood supply towards the site of repair” (Molloy et al., 2003).

When applied to a rat Achilles, IGF-1 was found to stimulate synthesis of DNA, collagen, and proteoglycans, as well as reduce time to functional recovery (Gulotta & Rodeo, 2009). It is crucial in the inflammatory and proliferative stages. The primary roles of IGF- I are to stimulate the proliferation and migration of fibroblasts at the injury site to increase collagen and ECM structure production during remodeling. IGF- I and PDGF-BB help to increase mitogenesis and cell division of tendon fibroblasts and surface cells, compared to when they are used individually (Molloy et al., 2003).

Table 21: *Growth Factor Pugh Analysis*

<b>Growth Factor Functions</b>	<b>Weight</b>	<b>PDGF-BB</b>	<b>FGF-2</b>	<b>TGF<math>\beta</math>-1</b>	<b>VEGF-2</b>	<b>IGF-1</b>
Collagen Production	1	1	1	1	0	1
Cell Proliferation	1	1	0	0	1	1
Protein Production	1	1	0	0	0	1
DNA Synthesis	1	1	0	0	0	0
Generation of Other Growth Factors	1	1	0	0	0	0
Improved mechanical properties	1	0	0	1	0	0

Migration of fibroblasts	1	0	0	0	0	1
Angiogenesis	1	1	1	0	1	0
Vascular Growth	1	0	1	0	1	0
Formation of granulation tissue	1	0	1	0	0	0
<b>Total</b>		<b>6</b>	<b>4</b>	<b>2</b>	<b>3</b>	<b>4</b>

To prioritize growth factors due to a limited budget, a Pugh analysis was performed to evaluate each growth factor against the needed healing functions shown in Table 21. PDGF-BB was ranked highest, followed by FGF-2 and IGF-1. PDGF-BB has been found to promote other growth factor production, specifically IGF-1 (Luo et al., 2018). Thus, the design team chose to prioritize PDGF-BB and FGF-2.

#### 4.4.2 Delivers a Therapeutic Agent

An important aspect of this project was the material needed to deliver the therapeutic agent of interest, PDGF-BB. Many drug delivery systems are dependent upon both the methods of delivery as well as the material. We prioritized the material selection for drug delivery as described in this section. Natural or synthetic materials could be used for the drug delivery component of our scaffold; however, we prioritized natural materials, because they are derived from a natural source and tend to elicit minimal adverse immune response. It is also typically easier to attach biological molecules to natural materials. In addition, they tend to better replicate and mimic the natural extracellular matrix. The limitations of natural materials include their high degradation rate, challenging reproduction process, and in some cases, poor mechanical properties (Silva et al., 2020). Table 22 below shows the benefits and limitations of each material investigated.

Table 22: *Benefits and Limitations of Natural Materials*

<b>Material</b>	<b>Benefits</b>	<b>Limitations</b>
Collagen	<ul style="list-style-type: none"> <li>- Various modalities such as meshes, hydrogels, sponges<sup>1</sup></li> <li>- Promotes cell proliferation and differentiation, ECM formation, and cell adhesion<sup>2</sup></li> <li>- Advisor has experience with this material</li> <li>- Ample research available on its use with growth factors</li> </ul>	<ul style="list-style-type: none"> <li>- Crosslinking agents may leach and cause unwanted immune responses<sup>1</sup></li> <li>- Many patents already exist</li> </ul>

Silk	<ul style="list-style-type: none"> <li>- Various modalities such as hydrogels, films, braided or knitted fibers<sup>1</sup></li> <li>- Support attachment and proliferation of several primary cells and cell lines<sup>1,2</sup></li> <li>- High drug loading capacity<sup>2</sup></li> <li>- Anti-microbial</li> <li>- WPI Professor Jeannine Coburn has experience with this material</li> <li>- Has been used to deliver growth factors</li> </ul>	<ul style="list-style-type: none"> <li>- Cell adhesion is limited<sup>1</sup></li> <li>- Improved mechanical properties are coupled with longer degradation rates<sup>1</sup></li> </ul>
Zein	<ul style="list-style-type: none"> <li>- Natural renewable source<sup>3</sup></li> <li>- Resistance to microorganisms<sup>4</sup></li> <li>- When electrospun, it has antimicrobial properties<sup>4</sup></li> <li>- High drug loading capacity<sup>3</sup></li> </ul>	<ul style="list-style-type: none"> <li>- Minimal literature on its use with growth factors</li> </ul>
Chitosan	<ul style="list-style-type: none"> <li>- Excellent biocompatibility and adhesive properties<sup>1,2</sup></li> <li>- Various modalities such as a sponge or hydrogel<sup>1</sup></li> <li>- Promotes fibroblast cell proliferation<sup>2</sup></li> <li>- Assists in the production of collagen I<sup>1</sup></li> <li>- Prevents scar tissue formation<sup>2</sup></li> </ul>	<ul style="list-style-type: none"> <li>- Low solubility<sup>7</sup></li> </ul>
Fibrin	<ul style="list-style-type: none"> <li>- Binds well with biological surfaces and molecules<sup>5</sup></li> <li>- Increases cell proliferation<sup>5</sup></li> </ul>	<ul style="list-style-type: none"> <li>- Risk of disease transmission<sup>2</sup></li> </ul>
Keratin	<ul style="list-style-type: none"> <li>- Naturally abundant<sup>6</sup></li> <li>- Can be made into porous, fibrous structures<sup>6</sup></li> <li>- Supports cellular attachment and promote cell proliferation<sup>6</sup></li> </ul>	<ul style="list-style-type: none"> <li>- Limited research on its use with growth factors</li> </ul>

1 (Silva et al., 2020)

2 (Reddy et al., 2021)

3 (Pérez-Guzmán & Castro-Muñoz, 2020)

4 (Lin et al., 2012)

5 (Weisel & Litvinov, 2017)

6 (Rouse & Van Dyke, 2010)

7 (Cheung et al., 2015)

Collagen is a versatile natural material that can be harvested from various donor sites such as bovine dermis or porcine intestine (Glowacki & Mizuno, 2008). It can be processed to form meshes, hydrogels, threads, or sponges. In addition to this, collagen can be crosslinked in several ways to improve the material's mechanical properties and increase its degradation time (Silva et al., 2020). Collagen has been widely researched and used in tissue engineering applications already, so there is a large volume of research available. Due to these advantages, collagen was of interest for this project. In addition to this, an advisor to this project, Professor Pins, has experience working with and researching collagen extensively.

Like collagen, silk can also be produced in various forms such as knitted or braided fibers, films or gels (Silva et al., 2020). Silk is another material that could be incorporated into

the final design due to its favorable properties. Silk is a natural material that can be produced from silkworms. Fibroin and sericin are the two proteins present in silk. However, sericin has been linked to adverse immune response and thus is required to be removed from silk before being implanted. Silk is a relatively tough and elastic material, which are favorable properties for a ligament repair scaffold (Kasoju & Bora, 2012). Silk is significantly stronger than other natural materials and can take longer to degrade (Silva et al., 2020). Along with its favorable properties, there was ample information on its use and Professor Jeannine Coburn of WPI is experienced in using silk for a multitude of studies. For these reasons, silk was also a material that was be considered for the final scaffold design.

Zein is a readily available material that has been studied for use in drug delivery scaffolds. Zein is easy to obtain as it comes from maize, a plant that is easy to grow and harvest. There are four main types of zein, but  $\alpha$ -zein and  $\beta$ -zein are the most commonly used forms. The difference between them is that the molecular weight in  $\alpha$ -zein is typically greater than that of  $\beta$ -zein (Pérez-Guzmán & Castro-Muñoz, 2020). Zein has many desirable properties for drug delivering scaffolds such as anti-microbial properties and the ability to form microspheres for drug delivery (Demir et al., 2017). One limitation of zein is that it has poor mechanical properties that must be improved through crosslinking and combining it with other materials. Based on the advantages and limitations of zein it appeared to be a promising candidate for the scaffold and thus was further considered.

Chitosan is a polymer that can form hydrogen bonds with other molecules to improve cell adhesion to the scaffold. This also allows for the proliferation of cells. To increase the performance of chitosan, it is often combined with hyaluronic acid and alginate as they are anionic and can form polyionic complexes with chitosan, which improve the adhesion of the scaffold as well (Reddy et al., 2021; Silva et al., 2020). Chitosan has less research available compared to other materials, but the studies that do exist show promising work, thus we considered this material further.

Due to its role in wound healing, fibrin was considered. Fibrin is derived from fibrinogen and is a protein found in blood plasma. It plays a vital role in biological functions such as hemostasis, angiogenesis, inflammation, and wound healing (Weisel & Litvinov, 2017). Fibrin helps form collagen, fibronectin, and other components of the ECM by aiding in fibroblast and

macrophage migration. Fibrin can be used to signal cell behaviors post-injury (Brown & Barker, 2014). Fibrin’s major drawback is that it attracts many biological materials, even those that are infectious and dangerous to cells (Reddy et al., 2021). Due to this and recommendations from project advisors, fibrin was not considered further for the scaffold.

Keratin is an intermediate filament derived from hair and wool when used as a biomaterial. Keratin is very easy to obtain as hair and wool are abundant. Keratin can be produced as fibers, films, and sponges (Rouse & Van Dyke, 2010). Due to the naturally renewable source that keratin is derived from and promising mechanical properties, keratin was further considered.

Table 23: *Material for Drug Loading Pugh Analysis*

Evaluation Criteria	Weight	Baseline	Collagen Sponge	Silk Hydrogel	Zein Electro-spun Mats	Chitosan Sponge	Keratin Films
Has it been used with PDGF-BB?	3	0	1	1	-1	1	1
Controlled Release	4	0	1	1	0	1	0
4-6 week Degradation Duration	3	0	1	-1	-1	-1	1
Biological Response	5	0	1	0	1	0	1
<b>Constraints</b>							
Cost	5	0	-1	1	1	1	-1
Material Availability	3	0	1	1	0	-1	-1
Equipment Availability	5	0	1	1	0	0	-1
<b>Total</b>			<b>18</b>	<b>17</b>	<b>8</b>	<b>6</b>	<b>4</b>

From the Pugh analysis in Table 23, it is evident that collagen sponges and silk hydrogels would be the best material options for the delivery of PDGF-BB. Both materials have been previously used with PDGF-BB and have sustained a controlled release profile. In addition, the materials and equipment needed to make these modalities are readily available to us. Keratin films ranked the lowest due to the lack of equipment and material availability as well as the limited research present on its use with growth factors. Similarly, zein electrospun mats and chitosan sponges ranked in the middle. This was due to their promising properties to deliver growth factors, but limited equipment and material availability. Based on the results of this Pugh analysis, we chose to move forward with collagen sponges and silk hydrogels. Once we had determined the materials that we would be using, the delivery method of growth factors was

discussed. We researched various mechanisms of delivery like physical absorption, physical encapsulation, layer-by-layer (LbL), heparin binding, and chitosan binding. More details of each mechanism are described below. Table 26 in Section 4.4.3 below shows the degradation rates of each material of interest. A full literature review on values research can be found in a Table in Appendix F.

### **Surface Adsorption**

The physical immobilization of growth factors onto the surface of different materials has served as a simple modality for the delivery of growth factors. The growth factors are not strongly retained on the scaffold with this method resulting in the initial rapid release of proteins to its environment (Ziegler et al., 2008). Furthermore, the binding of biomolecules to the scaffold surfaces can be relatively weak. Growth factors are expensive, so losing them due to poor binding is not acceptable. Our scaffold design will require more advanced modalities to strengthen the immobilization of growth factors to produce a sustained release profile for the growth factor we choose to load. Due to this poor binding, surface adsorption was no longer considered.

### **Physical Encapsulation**

Physical encapsulation encloses the growth factors into 3D polymer matrices by simply mixing them within the polymers, while still retaining its bioactivity. The interaction between the growth factors and the material relies on hydrophobic, hydrophilic-hydrophilic, and electrostatic interactions (Enriquez-Ochoa et al., 2020). With this method alone, growth factors can sequentially disassociate from a scaffold, but the method is inefficient as only a small fraction of growth factors can be bound to the scaffold this way. In addition to this, unpredictable release of growth factors was observed, making it a challenge to use in designs that required the release of a therapeutic drug over a long period of time. The physical immobilization of growth factors onto the surface of different materials has served as a simple modality for the delivery of growth factors. The growth factors are not strongly retained on the scaffold resulting in the initial rapid release of proteins to its environment (Ziegler et al., 2008). Furthermore, the binding of biomolecules to the scaffold surfaces can be relatively weak. Though physical encapsulation may yield inconsistent results its simplicity could make the fabrication of this scaffold easy and

materials with high permeability can be used as a casing to furthermore encapsulate the growth factor within our device to allow for a sustained release of more than 2 weeks. It is for this reason that we will consider physical encapsulation as a viable method of delivering our chosen therapeutic agent.

### **Layer-by-layer (LbL)**

The layer-by-layer (LbL) self-assembly method proves to be an effective way to deliver a controlled release of growth factors that mimic the natural tissue regeneration process. In this process, multiple strata, bi-layered, or tetra layered coatings are used for the controlled delivery of growth factors. Electrostatic interactions between polyelectrolytes and growth factors are used to deposit polymer coatings onto surfaces (Wang et al., 2017). In a study, LbL films were constructed with tetralayer repeat films of poly (acrylic acid) and chondroitin sulfate and loaded with BMP-2 and VEGF. The scaffold exhibited a sustained release of over 2 weeks with no burst release. In addition, the amount of growth factor to be released can be controlled by adjusting the number of layers in the scaffold as suggested by a study (Kulkarni et al., 2014). LbL is a promising method we can use in conjunction with electrospun films to increase the growth factor retention rate and produce a scaffold with a sustained release over a two-week period.

### **Heparin Binding**

The ECM is a dynamic microenvironment that regulates multiple processes and acts as a reservoir for growth factors due to their ability to bind multiple molecules with high affinity, like heparin proteoglycans (Wang et al., 2017). Many growth factors such as BMP-2, BMP-7, VEGF, PDGF-BB and FGF-2 interact specifically with the heparin sulfate of the ECM. Several studies have found that by integrating heparin into electrospun or lyophilized scaffolds, an increased retention of growth factors as well as a slower release rate was observed. Such a study assessed the release rate of growth factor FGF-2 bound by heparin which resulted in 52% of the loaded growth factor releasing in the first 28 days (Zern et al., 2010). In another study, 90% of FGF-2, VEGF, BMP-2, and HGF were successfully encapsulated in a heparin nano sponge by photo crosslinking which demonstrated a sustained release of 60 days (Choi et al., 2017). Heparin proves to be a viable option for delivering the growth factor to the patient for several weeks as it retains the growth factor within the scaffold for long periods of time due to its ability to bind to multiple molecules with high affinity.

## **Chitosan Binding**

Polysaccharides such as chitosan are comprised of multiple monosaccharaides joined together by glycosidic linkages. With regards to the preparation of growth factor encapsulated NPs, polysaccharides have shown to be promising for their abundance, low toxicity, high stability, low cost, biocompatibility, and presence of various functional groups (Wang et al., 2017). In a study conducted by Rajam, he developed EGF-incorporated and FGF-incorporated chitosan copolymers with tripolyphosphate (TPP) NPs. The drug loading capacity and loading efficiency of these NPs was  $91 \pm 1.5\%$ . On day 35, the cumulative release of EGF and FGF from the delivery systems was approximately 83% and 84%, respectively, without an initial burst release (Rajam et al., 2011). This study shows that this release resembles our design goal of having our growth factor elude from our scaffold for a minimum of two weeks. However, in an additional study, hyaluronic acid-chitosan NPs were prepared for the delivery of growth factors, VEGF and PDGF-BB. The NPs retained 94% of VEGF and 54% for PDGF-BB. The elution studies showed that PDGF-BB was released over a one-week period, whereas VEGF was released within 1 day (Tan et al., 2011). This study shows that chitosan has poor solubility in physiological conditions due to its strong intermolecular hydrogen bonding and would not be suitable for our design under such conditions as the growth factor would not be retained within the scaffold for more than two weeks. Chitosan may prove to be successful in conjunction with polymers, but as we are producing a scaffold with natural materials, it shows that it would not be a sufficient delivery method for growth factors.

After investigating these numerous modalities for loading growth factors to achieve sustained release profiles for our scaffold it was concluded that material selection was prioritized. This influenced what growth factor loading technique were to be used for our device.

### **4.4.3. Mechanically Sound**

As described in Section 4.4.2, collagen, silk, zein, chitosan, and keratin were further considered as materials that would be best for the drug loading portion of our design as described by their advantages and limitations. In addition, we also researched dermal matrices and synthetic materials as these materials had more potential to provide desirable mechanical properties. Synthetic materials can be advantageous for ease of processing and altering of properties, making reproduction much easier and more accurate and precise. The limitations of

synthetic materials are that they may not completely degrade in the body, or they may produce acidic degradation products (Silva et al., 2020). The synthetic materials that were considered included poly(L-lactide) (PLLA), poly lactic-co-glycolic acid (PLGA), polycaprolactone (PCL), and polyethylene glycol (PEG). PLGA was critical to research as it was used in the previous UCL MQP’s design, but overall rendered the scaffold ineffective because of its high stiffness. To avoid a similar problem, the material properties, advantages, and limitations of PLGA needed to be understood. The benefits and limitations of each material considered are in Table 24 below.

Table 24: *Benefits and Limitations of Synthetic Materials and Dermal Matrices*

Material	Benefits	Limitations
PLLA	<ul style="list-style-type: none"> <li>- Can maintain its tensile strength for up to 8 months (25-30 N)</li> <li>- Slow degradation rate<sup>1</sup></li> <li>- Excellent biocompatibility<sup>1</sup></li> <li>- Used in ligament reconstruction surgeries</li> </ul>	<ul style="list-style-type: none"> <li>- Synthetic</li> <li>- Hydrophobic – not good for cell adhesion<sup>1</sup></li> <li>- Brittle<sup>2</sup></li> <li>- Acidic degradation products<sup>1</sup></li> </ul>
PLGA	<ul style="list-style-type: none"> <li>- Excellent cell adhesion and proliferation<sup>1,2</sup></li> <li>- Degradation time can be altered<sup>2</sup></li> </ul>	<ul style="list-style-type: none"> <li>- Synthetic</li> <li>- Confirmed to be too stiff by the client</li> </ul>
PCL	<ul style="list-style-type: none"> <li>- Promotes angiogenesis and cell proliferation<sup>2</sup></li> <li>- Degrades slowly<sup>2</sup></li> <li>- Desirable mechanical properties</li> </ul>	<ul style="list-style-type: none"> <li>- Synthetic</li> <li>- Poor bioactivity<sup>1</sup></li> <li>- Hydrophobic – bad for cell adhesion<sup>1</sup></li> </ul>
PEG	<ul style="list-style-type: none"> <li>- Good elasticity<sup>1</sup></li> <li>- Allows for adhesion of biological molecules<sup>1</sup></li> <li>- Mucoadhesive<sup>1</sup></li> <li>- Easily modifiable<sup>2</sup></li> </ul>	<ul style="list-style-type: none"> <li>- Bio-inert, so cell interaction is limited<sup>1</sup></li> <li>- Generates structures that are insoluble<sup>1</sup></li> </ul>
Acellular Dermal Matrix	<ul style="list-style-type: none"> <li>- High strength and failure load</li> <li>- Flexible</li> <li>- Currently used in ligament surgeries</li> <li>- Multiple possibilities for anchoring to ligament</li> </ul>	<ul style="list-style-type: none"> <li>- Slow degradation rate</li> </ul>

1 (Silva et al., 2020)

2 (Reddy et al., 2021)

To determine whether these materials met our design specifications, we researched the material properties of these materials in the modalities that we would use them: gels, films, sponges, and dermal matrices. Most commonly only the modulus and fracture strength were reported. To calculate stiffness from the reported modulus we used Equation A. To calculate the failure load from the reported fracture strength, we used Equation B. Where A is the cross-

sectional area of the scaffold design, L is the length of the scaffold design, E is the modulus, K is the stiffness, and  $\sigma$  is the failure strength.

As you can see, the greater the modulus and area and the smaller the length, the larger the stiffness. While on the other hand, the smaller the modulus and are and the greater the length, the greater the modulus. Similarly, for failure load, the larger the cross-sectional area of the scaffold the larger the failure load. Thus, because the modulus of materials can vary as well as the dimensions of the scaffold, the range between the maximum and minimum calculated values for the stiffness and failure load of each material are reported in Table 25 below. A detailed outline of material properties, like modulus and failure strength, found in literature can be found in Appendix G.

Table 25: *Material Property Ranges for the Materials being Further Investigated*

Material	Stiffness (N/mm)	Failure Load (N)
Collagen Sponge	0.00375 to 0.428	0.0375 to 6.14
Collagen Threads	38.3 to 1,120	200 to 2,410
Silk Hydrogel	0.0692 to 6,980	105 to 29,300
Zein Electrospun Mats	6.56 to 78.8	5.93 to 35.6
Chitosan Sponge	1.28 to 15.3	35.3 to 212
Keratin Films	188 to 2250	59.3 to 981
Acellular Dermal Matrix	2.31 to 185	52.8 to 831

From Table 25, you can see that acellular dermal matrix, zein mats, chitosan sponges, and silk hydrogels have stiffness values that fall in the range that we are trying to achieve (3 and 17 N/mm), collagen sponges, collagen threads, and keratin films do not meet this criterion. Collagen sponges and zein mats do not meet the failure load criterion, and silk hydrogels well exceed it. However, keratin films, chitosan sponges, collagen threads and acellular dermal matrix meet this. Silk hydrogels have good mechanical properties when they are crosslinked. Professor Coburn has expressed that we may experience issues with the drug not releasing from the gel if it is altered in this way, thus silk was no longer considered for the structural component of the device. This leaves chitosan sponges and acellular dermal matrix as the most promising materials for the structural support design of this design.

In addition to researching the Young's modulus and fracture strength, we investigated the degradation rate of the material as this was another essential aspect in choosing the scaffold's

material. Thus, we researched the materials being considered to understand their degradation *in vivo* or *in vitro*. A summary of the degradation rates can be found in Table 26 below.

Table 26: *Degradation Rate Ranges for the Materials being Further Investigated*

Material	Degradation Rate (weeks)	Sources
Collagen Sponge	1 to 4	(Noah et al., 2002; Ueda et al., 2002)
Collagen Thread	4 to 26	(Ge et al., 2006)
Silk Hydrogel	15	(Hopkins et al., 2013; Leng et al., 2017)
Zein Electrospun Mats	10 to 35	(Y. Wang et al., 2013; Yao et al., 2009)
Chitosan Sponge	0.25 to 4	(Han et al., 2014; Stinner et al., 2010)
Keratin Films	0.5 to 6	(Borrelli et al., 2015; Vasconcelos et al., 2008)
Dermal Matrices	-	

Silk hydrogels, zein electrospun mats, and collagen threads have longer degradation rates than desired. Collagen sponges and keratin films, depending on how they are processed, degrade up to 4 weeks and 6 weeks, respectively. No data was found on the degradation rate of dermal matrices. Finally, we put together a decision matrix, shown in Table 27, to determine what material would be best for any portion of our design that required mechanical support.

Table 27: *Support Material Pugh Analysis*

Evaluation Criteria	Weight	Baseline	Collagen Sponge	Collagen Threads	Silk Hydrogel	Zein Electrospun Mats	Keratin Films	AcellularDermal Matrix
Stiffness > 3 and < 17 N/mm	5	0	1	-1	0	1	1	1
Failure Load > 13 N	5	0	-1	0	0	0	0	1
4-6 week Degradation	3	0	1	-1	-1	-1	1	-1
Biological Response	5	0	1	1	0	1	0	1
<b>Constraints</b>								
Cost	5	0	-1	-1	1	1	1	0
Material Availability	3	0	1	1	1	0	-1	1
Equipment Availability	5	0	1	1	1	0	-1	1
<b>Total</b>			<b>1</b>	<b>0</b>	<b>10</b>	<b>12</b>	<b>5</b>	<b>20</b>

#### **4.4.4 Reproducibility**

The potential manufacturing methods and feasibility were important to consider so that we achieved reproducibility. To ensure reproducible production, the manufacturing methods that were considered included electrospinning, crosslinking, lyophilization, sonication of hydrogels, decellularization, purification of singular growth factor, and sterilization.

#### **Electrospinning**

Electrospinning was considered to produce films that could be layered for the scaffold design. Electrospinning is a process where a polymer solution is extruded from a syringe and subjected to a high-power supply. There are several elements to this process that can be modified to allow for reproducibility. These elements included the polymer concentration, solvent volatility, solution conductivity, applied voltage, and the gap between the syringe and collector (Deitzel et al., 2001). The surface area, morphology, mechanical performance, and length can be modified to best support cell seeding and proliferation (Cui et al., 2010). The technique is advantageous for tendon regeneration, and by extension, ligament regeneration, specifically because the fibers can mimic native structure. It can also be used to facilitate the inclusion of growth factors (Díaz-Gómez et al., 2014). It can be used to produce natural and synthetic fibers from materials such as collagen, silk, PLLA, PCL, PLGA and PLA, or composites of natural and synthetic materials (Silva et al., 2020). This method is advantageous because of long, continuous fibers with a controlled diameter. When these scaffolds are coated with growth factors, cell attachment, cell proliferation, and ECM deposition are enhanced (Silva et al., 2020).

Although this method seemed promising, there were several limitations. The fibers are typically produced in 2D mats, which limits 3D geometry. We were unable to fully consider this manufacturing technique because we did not have access to the equipment needed. An external manufacturing company that has the capabilities to electrospin for such applications as ours did not have the bandwidth and the service would have been beyond our financial limitations. Due to the capacity of the budget and timeline, this method was not utilized to develop prototypes or the final design.

#### **Crosslinking**

Another method to create a reproducible product capable of having precise and accurate mechanical properties, delivery capabilities, shelf life, and degradation was crosslinking. Crosslinking is a technique that can be used to alter the properties of a material, which makes it of use in scaffold design. For collagen fibers, glutaraldehyde, cyanamide, carbodiimide, and dehydrothermal crosslinking have been studied (Zeugolis et al., 2009). In collagen threads specifically, cross-linking has been shown to decrease the rate of fibroblast outgrowth on the surface of threads in some studies. This leads researchers to believe that biochemical signaling cues should be considered when aiming to increase the rate of cellular ingrowth or tissue regeneration (O'Brien et al., 2016). Gels, threads, sponges, and dermal matrices are all forms of materials that can undergo crosslinking. During the design process, we considered crosslinking as a manufacturing technique because it could reproducibly improve mechanical properties, load therapeutic agent, and decrease the rate of therapeutic agent release, however it was only deemed necessary to the fabrication of the final design because the collagen sponges used needed to be crosslinked to be sterilized. We were able to meet the other design specifications through other methods.

### **Lyophilization**

Lyophilization of porous scaffolds was another manufacturing technique used to create reproducible devices. Three-dimensional scaffolds are advantageous because they allow for cell communication, infiltration into the scaffold, and nutrient transport. Freeze-drying, also known as lyophilization, is a technique that assists with forming a 3D porous scaffold, or a sponge, for use in tendon regeneration (Li et al., 2020). One study looked at the fabrication of a 3D SF sponge that was reinforced with nonwoven silk. A nonwoven mat of silk was created and then distilled to create a transparent silk solution. Freeze drying occurred for 2 days and then the scaffold was crosslinked with ethanol. The porosity was tested using liquid displacement. Higher concentrations of SF were shown to enhance the mechanical properties of the scaffold, however tensile strength was too low to withstand implantation and suturing. This could be improved by embedding woven, knitted, or braided microfiber fabric. The walls of the SF sponge also had more adhesion sites for cell attachment and proliferation. Higher proliferation rates occurred in scaffolds with lower density and higher porosity (Li et al., 2020).

Lyophilization has been a method used in the WPI's Professor Pins Lab to make collagen sponge scaffolds. Due to the accessibility of the collagen material and the lyophilization protocol and equipment, we decided to utilize collagen scaffolds that had been manufactured in this way. However due to time constraints, we used premade collagen sponges rather than fabricating them during the time of the project.

### **Decellularization**

Decellularization was a manufacturing technique that was considered to produce a reproducible extracellular matrix. Acellular tissue was considered because of its ability to maintain native tissue properties along with its biocompatibility as a natural matrix. The process of decellularizing tissue removes the cells and growth factors in the tissue leaving behind the extracellular matrix (ECM) which contains collagen fibers and proteoglycans, allowing the matrix to maintain tensile strength. In addition to maintaining mechanical strength that is beneficial for the casing material, acellular dermal matrices have recellularization capabilities that help with cell migration onto the scaffold in vivo (Nikolova & Chavali, 2019). Generally, the protocols to decellularize a tissue include extracting the samples of tissue at the desired thickness and allowing the tissue to incubate in a decellularized solution made from chemicals such as acids, bases, and surfactants to lyse through cells (Gilpin & Yang, 2017). This type of tissue was advantageous to strengthen the design and assist cell migration as a casing material. Specifically, we were able to acquire an ADM for the casing of our silk hydrogel-infused collagen sponge. The purpose of the casing was to decrease the elution rate of the growth factors from the scaffold to the UCL to avoid an initial burst release and control the release of growth factors.

### **Sonication**

The process of sonication is used in biomedical applications to create hydrogels. Hydrogels can be used as drug delivery systems and have been widely used in medicine. They are biocompatible and easily encapsulate hydrophilic drugs. The stiffness of these gels can range from 0.5 kPa to 5 MPa and can be manipulated to best suit the desired application (Li & Mooney, 2016). Collagen-platelet rich plasma (PRP) hydrogels have been shown to significantly improve the load at yield, maximum load, and linear stiffness of the ACL (Murray et al., 2007). In another study, a fiber-reinforced hydrogel (FRH) was shown to have a similar structure to

native tendon, which has similarities to ligament structure. Ultra-high molecular weight polypropylene (UHMWPE) fibers were impregnated with biosynthetic polyvinyl alcohol/gelatin hydrogel (FRH-PG) or polyvinyl alcohol/gelatin (FRH-PGS). The tensile strength of these was like that of a human Achilles' tendon (No et al., 2020). Silk fibroin hydrogels have also been shown to promote wound healing, and release FGF-1 over an extended period (He et al., 2019). Based on prior success and their properties, hydrogels were further explored for their drug encapsulating potential. Since the gels can be pre-designed to meet a specific need, they were appealing to achieve a reproducible design. Specifically, we decided to utilize sonication to produce hydrogels made of silk because the silk material and basic fabrication protocol structure were provided by the lab of WPI professor Jeanine Coburn.

### **Attainment of Isolated Growth Factor**

As previously discussed, isolated growth factors were chosen as therapeutic agents. Based on their role in wound healing in ligaments, the human growth factors PDGF-BB and FGF-2 were chosen as the most important to our final design. Since the reproducibility and cost of our device were prioritized, we were only able to purchase one of these growth factors, so we chose PDGF-BB. Platelets are a natural and abundant source of growth factors in the body. The  $\alpha$ -granules within platelets contain growth factors (Rao et al., 2019). Human PDGF-BB was purchased from ProSpec, a company which offers sterile filtered lyophilized PDGF-BB powder for purchase that has been purified by proprietary chromatographic techniques.

In addition to these various materials manufacturing techniques, sterilization techniques were used to ensure that our design is reproducible. These included protocols that will be further discussed to sterilize the PDGF-BB loaded silk hydrogel, collagen sponges, and ADM.

### **4.4.5 Surgically Compatible**

To achieve surgical compatibility, we considered different sizes of the scaffold in addition to methods to anchor the scaffold to the ulnar collateral ligament.

#### **Scaffold Size**

As previously detailed, the size specification for the scaffold design needed to be that which allowed it to be implantable in 10 cm incision window and within the dimensions of 15

mm x 40 mm x 3mm. The scope of this project's timeline and budget only allowed us to make half size scaffolds.

## **Fibrin Glue**

Fibrin glue is a type of surgical adhesive that has been used for many years. Tisseel, a commercial fibrin glue, has been on the market for more than 25 years and has been used in over 9.5 million surgical procedures (Valbonesi, 2006). Fibrin glues are commonly used to enhance surgical hemostasis and ensure effective tissue adhesion (Fibrin Glue - an Overview | ScienceDirect Topics, n.d.). Fibrin glues are the only materials that are approved by the Food and Drug Administration for adhesive and sealant applications. Fibrin glue degrades within 10-14 days within the body. We hoped to use fibrin glue as a fixation method to secure our scaffold to the UCL due to its many benefits in wound healing and ability to effectively fix a scaffold to a ligament and as a method to adhere the casing material to itself. However due to financial constraints, we chose to prioritize material purchases other than fibrin glue that ensured better therapeutic agent delivery and cell proliferation effects.

## **Sutures**

Another means that our device could be fixed to the ligament anatomy is through sutures. There have been several iterations in the evolution of suture repair methods for tendons and ligaments. In comparison to fibrin glue, sutures have a much longer degradation period as they last longer in the body. It is important to note that early mobilization is pertinent to obtaining good functionality of the sutures. If the sutures are not adequate, then the risk of rupturing increases. Thus, high repair strength to overcome early mobilization and avoid rupture (Rawson et al., 2013). During the design process, we were concerned that suturing may damage the scaffold when securing it to the ligament and degrading over time. Since we had limited financial and time resources, the fixation method of suturing was not further considered, and other scaffold functions were prioritized. However, if this method is to be chosen for a future project, it would be imperative to select material that will be strong enough to endure the stresses yielded by the motion of the arm.

## Netting

Another alternative fixation method, netting, was discussed during the design process. This alternative was discussed with hopes to mitigate scaffold damage that could occur with suturing. The netting would overlay on top of the scaffold and the ends of the netting would be sutured to the native ligament as shown in Figure 16. It is important to note that this method of fixation is not current with standard and practiced suturing methods and would be a unique fixation method. For this reason and because we had limited financial and time resources, the fixation method of netting was not further considered.

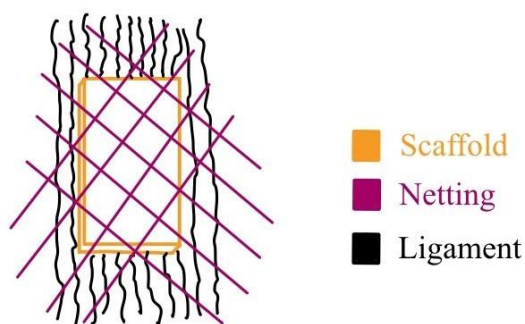


Figure 16. *Netting Method for Fixation.*

## 4.5 Alternative Designs

Based on the modeling research that was done, and the feasibility of the conceptual designs, the layer-by-layer filaments design and the encased porous scaffold design were chosen for further consideration and modeling. The encased sponge was highly considered as the silk hydrogel and collagen sponges proved to be the most viable option for drug delivery according to literature and ADM proved to be an ideal casing material for the design as well. This decision was made using Pugh analyses for each of the design considerations mentioned in Section 4.4. These Pugh Analyses were created considering the prioritized primary objectives, secondary objectives, and specifications and constructed using extensive literature research discussed in Section 4.4.

### 4.5.1 Layer-by-Layer Filaments

After consideration of many unique design configurations and elements, the layer-by-layer filament method, shown in Figure 17, appeared to be one of the most promising. This was for several reasons, including the ability to elute a therapeutic agent, favorable mechanical properties, biocompatibility, and surgical compatibility.

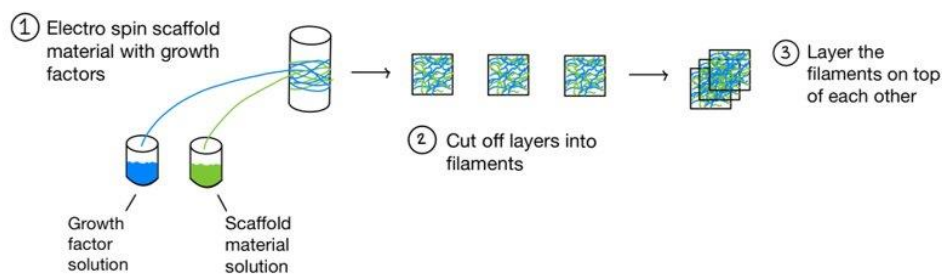


Figure 17. *Drawing of the Layer-by-Layer Filament Design.*

This design fulfills the objectives and functions of our final design. Growth factors can be incorporated into the solutions that are used to process and manufacture electrospun fibers, which are the main component of this design. The electrospun fibers would then be layered on top of each other. The growth factors we considered for this design are FGF-2 and PDGF-BB. The surface area of this design is one of the highest, meaning it has the greatest binding area for growth factors, and thus has a high drug loading capacity. As the outer layers of the scaffold degrade, interior layers would be exposed to the injury site which would ensure a continuous delivery of growth factors over the desired two-week time period. Electrospinning is currently in use by many companies and is accessible. BioSurfaces, Inc. (Ashland, MA) is an example of a company that has experience spinning the materials we are considering, which include zein and collagen. The electrospinning process is reproducible as it ensures accurate and precise reproduction of the scaffold. The mechanical properties from literature of these materials are also in the specified range that we are looking at for our scaffold. These properties also depend on the dimensions of the scaffold, which can be controlled by adding or removing layers. The films' mechanical properties could also be altered using crosslinking. This scaffold would be straightforward to implant if fibrin glue or sutures were used, as surgeons have ample experience with both fixation methods (Magit, 2021).

After speaking with Biosurfaces, Inc., who would help us manufacture this design, they expressed that collagen would not fit within our budget and that it would need to be completed with zein. They sent us a sample of electrospun zein for us to test for the correct mechanical properties. It was discovered that this material would not exhibit the properties needed for the scaffold device and thus this design was not considered further.

#### 4.5.2 Encased Porous Scaffold

The second design we considered further was the encased porous scaffold, shown in Figure 18. Some of the main benefits of this design are the ability to load a large capacity of therapeutic agents, and favorable mechanical properties. A sponge loaded with growth factors would be created. Then a hydrogel loaded with additional growth factors would be injected into the sponge. Once these were combined, this silk hydrogel loaded collagen sponge would be completely encased in ADM.

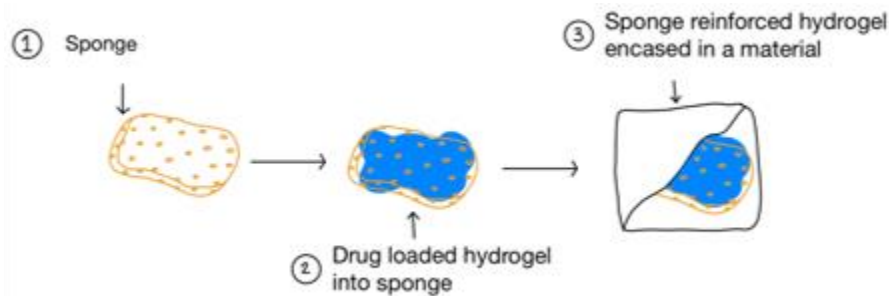


Figure 18. *Drawing of the Encased Porous Scaffold Design.*

This design allows for one of the largest amounts of growth factors to be incorporated, both within the sponge itself and encapsulated within the hydrogel. Hydrogels specifically can contain a large volume of growth factors and release them over extended periods of time (F. Wang et al., 2020). This is key for ligament healing, as the therapeutic agent would be delivered to the injury site throughout the duration of the wound healing process. The sponge reinforced hydrogel would then be encased in ADM to further slow the drug release profile. The diffusion rate of the material could be tested and adjusted if necessary to reach a diffusion rate that would assist drug elution over a two-week period. The surgeon could attach the scaffold to the ligament using fibrin glue or suturing techniques, as with the first design. Having many different components to this design would make reproducibility and manufacturing more challenging from

a financial perspective, but if the design proved to be beneficial for wound healing, this may be justified.

#### **4.6 Mathematical Modeling**

Mathematical models can help to predict the nature in which biologic systems operate. As such, conceptual scaffold designs can be mathematically modeled to better understand diffusion of a solute through a membrane and release of a drug from a scaffold. Specifically, mathematical equations are derived to show functional relationships between experimental parameters. By predefining known parameters and developing models with iterative values for unknown constants, a series of theoretical models can be made to determine the diffusion coefficient of a substance through a membrane or the mass fraction of a drug eluding from a scaffold with respect to time. By developing these models, we will be able to determine a range of ideal curves that will best model the elution and diffusion of our scaffold in relation to our design goals. Each model will be based on our goal of having a sustained release of our growth factor for four weeks. Of the curves generated, we will assess which curves exhibit the most ideal sustained release.

To model the diffusion of a solute through a membrane we will be using a mathematical model derived from Fick's law which relates to a two-chamber diffusion system like that of an Ussing chamber (Charalel et al., 2012). This model is described by both equation C and equation D. This model will be used as its parameters directly relate to our testing conditions for diffusivity of our growth factor through the ADM. These include  $N$ , the total solute mass in the system,  $V$ , the total volume in the system,  $h$ , the thickness of the membrane,  $A$ , the cross-sectional area of the membrane exposed to solute,  $V_1$ , the volume in chamber 1,  $V_2$  the volume in chamber 2,  $C_2$ , the concentration of growth factor eluded through the membrane, and  $D$ , the diffusion coefficient of the system measured in  $\text{cm}^2/\text{day}$ . We determined the diffusion coefficient of BSA in DPBS (-) across ADM in  $\text{cm}^2/\text{second}$  from the measured concentrations using Equations A and B where  $N$  is the total solute mass in system (6.8 mg),  $V$  is the total volume (6.8 mL),  $C$  is the protein concentration in the acceptor chamber at a given time in  $\text{mg/mL}$ ,  $h$  is thickness of the barrier (0.40 mm),  $t$  is time in days,  $A$  is surface area of the barrier ( $0.709 \text{ cm}^2$ ), and  $\tau$  is the scaling factor (Charalel et al., 2012).

$$C_i = -\left(\frac{N}{V}\right) e^{\left(\frac{D_i}{86400}\right)\left(\frac{t}{\tau}\right)} - 1 \quad (C)$$

$$\tau = \frac{\left(V_1 + \frac{Ah}{2}\right)\left(V_2 + \frac{Ah}{2}\right)}{AV} \quad (D)$$

A series of predictive curves (Figure 19) were generated by iterating the mathematical model with iterating realistic diffusion coefficient values using MATLAB. The MATLAB code that went into generating these curves can be found in Appendix H. The diffusion coefficient values were iterated from 0.002 cm<sup>2</sup>/day to 0.014 cm<sup>2</sup>/day. A graph plotting mass ratio of eluded BSA to total BSA loaded was constructed based on the iterating diffusion profiles as you can see in Figure 19. From the graph we can determine a range of curves that will represent an ideal sustained release of our growth factor that will elude over 4 weeks and will maximize the amount of growth factor eluded from our scaffold. We have determined our ideal diffusion profiles to have a diffusion coefficient range values of 0.006 cm<sup>2</sup>/day to 0.008 cm<sup>2</sup>/day. This range is indicated by the dashed black curves. Once we receive experimental data, we can fit the data to this model and see if it corresponds to our ideal diffusion coefficient range of values.

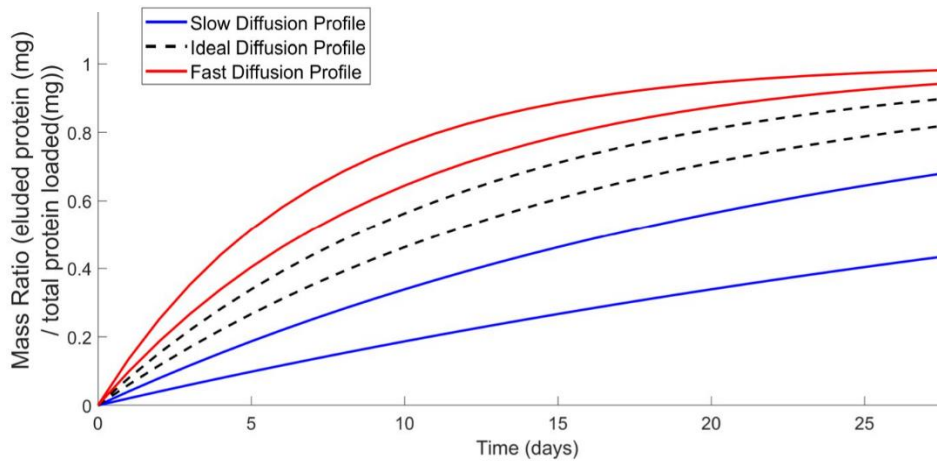


Figure 19. *Diffusion Mathematical Model of Protein through Acellular Dermal Matrix.*

## **5.0 Verification of Final Design**

This section outlines the fabrication of the design components and the test system to evaluate the components of the implantable scaffold design to characterize the safety and efficacy. This includes PDGF-BB concentration testing, BSA diffusivity testing, and tensile testing to the sponge and casing. The protocols that are outlined have been developed to ensure the design components meet the defined design specifications. The sample sizes were adjusted depending on the number of scaffold devices that are able to be created considering budget and time limitations.

### **5.1 Fabrication of Designs**

The following section details the fabrication for each component of the final design and the molds we used to make it, most notably including the PDMS mold, silk hydrogel, collagen sponges, and ADM. Our sterilization protocols are also discussed. The Bill of Materials for the project can be found in Appendix I.

#### **5.1.1 PETG Inverse Mold**

We used SolidWorks to design a part, shown in Figure 20 below, that was needed to make the PDMS molds. We then 3D printed the part using polyethylene terephthalate glycol (PETG). We selected PETG because it can withstand temperatures of 70°C without deforming. We then smoothed any ridges on the mold using sandpaper to ensure a smooth topography for the gel scaffolds and make it easier to remove the scaffolds from the molds.

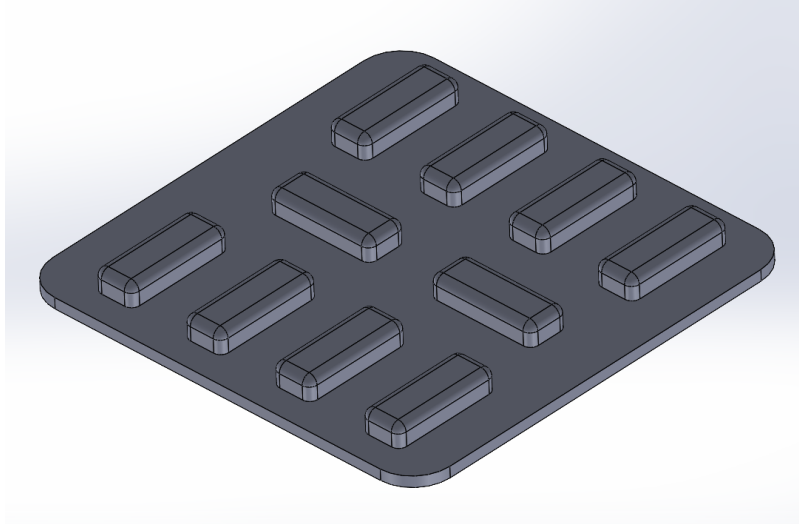


Figure 20. *Image of Inverse PETG Mold used to Make PDMS Mold*

### **5.1.2 PDMS Mold**

We used PDMS (Elastomer 182) to create the molds for the scaffolds used for initial and final testing. We chose it for its ease of access and its flexibility as a material. To make the PDMS molds, we mixed 10 parts of the PDMS Base with 1 part of the curing agent. We then degassed this mixture in a vacuum for about 30 minutes. Every five minutes, we released the pressure, so that the bubbles on the surface dissipated. After the PDMS alone had been degassed, we poured the mixture into a square 10 mm culture plate that contained the inverse mold. We taped the PETG mold to the bottom of the plate using double-sided scotch tape to prevent air bubbles and ensure it did not rise throughout the curing process. We again degassed this plate in the vacuum for 15-30 minutes until no bubbles were seen. Finally, we placed it into the oven at 70°C for up to 3 hours. The mold was periodically checked to determine when it was fully cured and then removed from the plate.

### **5.1.3 Silk Hydrogels Preparation**

We fabricated silk hydrogels by sonicating 5 % wt. silk aqueous solution for 60 seconds to form a silk pre-gel solution. We then would add either BSA or PDGF-BB to the pre-gel solution and add it into the PDMS molds to fabricate either silk hydrogel scaffolds or collagen sponge reinforced hydrogel scaffolds. The protocol for the fabrication of these hydrogels can be found in Appendix J.

#### **5.1.4 Collagen Sponges**

Collagen sponges were provided to us by the lab of the advisor, Professor Pins. The glycosaminoglycan (GAG) collagen was fabricated from self-assembled type I collagen (CI) molecules. Collagen membranes were fabricated by mixing the collagen solution with salt solutions and then placed in a laminar flow hood for controlled drying (Bush & Pins, 2010). The collagen sponges were then ultraviolet (UV) crosslinked for 30 minutes to ensure that they didn't dissolve in solution during the sterilization process.

#### **5.1.5 Acellular Dermal Matrix Casing**

The process of decellularizing tissue removes the cells and growth factors in the tissue leaving behind the extracellular matrix (ECM) which contains collagen fibers and proteoglycans, allowing the matrix to maintain tensile strength. Generally, the protocols to decellularize a tissue include extracting the samples of tissue at the desired thickness and allowing the tissue to incubate in a decellularized solution made from chemicals such as acids, bases, and surfactants to lyse through cells (Gilpin & Yang, 2017). This type of tissue was advantageous to strengthen the design and assist cell migration as a casing material. Specifically, we were able to acquire acellular dermal matrix for the casing of our silk hydrogel-infused collagen sponge.

#### **5.1.6 Sterilization of Scaffold**

To meet design constraints and ensure that our design is sterilizable, we implemented protocols to sterilize the components that comprise our final scaffold which include the PDGF-BB loaded silk hydrogel, collagen sponges, and ADM. We conducted all fabrication of the final scaffold in a biosafety cabinet (BSC) to prevent contamination. We sterilized all tools, machinery, and materials utilized in the fabrication of our final design through autoclaving or thoroughly wiping materials down with 70 % Ethanol before being placed inside the BSC. All sterilization protocols for the PDGF-BB loaded silk hydrogel, collagen sponges, ADM, machinery, and tools can be found in Appendix K.

### **5.2 Design Verification**

Before we conducted final testing, we ran some initial tests to gain more information about the design components and to confirm protocols before we completed the final design. The methods and results of these experiments are discussed in the following section.

### 5.2.1 Effect of Various PDGF-BB Concentrations on Cell Proliferation

To determine the best concentration of PDGF-BB to use for the scaffold, different concentrations were considered and tested. These included 0, 0.167, 0.416, 0.677 and 1.0  $\mu\text{g}/\text{mL}$ . The range was based on literature values and the content of PDGF-BB in 10 mL of PRP. Each concentration was seeded in 1 mL of culture media with 30,000 NIH 3T3 mouse fibroblast cells in triplicate. Each well in the 12-well plate was imaged on days three and five and cells were counted using a hemocytometer to determine the increase in cell proliferation due to PDGF-BB. The full protocol is shown in Appendix L. Some representative images taken with Zeiss Primovert Inverted Microscope and Zen Software are shown below in Figure 21.

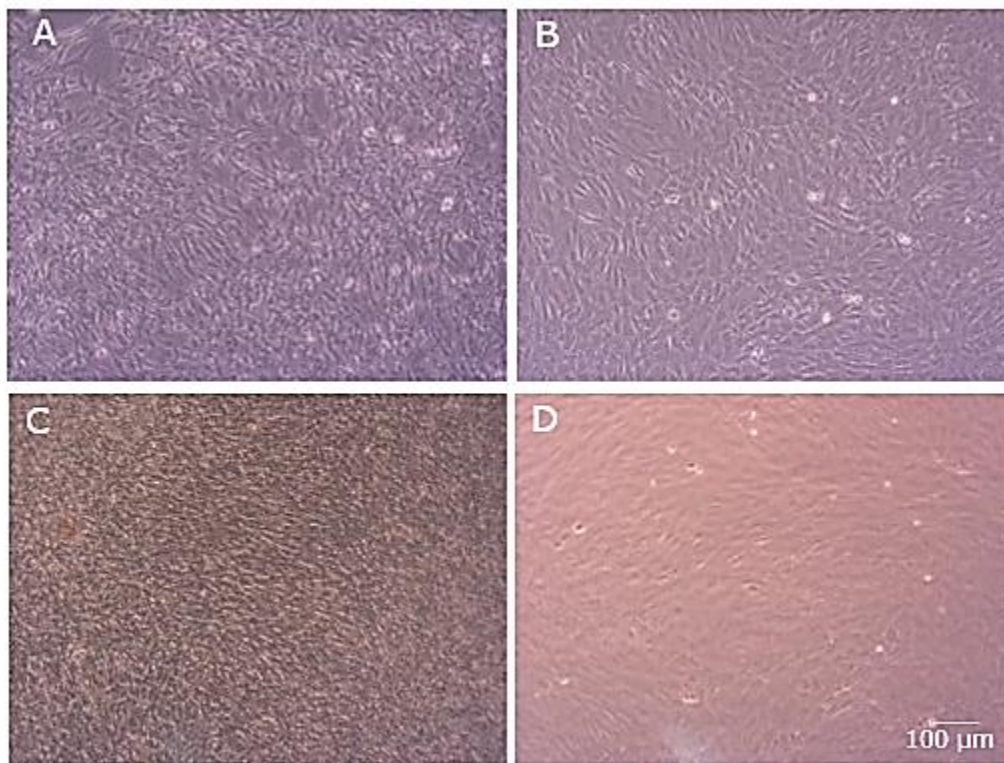


Figure 21. Images of NIH 3T3 cells A) After 3 days in culture with 1.0  $\mu\text{g}/\text{mL}$  PDGF-BB. B) After 3 days in culture with 0.0  $\mu\text{g}/\text{mL}$  PDGF-BB. C) After 5 days in culture with 1.0  $\mu\text{g}/\text{mL}$  PDGF-BB. D) After 5 days in culture with 0.0  $\mu\text{g}/\text{mL}$  PDGF-BB.

Table 28: Final Cell Count Averages and Percent Increase Compared to Controls.

Concentration ( $\mu\text{g}/\text{mL}$ )	0.167	0.417	0.667	1	0
Day 3 Average (N=3)	394,167	473,333	573,333	678,333	310,000
% Compared to Day 0	127%	153%	185%	219%	100%

Day 5 Average (N=3)	1,885,000	2,188,333	2,460,833	2,740,000	701,875
% Compared to Day 0	269%	312%	351%	390%	100%

Table 28 shows the average cell count for each concentration on days three and five. The testing showed that the highest concentration of PDGF-BB, 1.0  $\mu\text{g/mL}$ , resulted in the highest rate of proliferation. A single factor ANOVA test was used to prove statistical significance, and individual post-hoc comparisons are shown by \* in Figure 22 where the p value was 0.005 after a Bonferroni correction and n=3. The main effect was shown as there was a significant effect between each concentration of growth factor on days three ( $p < 0.05$ ) and five ( $p < 0.05$ ). Based on these conclusions, we chose the concentration of growth factor in the final design to be 1.0  $\mu\text{g/mL}$ .

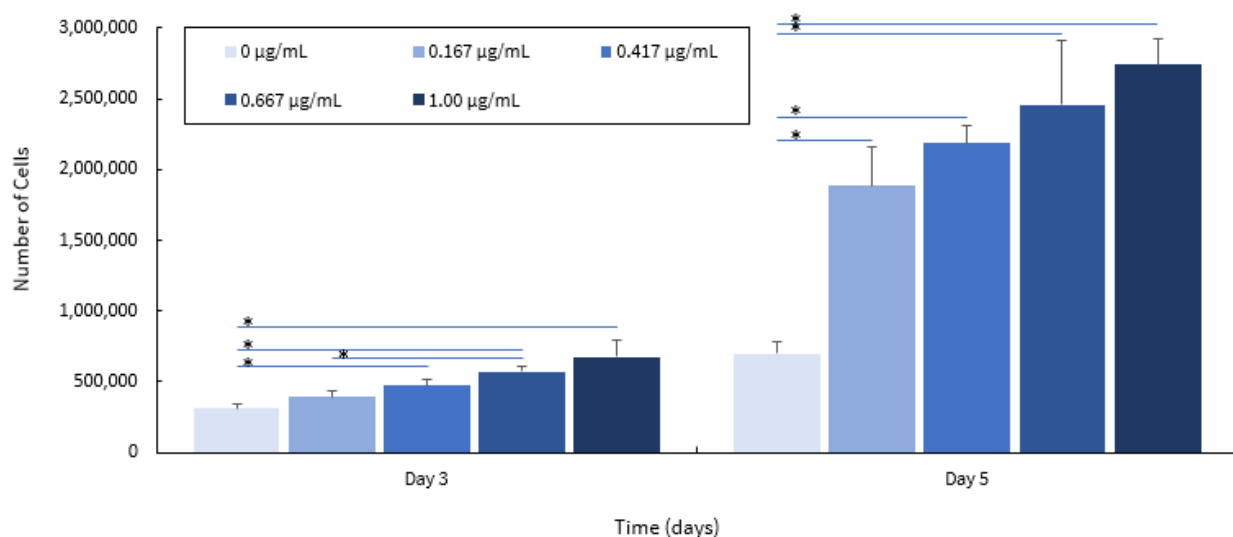


Figure 22. Cell Count versus Time in Culture of Different Concentrations of PDGF-BB in Culture

This test is somewhat limited because cells were counted manually, averaged, and multiplied by the total volume to find the total count. The cells were also 100 % confluent on day five, and based on this confluency, the number of cells seeded for the final experiment decreased to 20,000 cells.

### 5.2.2 BSA Diffusivity through Acellular Dermal Matrix Casing

We calculated the diffusion coefficient of BSA through diffusivity testing of the ADM casing to model its diffusion to understand if the casing would help extend the release profile of PDGF-BB. We utilized an Ussing Chamber shown in Figure 23 to test the mass transfer of 2

mg/mL BSA in DPBS (-) from one enclosed chamber through ADM to an acceptor chamber of DPBS (-) without BSA.

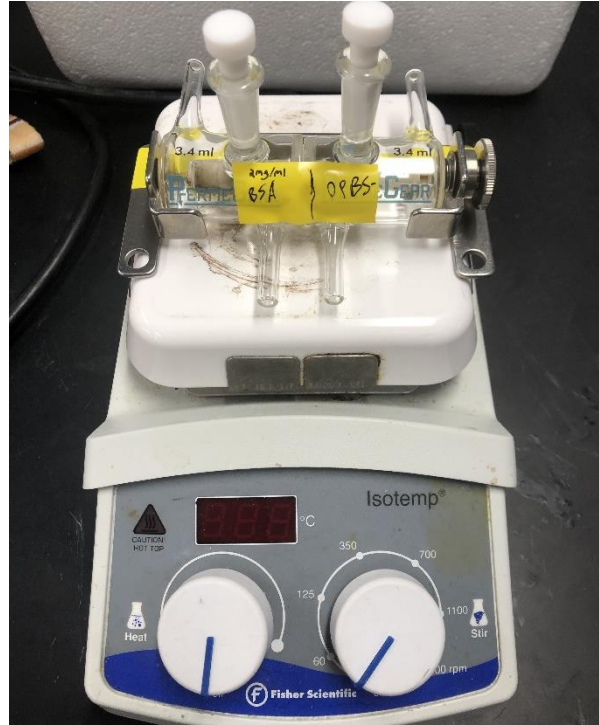


Figure 23. Casing Diffusion System including Ussing Chamber and Magnetic Shaker Plate.

Every 24 hours for 7 days, we collected 100  $\mu\text{L}$  samples from the acceptor chamber and measured protein concentration with a BCA Assay. We determined the diffusion coefficient of BSA in DPBS (-) across the ADM in  $\text{cm}^2/\text{second}$  from the measured concentrations using Equations E and F where  $N$  is the total solute mass in system (6.8 mg),  $V$  is the total volume,  $C_2$  is the protein concentration in the acceptor chamber at a given time in  $\text{mg/mL}$ ,  $h$  is thickness of the barrier (0.40 mm),  $t$  is time in days,  $A$  is surface area of the barrier ( $0.709 \text{ cm}^2$ ), and  $\tau$  is the scaling factor (Charalel et al., 2012).

$$D = -\ln\left(1 - \left(\frac{C_2(t)}{\frac{N}{V}}\right)\right) \cdot h \cdot \frac{\tau}{t} \quad (\text{E})$$

$$\tau = \frac{(V_1 + \frac{Ah}{2})(V_2 + \frac{Ah}{2})}{AV} \quad (\text{F})$$

We determined the diffusion coefficient of BSA through the ADM to be  $9.07 \pm 7.38 \text{ cm}^2/\text{s} \times 10^{-8}$  ( $n=7$ ). The BSA concentrations in the acceptor chamber on days 0, 1, 2, 3, 4, 5, 6, 7

were 0.00 mg/mL, 0.00 mg/mL, 0.0385 mg/mL, 0.0498 mg/mL, 0.0966 mg/mL, 0.150 mg/mL, 0.182 mg/mL, 0.190 mg/mL respectively. By Day 7, 8.28% of the BSA had diffused through the ADM, supporting the hypothesis that the ADM casing would slow down the release of PDGF-BB to the injury site. The release of BSA through the ADM is shown in Figure 24. Since the concentration of the acceptor chamber was determined experimentally, we assumed no loss in mass besides sample collection to calculate the concentration of the donor concentration at each time point. It is important to note that the effects of ADM on the readings from the BCA were not accounted for. The BCA would have been able to read the dissociated collagen from the ADM, however for this experiment, this was considered negligible. Using the linear fit of the concentration, was determined that the system would reach equilibrium after 37.5 days.

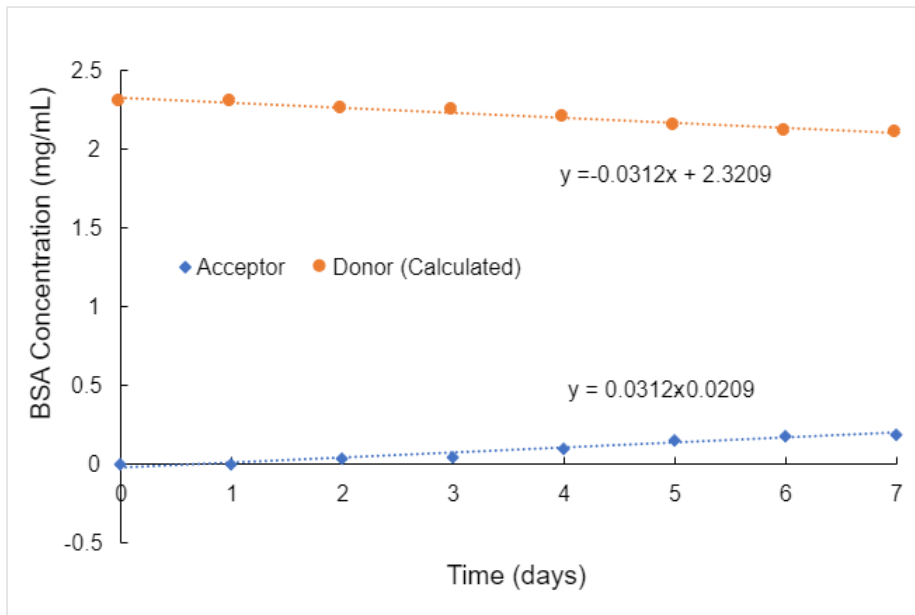


Figure 24. Graph of BSA Diffusion through Acellular Dermal Matrix Over Seven Days.

By using a diffusion mathematical model, we can overlay our experimental BSA diffusion through our bovine dermis data onto it as shown in Figure 25. From the predictive model we determined that our ideal curves would allow for the longest sustained release while also eluding the most BSA proteins. The diffusion coefficient that was yielded from our experimental BSA data was  $7.84 \times 10^{-3} \text{ cm}^2/\text{day}$  and is represented by the pink dotted line in Figure 25. As you can see from fitting our experimental data to our mathematical model for diffusion our BSA data falls between our ideal curves and ideal diffusion coefficient range of  $0.006$  to  $0.008 \text{ cm}^2/\text{day}$ . This validates our decision to utilize the ADM as it is a material that

exhibits a sustained release for up to four weeks while also maximizing the amount of BSA that is eluted through the casing in that time.

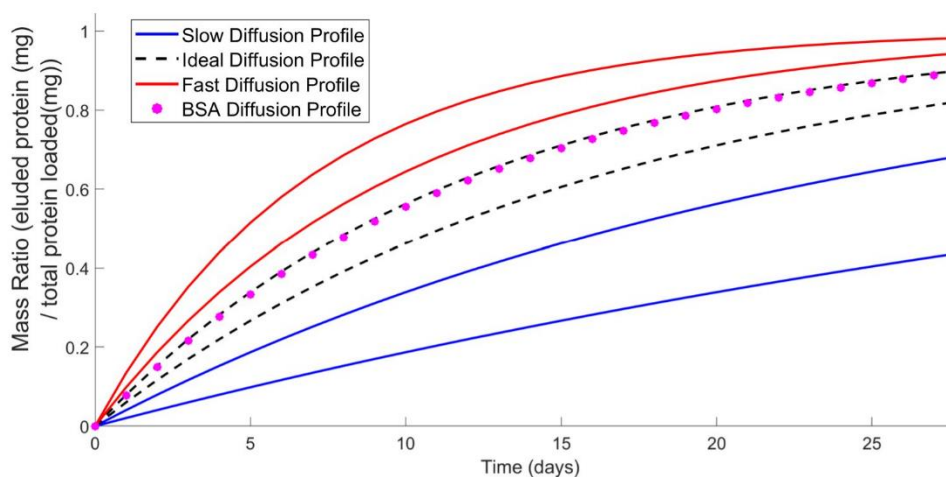


Figure 25. Diffusion of BSA through Acellular Dermal Matrix Fitted to Diffusion Mathematical Model.

### 5.2.3 Uniaxial Tensile Testing of Acellular Dermal Matrix

The purpose of the mechanical tensile testing is to characterize the scaffold's ability to meet the specifications that it must have a stiffness between 3 and 17 N/mm and failure load greater than 13 N to ensure the device can withstand surgical manipulation. These properties will be evaluated using an Instron test method and procedure outlined in Appendix M. As dermis is an anisotropic material, 5 samples of the first direction (D1), and 5 samples of the second direction (D2) were tested as shown in Figure 26.

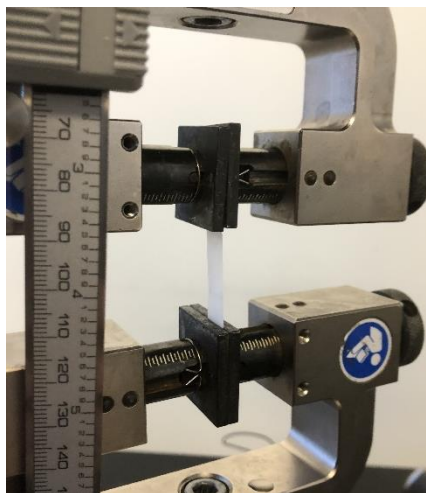


Figure 26. ADM in Instron before Tensile Testing

The modulus will be identified by finding the slope of the stress strain data from the Bluehill software based on the initial cross-sectional area of the scaffold and the tensile strength will be the maximum tensile load. Due to limited resources, only one sheet of hydrated acellular dermal matrix was tensile tested even though in the final design, two sheets will be fixed together to create a pocket. Due to this, we will assume that the stiffness and failure load will be scaled up by magnitude of two. A two tailed unpaired t-test will be performed to evaluate whether the results fall within the specification range. The stress strain curves for all ten samples are found in Figure 27.

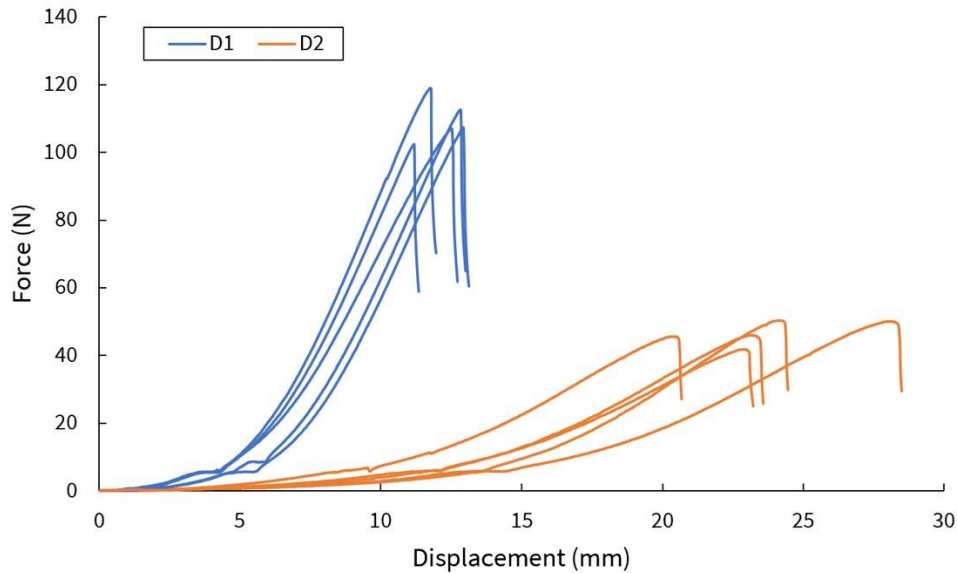


Figure 27. Stress vs Strain Curve for Acellular Dermal Matrix

Table 29: Values Obtained from Dermal Matrix Testing

Data Measured	Direction 1	Direction 2
Length (mm)	18.81 ± 2.7	17.81 ± 1.7
Width (mm)	8.02 ± 0.8	8.34 ± 0.5
Thickness (mm)	0.31 ± 0.1	0.29 ± 0.03
Failure Load (N)	109.91 ± 6.24	45.05 ± 5.83
Stiffness (N/mm)	18.33 ± 1.35	4.59 ± 0.63

The results of our dermal matrix testing can be seen in Table 29. From these results we can conclude that the mechanical properties of the machine direction are a magnitude greater in all aspects but both directions still uphold our scaffolds mechanical specifications.



## 6.0 Final Design and Validation

This chapter outlines the validation testing that was done on the design components, as well as the method used to create the design. Initial and final drug elution testing was conducted, along with cell proliferation and diffusivity testing. This chapter also includes feedback from the client when presented with the final design.

### 6.1 Final Design

To create the final design, we made polydimethylsiloxane (PDMS) molds. We sonicated silk fibroin solution at 5 wt% in 1.5 mL batches for 90 seconds. Then, we added 1.00  $\mu\text{g/mL}$  of PDGF-BB to the silk pre-gel solution. Using a positive displacement pipet, we injected 150  $\mu\text{L}$  of pre-gel into the PDMS mold, placed a collagen sponge on top, and then injected another 150  $\mu\text{L}$  of pre-gel solution into the mold. We placed the collagen sponge reinforced hydrogels into a vacuum chamber for 20 minutes to release air bubbles. The scaffolds sat at 20  $^{\circ}\text{C}$  in a dark box for 48 hours to gel. The dimensions of the final hydrogel were 20 mm x 7.5 mm x 2 mm and the dimensions of the dermis were 24 mm x 10 mm x 0.4 mm. Figure 28 shows the final design components.

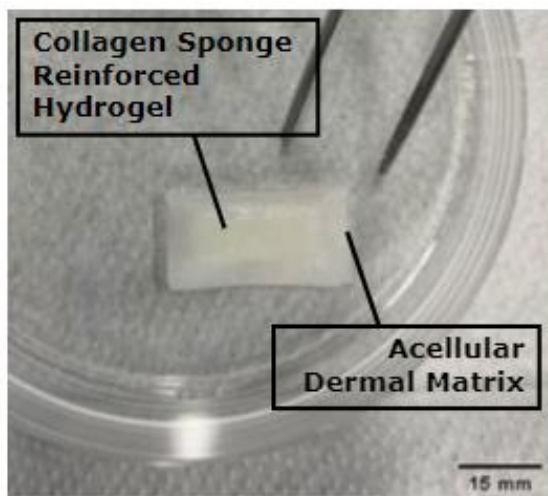


Figure 28. *An Image of the Final Design Components*

### 6.2 Design Validation

Following the design process and design iterations and testing previously described and detailed in the Gantt Charts in Appendix D, a final design was created and tested.

### 6.2.1 Initial BSA Drug Elution on Various Scaffold Designs

The purpose of the drug elution testing is to characterize the release profile of growth factor from the design to ensure that enough therapeutic agent is loaded and released from the device to meet our specifications and objectives. The implant needs to release 300 ng of PDGF-BB over a period of at least 2 weeks. Seventy percent of growth factors should be retained in the scaffold after the first five days. The initial drug elution modeling will be completed with a model protein, bovine serum albumin (BSA). We loaded 260  $\mu\text{g}$  of BSA into two different scaffold conditions: silk hydrogels (SA), collagen sponge reinforced hydrogels (SAC). We then conducted a BCA Assay to analyze our preliminary trials as it is an inexpensive way to measure albumin concentrations. Because the assay measures various amino groups and is not protein specific, the BCA assay will read protein concentrations from the collagen sponges. By measuring the collagen sponge on its own, we could attempt to account for how much albumin alone is eluted from the collagen sponge reinforced hydrogel.

Next, we suspended five scaffolds of each condition in 1 mL of DPBS (-), and supernatant samples of 1 mL were taken at 0, 1, 2, 3, 4, 7, 10 and 14 days from suspension. The protocol for this testing is outlined in Appendix N. Figure 29 shows the amount of BSA released at each time point for each test condition. Because the BCA assay could read the collagen protein, the amount of protein released from C was subtracted from the SAC scaffold (represented in yellow). From this data, the general trends show that SAC scaffolds sustained a

more controlled release than the SA scaffolds, which had a large burst release. This indicates that collagen is advantageous in lengthening the release period of albumin.

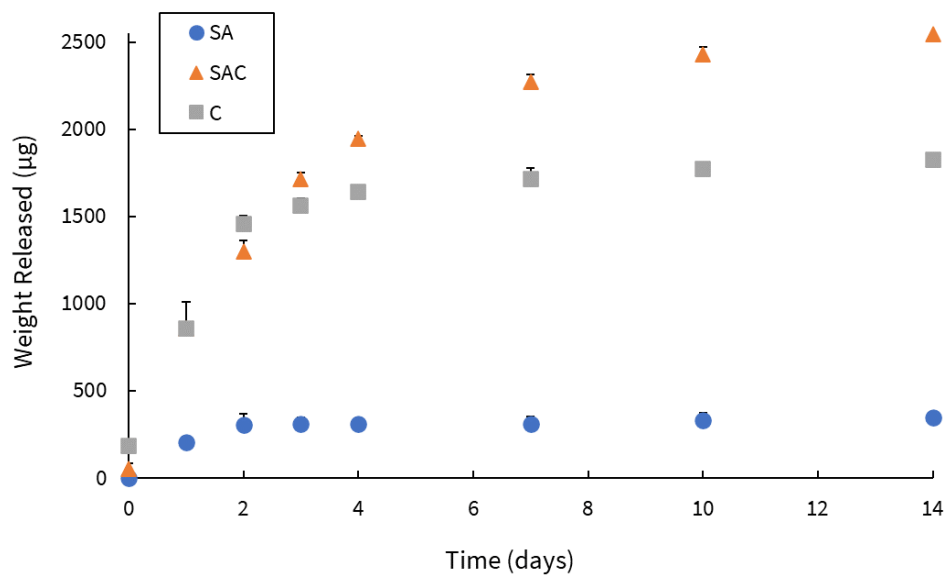


Figure 29. Graph of the Raw Cumulative Release Data of BSA from the Three Tested Conditions

As explained before, the release from the collagen sponge by itself needed to be subtracted from the collagen sponge reinforced hydrogel in order to get just the release of BSA

and not the release of collagen and BSA. Figure 30 below shows the cumulative release of BSA from these two scaffolds: silk hydrogels and collagen sponge reinforced hydrogels.

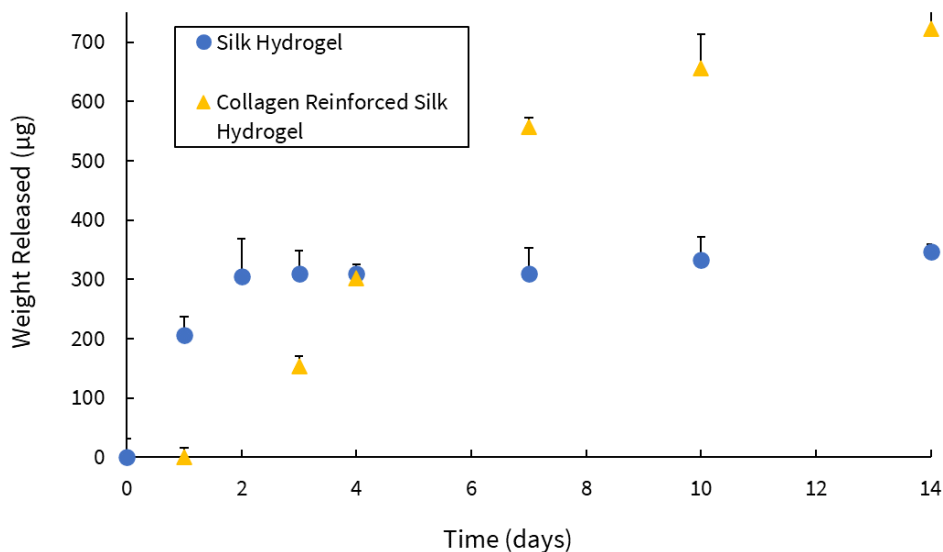


Figure 30. Graph of the Cumulative Release of BSA from the Silk Hydrogel Design and the Calculated Sponge Reinforced Hydrogel

From this study, we determined that the sponge reinforced hydrogel showed a more sustained release of BSA, as the silk hydrogel's BSA release plateaued after day two.

### 6.2.2 PDGF-BB Elution Testing

From the initial drug elution testing completed with BSA, we determined the final design to be a collagen sponge reinforced silk hydrogel loaded with PDGF-BB and encased in acellular dermis to slow the rate of release. We also determined the concentration of growth factor that would be used from the cell proliferation testing results presented in Section 5.2.1. We were unable to perform drug elution testing with the casing due to budget constraints constricting our ability to construct a viable sealing for the casing, so the sponge reinforced hydrogel was used for final drug elution testing, using the protocol shown in Appendix N. Again, we suspended five sponge reinforced silk hydrogel scaffolds loaded with PDGF-BB in 1 mL of DPBS (-), and as much supernatant was removed as possible on each sampling day before being replaced by fresh DPBS (-). For this testing, we used a Human PDGF-BB ELISA Kit to determine the concentrations of PDGF-BB eluted from five representative scaffolds.

We assumed that there were equal concentrations of PDGF-BB in each scaffold as well as that each supernatant sample was a homologous solution. Figure 31 below shows the cumulative percent of drug released over a ten-day period.

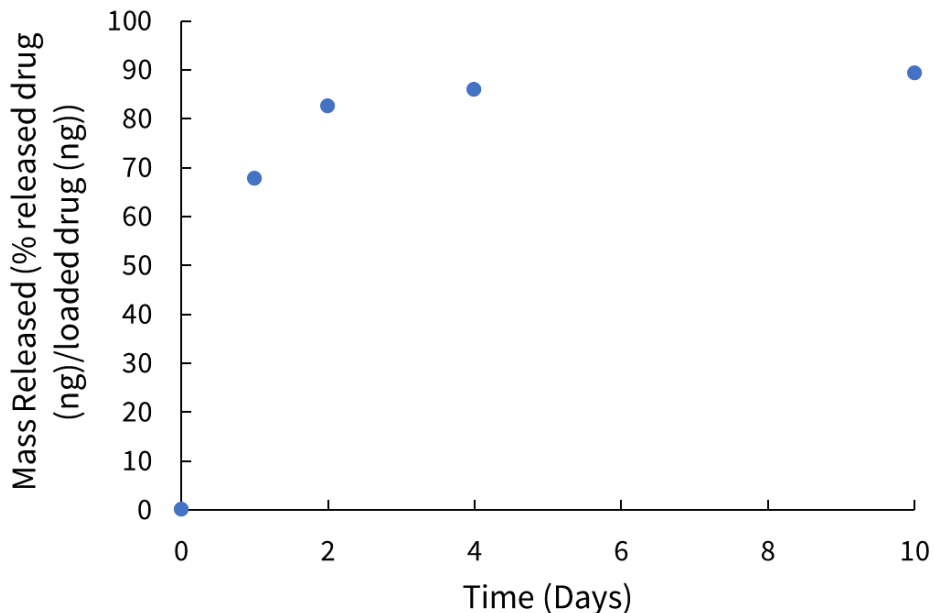


Figure 31. *Graph of the Cumulative Release of PDGF-BB from the Collagen Sponge Reinforced Silk Hydrogel*

The sponge reinforced hydrogel released most of the PDGF-BB in the first two days, with nearly 90% of PDGF-BB released from the sponge reinforced silk hydrogel by day 10.

### 6.2.3 Effect of Eluted PDGF-BB on Cell Proliferation

The purpose of our cell proliferation testing was to characterize the final design's eluted growth factor's efficacy in increasing cell proliferation, which would indicate favorable outcomes for cell migration and angiogenesis once the scaffold is implanted in the body. We used Passage 11 CRL 2097 human fibroblastic cells cultured in 10% FBS culture media, as noted in Appendix L. After we completed the concentration testing, the concentration of PDGF-BB to be used in the scaffold was determined to be 1.0  $\mu\text{g}/\text{mL}$  (Section 5.2.1). To assess the effect of the loaded PDGF-BB on cell proliferation, 100 $\mu\text{L}$  of supernatant from the final drug elution protocol (Section 5.3.2) was placed onto 20,000 cells in each well of a 24-well plate in order to assess the effectiveness of the amount of eluted growth factor on cell proliferation after it has passed through the collagen reinforced silk hydrogel and dermal matrix. Four different scaffolds

from drug elution days 1, 2, 3, 4, 7 and 10 were analyzed on days 3 and 5 after the supernatant was added to the wells. The protocol is outlined in Appendix L.

The test assumes an even concentration of cells throughout the entire sample. It also assumes that the conditions between each experimental setup are kept constant. The volume of eluted supernatant solution being added to the culture plate is negligible. It is assumed that if cells are showing increased proliferation, the PDGF-BB would also facilitate angiogenesis and other important functions in the healing process when the device is implanted in vivo, although further testing is needed. The concentration of PDGF-BB in 10% Fetal Bovine Serum (FBS) (used for media) is negligible.

We analyzed the cells using a BrdU Cell Proliferation Assay, which we trialed before use in the final test to ensure accuracy. Images were taken of each well without UV, with a DAPI filter, and with a FITC filter for each scaffold that was analyzed for each drug elution time point. Representative images are shown in Figure 32.

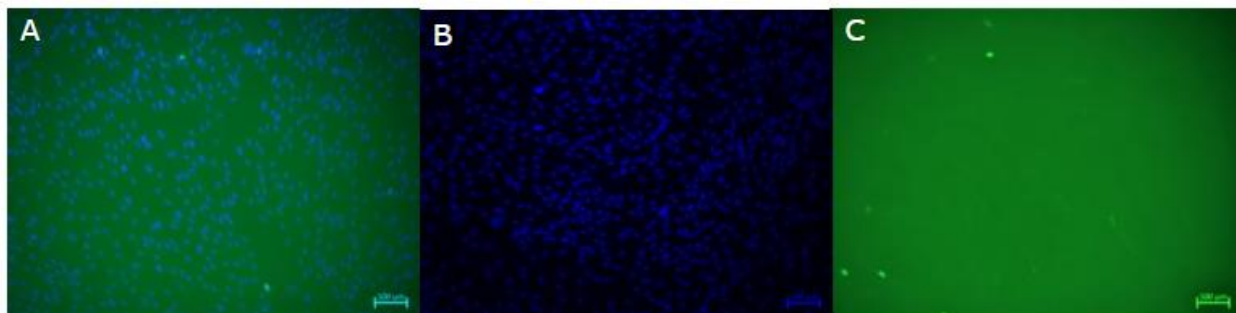


Figure 32. *Representative Images from BrdU Assay five days after adding supernatant. A) Combined image of DAPI and BrdU positive cells. B) Image of DAPI positive cells. C) Image of BrdU positive cells.*

From these images, ImageJ was used to count each individual cell and from there, find the percentage of DAPI to BrdU positive cells. The percentages are shown below in Figure 33.

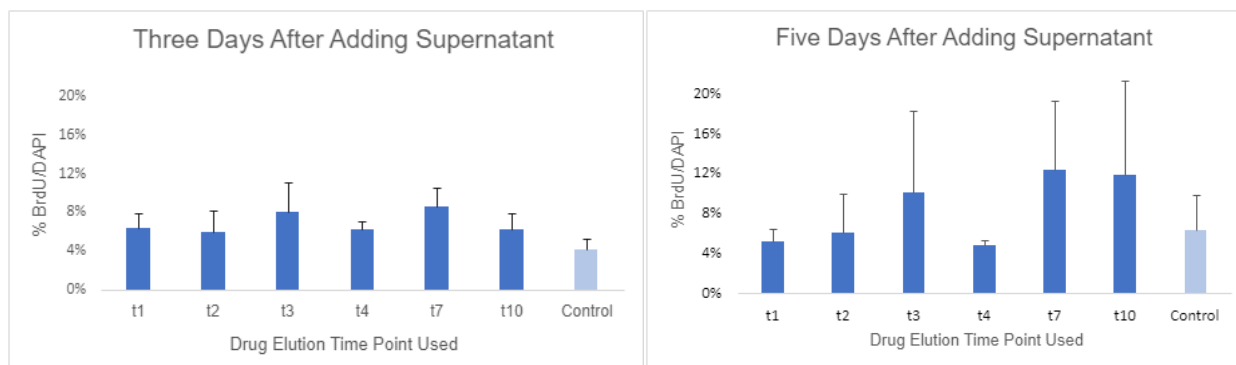


Figure 33. *BrdU/DAPI Positive Cells After Three and Five Days with Supernatant. Error bars represent standard deviation between the four scaffolds for each time point*

### 6.2.4 PDGF-BB Diffusion through Acellular Dermal Matrix Casing

The purpose of the diffusivity testing of the casing was to characterize the ability for PDGF-BB within the hydrogel to permeate out to the surrounding environment to understand if the casing would help extend the release profile of PDGF-BB. The protocol can be found in Appendix M. We utilized an Ussing Chamber with the scaffold including the PDGF-BB loaded collagen sponge reinforced silk hydrogel and acellular dermal matrix casing all sandwiched between chambers containing DPBS (-), as shown in Figure 34. Every 24 hours for 10 days, we collected 100  $\mu$ L samples from both chambers and measured protein concentration with a Human PDGF-BB ELISA Assay. The assumptions of this protocol are uniform properties of the acellular dermal matrix and uniform growth factor concentrations.

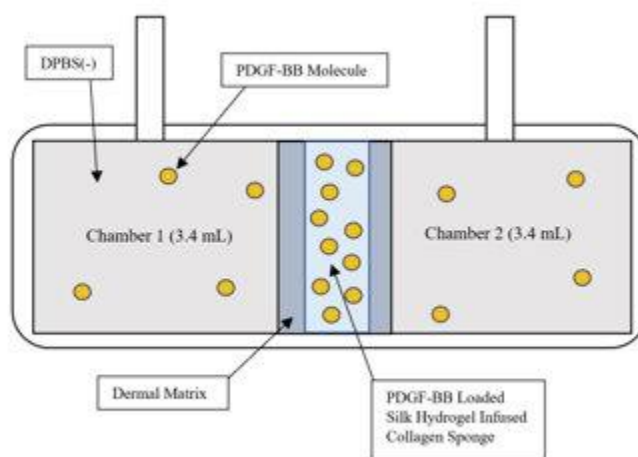


Figure 34: *Casing Diffusion System including Ussing Chamber and Magnetic Shaker Plate.*

We determined the diffusion coefficient of PDGF-BB out of the scaffold through the acellular dermal matrix to be  $9.14 \times 10^{-8} \pm 1.1 \times 10^{-7} \text{ cm}^2/\text{s}$ . By Day 12, 18.3% of the PDGF-BB had diffused through the ADM, indicating that the dermal matrix is an appropriate material to reduce burst release of PDGF-BB and elongate the elution period.

By using a diffusion mathematical model, we can overlay our experimental PDGF-BB diffusion through our ADM data onto it as shown in Figure 25. From the predictive model we determined that our ideal curves would allow for the longest sustained release while also eluding the most PDGF-BB proteins. The diffusion coefficient that was yielded from our experimental PDGF-BB data was  $7.90 \times 10^{-3} \text{ cm}^2/\text{day}$  and is represented by the pink dotted line in Figure 35. As you can see from fitting our experimental data to our mathematical model for diffusion our PDGF-BB diffusion profile falls between our ideal curves and ideal diffusion coefficient range of 0.006 to 0.008  $\text{cm}^2/\text{day}$ . This validates our decision to utilize the ADM as it is a material that exhibits a sustained release for up to four weeks while also maximizing the amount of PDGF-BB that is eluted through the casing.

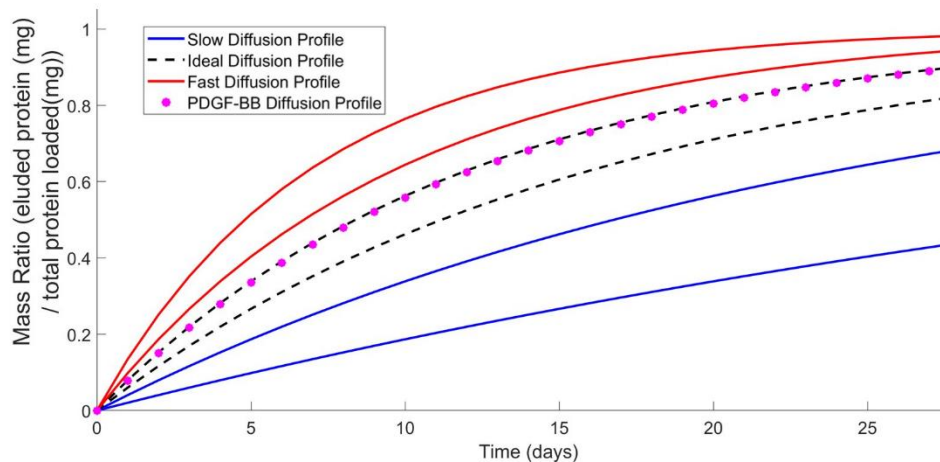


Figure 35. Diffusion of PDGF-BB through Acellular Dermal Matrix Fitted to Diffusion Mathematical Model.

### 6.3 Client Feedback

We presented the final product to the client and user, Dr. Magit, for feedback and validation. To present the full capabilities we fabricated several sizes for our client to hold and look at both with and without dermal matrix casing, although the adhesive used to encase the dermal matrix around the scaffold device did not cure in time for this evaluation. The sizes were

7.5 mm by 20 mm by 2mm, 10 mm by 30 mm by 2mm, and 15 mm by 40 mm by 2 mm.

According to Dr. Magit, the largest size would be covering the whole ligament while the smallest would be best to use because it would work in the small spaces. The repairable tears are usually the ones at the proximal and distal insertion ends of the ligament which have small spaces to work with. These types of tears, such as when the ligament pulls off the ulna are often very painful and typically heal poorly.

Some next steps that Dr. Magit emphasized were to do a suture pull out test to evaluate the dermal matrix's ability to stay intact when sutured to the ligament. Dr. Magit would suggest a suture net type fixation method such as a suture bridge or a figure of eight suture method to keep the device secured to the healing ligament. Dr. Magit also expressed concerns about fibrogenesis which could result in scar tissue from the isolated growth factor or scaffold device in contact with tissue. To address this, further evaluation would need to be made and Dr. Magit emphasizes the importance of animal testing in vivo as a next step. Dr. Magit also asked about so asked about the usability and logistics of using the device and assembling it in the operating room. A user manual would need to be created in future work on this project. We discussed options to create a kit containing the inner collagen sponge reinforced silk hydrogel, adhesive, and dermal matrix which could be hydrated and assembled in the operating room. Overall, Dr. Magit's feedback was very positive and confident in the strides this project made for this device.

## **7.0 Discussion**

In this chapter we will discuss the meaning of our testing results and compare them to literature. We will also discuss the impact of our design on the world around us, including topics such as economics, environment, society, politics, ethics, safety, manufacturability, and sustainability.

### **7.1 Drug Elution Studies**

To assess the drug release profile of PDGF-BB from our scaffold design, we completed various testing. Initially, we modeled the release profile with BSA to determine whether a silk hydrogel loaded protein or sponge reinforced silk hydrogel loaded with protein would allow for a more desirable release profile. After we selected a design from these tests, we completed the drug elution testing with the final scaffold design and loaded it with the proper amount of PDGF-BB.

#### **7.1.1 Initial BSA Drug Elution on Various Scaffold Designs**

Our team initially tested the drug elution from two scaffold designs: a silk hydrogel and a collagen sponge reinforced hydrogel. These hydrogels we loaded with a model protein known as bovine albumin serum (BSA). From this study, we determined that the sponge reinforced hydrogel showed a more sustained release of BSA where it starts to plateau at day 10, while the silk hydrogel's BSA release plateaued after day 2. Although there are no studies that test collagen sponges reinforced albumin loaded silk hydrogels; the components have been tested individually. One study showed silk hydrogels released albumin for about 3 days, with a small continual release till day 10, similar to what we found (Yan et al., 2017). Another study showed the release of human albumin serum from collagen sponges where about 95% of albumin was released in 1 day (Maeda et al., 1999). Again, showing a quick burst release that we observed in our study.

We did have some trouble measuring the percentage of PDGF-BB released from the sponge reinforced hydrogel as we subtracted the amount of collagen by itself from the collagen sponge reinforced hydrogel loaded with BSA. We realized at the end of the project; we should have instead tested unloaded collagen sponge reinforced silk hydrogel as the control to subtract from the loaded scaffold. As the rate of collagen releasing from the collagen sponge alone differs

from when it is combined with the silk hydrogel. We would recommend this control for future testing. In addition, despite the fact that silk does not contain any amino acids that can be read by the BCA assay we would still suggest testing it for completeness.

### **7.1.2 Final PDGF-BB Drug Elution from Collagen Sponge Reinforced Hydrogels**

Our final drug elution testing showed that about 90% of PDGF-BB was released in a 10-day period, with an 80% burst release in the first two days. As we predicted, this was quicker than our design specification of at least a two-week release period. This testing verified the need for the acellular dermal matrix to help further control the release of PDGF-BB over the desired period.

Although there are no studies that test collagen sponges reinforced PDGF-BB loaded silk hydrogels, the components have been tested individually. One study showed various silk-chitosan hydrogels releasing PDGF-BB for about 3 days, similar to what we found (Min et al., 2022) Another study using silk-chitosan hydrogels for PDGF-BB delivery found that by day 10 most of the growth factor had been released from the system (Wu et al., 2016). This may be longer than what we found, due to the fact that it was combined with chitosan while ours was not. In addition, their silk was combined with PEG2000, which may have also increased the binding ability of PDGF-B. For the release from a collagen sponge, we compared the values we found to an article that used collagen sponges to deliver recombinant bone morphogenetic protein 9 (rhBMP9), another growth factor. They found that rhBMP9 released from the collagen sponge for up to 10 days, again yielding similar results to our study (Fujioka-Kobayashi et al., 2017).

We did have some trouble with running the ELISA assay, as we needed to dilute our sample to ensure they were in a readable range. We loaded 300 ng into each scaffold and the upper limit of the ELISA assay for PDGF-BB is 2 ng. Because we were not entirely sure how much PDGF-BB would be released at each time point we were not sure how much to dilute by. Many of our samples read below the blank buffer, thus suggesting we diluted our samples by too much. We still have all of our samples stored, and hope that they can be run again in the future.

## **7.2 Cell Studies**

Our initial healing promotion objective was to augment and support the regeneration of the ligament to stimulate cell proliferation, migration, and synthesis of fibroblasts, restore the aligned matrix deposition, form granulation tissue, and stimulate angiogenesis. This is mainly related to the healing promotion objective. Due to our budget and time constraints, measuring matrix deposition, granulation tissue formation, and angiogenesis was not possible. We chose to focus on cell proliferation of fibroblasts to draw conclusions about the potential of the device to assist in UCL healing. The initial and final testing are described below.

### **7.2.1 Effect of Various PDGF-BB Concentrations on Cell Proliferation**

Based on literature values, we chose to test concentrations of PDGF-BB that were in the range of 200-1200 ng/mL (Thomopoulos et al., 2010; Wei et al., 2006). We were able to measure cell proliferation through the synthesis of fibroblasts, and from this data, we can make conclusions about the potential of the design to stimulate the formation of granulation tissue and angiogenesis. Through our analysis, we found that the highest PDGF-BB concentration, 1.0  $\mu\text{g/mL}$ , yielded the highest cell count. We chose to use this concentration for our scaffold as a result since we believed it would be the best concentration to promote healing and achieve our objective.

The limitations for this test are the budget and materials used. This test should be replicated with human CRL 2097 fibroblast cells, which were used for final testing, rather than the mouse cells that were used for this testing. It also would have been better to analyze the results of this study using the BrdU Proliferation Assay rather than counting cells. Trypan blue also should have been used when counting cells in order to assess their viability. The cell counting technique that was used has room for human error.

### **7.2.2 Effect of Eluted PDGF-BB on Cell Proliferation**

Based on literature mentioned in the previous section and our initial testing, we decided to add 150  $\mu\text{L}$  of eluted supernatant to our design. We believed that since the concentration in the scaffold was 1.0  $\mu\text{g/mL}$ , there would be statistically significant increase in cell proliferation in the presence of the eluent. In periodontal ligaments, 10 ng/mL of PDGF-BB was used and was proven to act as a strong mitogenic agent (Marcopoulou et al., 2003). If 50% of PDGF-BB had

eluted on day one (150 ng), the concentration of growth factor in culture would be 150 ng/mL. This means that the limitation in our study was likely due to an inadequate transfer of PDGF-BB into the culture. There was a higher % of BrdU positive cells after five days in culture than after three days in culture, but it was not statistically significant. Further testing is required to fully assess the healing promotion of our design.

This test was conducted with passage 11 CRL 2097 human fibroblast cells. There is an aging affect associated with cells with higher passage numbers. It would also be helpful to test other cell types that are relevant in the healing process such as cytokines, neutrophils, and macrophages to assess the healing process further, as well as ligament cells themselves. This test was also conducted in a biosafety cabinet with materials that are used by many other individuals outside of us, which adds variability.

In hindsight, we should have used more of the eluent or we should have planned the testing timeline better so that we could measure the concentration of PDGF-BB that was eluding from the scaffold, and then we could have created culture media with the same concentration of PDGF-BB. We unfortunately did not have time to do any re-testing due to time constraints.

### **7.3 Diffusion Studies**

To assess the viability of a ADM to encase the scaffold design to help control drug release, the diffusion of growth factor was modeled using an Ussing chamber system and BSA. The resulting diffusion coefficient was comparable to that found in literature and suggested that the ADM would help reduce burst release. We determined the diffusion coefficient of BSA through the ADM to be  $9.07 \pm 7.38 \text{ cm}^2/\text{s} \times 10^{-8}$  (n=7). This value is comparable to one study that found that the diffusion coefficient of BSA across a human cornea membrane to be  $3.1 \pm 1.0 \times 10^{-8} \text{ cm}^2/\text{s}$  (Charalel et al., 2012). Thus, the ADM would aid in the ligament healing by helping to elongate the release of the PDGF-BB.

Next, we conducted a diffusion study using an Ussing chamber in which a layer of ADM, then PGDF-BB loaded collagen sponge reinforced silk hydrogel then another layer of ADM, were sandwiched between two chambers of DPBS (-). Similarly, to the study with BSA, the diffusion coefficient was determined, and we concluded that the ADM was an appropriate material to reduce burst release and elongate drug elution from the scaffold. The limitation to

these findings is that there are several other factors that have been omitted that contributing to the diffusivity of PDGF-BB across a membrane in the body such as vascular flow, temperature and pressure, and cell binding and chemical pathways that may also affect concentration gradients associated with diffusion.

## **7.4 Tensile Testing Study**

We were able to successfully measure the failure load and stiffness of our proposed scaffold design by tensile testing the anisotropic ADM that would serve as the casing in two directions. In our analysis we found that the average failure load and stiffness of the ADM in one direction was  $109.91 \pm 6.24$  N and  $18.33 \pm 1.35$  N/mm, respectively and in the other direction it was  $45.05 \pm 5.83$  N and  $4.59 \pm 0.63$  N/mm, respectively. These values align with our mechanical design constraints that stated that our design was to have a failure greater than 13 N and a stiffness between 3 and 17 N/mm. This means that our scaffold would be mechanically sound and would not be compromised due to surgical manipulation during implantation.

The limitations of this test include that we were only able to acquire a certain range thickness for the ADM of 0.4 mm to 0.7 mm. If we were able to acquire a thickness range of 0.1 mm to 0.15 mm, we would have been able to tensile test two sheets of ADM which would most resemble our final scaffold design.

## **7.5 Impact Analysis**

To understand the impact of our design it is important to consider potential changes and implications in several areas. These areas include economics, environmental impacts, societal impacts, political ramifications, ethical concerns, health and safety, annotatability and sustainability.

### **7.5.1 Economics**

By providing an alternative procedure for developing athletes, an economic decision can be made to choose a less invasive and intrusive surgery such as Tommy John surgery. The restoration of a player's native UCL has positive economic effects as it allows the individual to continue to strengthen their elbow ligaments promoting the longevity of the UCL and reducing the risks of complications down the road into older age in which they may require costly surgeries and rehabilitation. The cost of a UCL reconstruction would be like the cost of the

implantation of the reparative device. Even though a reconstruction is more intensive and requires the extraction of autograft from the patient which lend it to be a costly procedure amounting from \$5,000 to upwards of \$26,000, the growth factors that are required for the reparative device are also very costly (*How Much Does Tommy John Surgery Cost?*, n.d.). However, since the implantable reparative device would return the baseball player back to playing in less time the amount of rehabilitation required is reduced and so is the cost of said rehabilitation. Since this device has the potential to be expanded to other ligament and tendon repair surgeries such as rotator cuff repairs, a broader customer market is attained and may reduce the amount of money patients must pay for said repair surgeries. Furthermore, there are greater incentives for professional baseball teams to return players to field as the franchise will make less money as they are in recovery from surgery. From 2004 to 2014, one hundred ninety-four MLB pitchers underwent UCL reconstruction, missing on average 180.2 days of the MLB regular season. Cost of recovery amounted to \$395 million, averaging \$1.9 million per player (Meldau et al., 2020). Due to the player returning to playing quicker with the reparative device in comparison to the UCL reconstruction, the team may opt for this procedure as to not lose as much money.

### **7.5.2 Environmental Impact**

There is an environmental impact associated with the manufacturing of a design of this nature. Each component needs to be made in a sterile environment, which requires a lot of chemicals such as bleach and isopropyl alcohol, as well as single use products. These have harsh impacts on the environment through their toxicity and lack of degradation. The fabrication of collagen sponges and silk hydrogels requires biological hazardous materials which need to be disposed of properly in order to minimize environmental impacts. Some of the materials used also require refrigeration to store and must be shipped before they can be used, which contributes to pollution.

### **7.5.3 Societal Impact**

There are likely several societal impacts from the production, sales and marketing of the designed product. There could be impacts on baseball leagues organization and funding if this product truly quickens healing and reduces recovery costs. There may also be an impact on youth sports if the risk of severe and permanent injury is mitigated by the product. Additionally, there

may be several other societal impacts such as greater athletic participation if the product were to be applied to other ligaments and types of injuries in the future. Although it is not known for sure, it is estimated that the cost of the surgical procedure to implant the device would be comparable to the current surgical reconstructive procedures. However, with a reparative rather than reconstructive method for partial tears, this will reduce the cost of physical therapy making the reparative device more accessible and equitable to a wider variety of financial status in patients and reducing the amount of time players have in order to recover, thus reducing the need to quit a sport.

#### **7.5.4 Political Ramifications**

The political ramifications of this project are likely insignificant. With this said it is possible that the new product may have political ramifications following novel biomedical research. Additionally, baseball leagues, which is a global market, may be impacted politically because of the opportunity for an alternative injury repair method for players.

#### **7.5.5 Ethical Concerns**

There are some ethical concerns with using silk fibroin as a material in the scaffold. In order to obtain silk fibroin solution, silkworms must be boiled alive in their cocoons or the pupa is removed before boiling, which still results in the death of silk worms (“The Silk Industry,” n.d.). In this sense, there is concern for animal safety. In addition, the casing is derived from fetal bovine dermis, which again raises concern for animal safety, as you are sacrificing a pregnant cow to obtain fetal bovine then get the dermis from the fetus (Jochems et al., 2002). Fetal bovine, however, is sacrificed for other reasons like fetal bovine serum (FBS), so one can argue that we are making use of waste products from this. Similarly, the collagen sponges used in this project are also derived from bovine dermis, but this time from adult cows. Again, there are ethical concerns of killing animals for the benefits of human health. But as mentioned before, bovine is currently sacrificed for various other reasons, like food. The most important aspect to all of this is that the animals are being treated humanely up until slaughter.

Alternatively, using silk cocoons could be used after the moth has emerged from the cocoon, which could reduce ethical concerns. This may however affect the properties of the silk product. Instead of killing pregnant cows to obtain fetal dermis for the obtainment of acellular

dermal matrix, we could use dermis from humans that have donated their organs, or dermis from cows that die a natural death. Collagen sponge materials could also be obtained from animals that have died a natural death.

#### **7.5.6 Health and Safety**

With regards to surgical procedures and implanting foreign objects into the body it is pertinent that the health and safety of our design is not overlooked. Ensuring sterility from fabrication to storage to implantation is important as it minimizes the risk of implant rejection and corresponding negative immune responses. Safety would be ensured through phased clinical trials to be completed after all necessary in vitro studies had been successfully completed. Patient monitoring throughout the clinical trials would be required to ensure health and safety.

#### **7.5.7 Manufacturability**

The goal of this project was to create a device that could be produced repeatedly and precisely as well as sterilely. The protocols to manufacture and sterilize the scaffold have been developed and are included in Appendix K as previously noted, although they would need to be reevaluated to scale up manufacturing in the future for larger production quantities. Fabrication would need to be completed efficiently in a sterile manufacturing plant. More resources would be required to mass produce scaffolds, which would require financial resources to purchase large quantities of our materials. This would require a reputable material distributor as well.

#### **7.5.8 Sustainability**

The production of our product would have some impact on renewable energy and environmental resources. Since silkworms are required to make the silk hydrogels, they would need to be taken care of throughout their life and reproduced to support manufacturing. The processes to store and use PDGF-BB and collagen also require energy due to refrigeration. There is also collagen used in this design which must be harvested from animals, so this adds energy as this material, along with the others, needs to be shipped considerable distances at times to reach manufacturing. This means that electrical energy is required to keep the design viable and to produce it with its many components.

## **8.0 Conclusions and Recommendations**

A PDGF-BB loaded collagen sponge reinforced hydrogel encased with acellular dermal matrix was successfully produced and able to have a controlled release of PDGF-BB that increased cell proliferation. This project was a successful stride for the concept to aid in ligament repair.

### **8.1 Recommendations and Next Steps**

In order to refine the design that has been started by our team, we have outlined several recommendations. These include testing modified materials, testing the sealed encased design, fixation, and animal testing. If the design is proven to aid in the healing process, it may also be applied to other ligaments.

#### **8.1.1 Test Different Silk Hydrogel Fabrication Solutions**

In the future, we recommend testing various concentrations of silk solution as this may affect how drug is eluted from the hydrogel. We recommend testing 1 wt%, 2.5 wt%, 5 wt%, 7.5 wt% and 10 wt%. Additionally, we would recommend testing variable sonication times.

#### **8.1.2 Test Collagen-PDGF-BB Composite Sponge**

We would also recommend fabrication collagen sponges that have the PDGF-BB added to the slurry solution that is used for lyophilization to make a collagen-PDGF-BB composite sponge. This may eliminate the need for the silk hydrogel component or give the scaffold more area for the protein to bind to. In addition, it could produce a better release profile than the sponge reinforced silk hydrogel design that we used in our device. Lastly, it could also allow for more than one type of growth factor to be included in the scaffold design by adding one to the collagen sponge and the other to the silk hydrogel.

#### **8.1.3 Use a Portfolio of Growth Factors**

PDGF-BB is an excellent growth factor choice as it helps regulate the production of other types of growth factors. However, using multiple growth factors in the scaffold design would be even more effective as you would not need to wait for the body to produce this on its own, which

could speed up the healing process. We wanted to use both PDGF-BB and FGF-2 but due to budget constraints, we were unable to test both types of proteins.

#### **8.1.4 Research and Test how to Seal the Casing**

The acellular dermal matrix casing needs to be sealed such that it is effective in slowing down the release of growth factors. Some ideas we had were to suture, fibrin glue, or tissue-weld it into a pocket so that it would stay together. Due to time, money, and resource constraints we were unable to test any of these options. The method for closure would need to be tested mechanically to ensure it would not fall apart during surgical manipulation and would need to be tested with drug elution to ensure there was a tight enough seal that the casing still released growth factors at the desired rate.

#### **8.1.5 Develop Method to Fixate the Scaffold to the Ligament**

To use the device effectively, it needs to be fixated to the injured ulnar collateral ligament without damaging the existing anatomy or the scaffold itself. This can be by fibrin glue, sutures, anchoring, or a netting method as previously described.

#### **8.1.6 Animal Testing**

Ultimately, this device would need to be tested on an actual ligament. This could be achieved by harvesting a ligament and testing it *ex-vivo*, or by implanting the device into a small model animal such as a rat or a rabbit.

#### **8.1.7 Apply the Scaffold to Other Ligaments**

Ultimately, this device should be tested for its ability to heal ligaments beyond just the ulnar collateral ligament. The size and amount of growth factors loaded onto the device may need to be altered in order to apply this device to other locations of the body. Some places it could be tested are the anterior cruciate ligament (ACL) which also has a synovial environment, medial collateral ligament (MCL) or rotator cuff.

### **8.2 Conclusion**

In conclusion, the project was successful in designing and testing a PDGF-BB loaded collagen sponge reinforced silk hydrogel encased in an acellular dermal matrix. This project

made strides in the concept of repairing grade II UCL tears. We modeled elution and diffusion testing using BSA loaded devices and then moved forward with loading with the final therapeutic agent, PDGF-BB. We were able to successfully deliver a sustained release of our therapeutic as determined by our drug elution and diffusion testing. This release timeline was also confirmed by mathematical modeling. As for healing promotion, further cell proliferation testing is required to assess how well the scaffold promotes healing of the UCL. The lack of significant results may be due to an inadequate amount of supernatant being used for the testing or too low of an initial concentration of growth factor. Additionally, we proved that the design is surgically compatible as our client confirmed it could be easily implemented in an operating room. We also confirmed that the design was mechanically sound as determined by our tensile testing results. Although the device was successfully produced and able to have a controlled release of PDGF-BB, we acknowledge that the recommendations previously explained should be considered to further refine the device. With the progress made in this project and future improvements, we believe the design that we created will have a significant impact in healing partial UCL tears as an alternative to current surgical practices.

## References

- 510(k) *Premarket Notification*. (n.d.-a). Retrieved April 27, 2022, from <https://www.accessdata.fda.gov/scripts/cdrh/cfdocs/cfpmn/pmn.cfm?id=K082176>
- 510(k) *Premarket Notification*. (n.d.-b). Retrieved April 27, 2022, from <https://www.accessdata.fda.gov/scripts/cdrh/cfdocs/cfPMN/pmn.cfm?ID=K071065>
- Acevedo, D. C., Shore, B., & Mirzayan, R. (2015). Orthopedic Applications of Acellular Human Dermal Allograft for Shoulder and Elbow Surgery. *Orthopedic Clinics of North America*, 46(3), 377–388. <https://doi.org/10.1016/j.ocl.2015.02.006>
- Aluigi, A., Vineis, C., Varesano, A., Mazzuchetti, G., Ferrero, F., & Tonin, C. (2008). Structure and properties of keratin/PEO blend nanofibres. *European Polymer Journal*, 44(8), 2465–2475. <https://doi.org/10.1016/j.eurpolymj.2008.06.004>
- Andrae, J., Gallini, R., & Betsholtz, C. (2008). Role of platelet-derived growth factors in physiology and medicine. *Genes & Development*, 22(10), 1276–1312. <https://doi.org/10.1101/gad.1653708>
- Apostolakos, J. M., Lin, K. M., Carr, J. B., Bedi, A., Camp, C. L., & Dines, J. S. (2020). The Role of Biologic Agents in the Non-operative Management of Elbow Ulnar Collateral Ligament Injuries. *Current Reviews in Musculoskeletal Medicine*, 13(4), 442–448. <https://doi.org/10.1007/s12178-020-09637-9>
- Awh, M. (2010, January 1). *Ulnar Collateral Ligament Tears of the Elbow*. Radsourc. <https://radsourc.us/ulnar-collateral-ligament-tears-of-the-elbow/>
- Babensee, J. E. (2020). Inflammation, Wound Healing, the Foreign-Body Response, and Alternative Tissue Responses. In *Biomaterials Science* (pp. 737–746). Elsevier. <https://doi.org/10.1016/B978-0-12-816137-1.00048-9>
- Barber, F. A., Herbert, M. A., & Coons, D. A. (2006). Tendon Augmentation Grafts: Biomechanical Failure Loads and Failure Patterns. *Arthroscopy: The Journal of Arthroscopic & Related Surgery*, 22(5), 534–538. <https://doi.org/10.1016/j.arthro.2005.12.021>
- Biomechanics: Ulnar Collateral Ligament—Dec 18, 2008—Blog—TexasLeaguers.com*. (2008, December 18). <https://texasleaguers.com/blog/2008/12/18/biomechanics-ulnar-collateral-ligament>
- BIOREZ – The future of tendon and ligament healing*. (n.d.). Retrieved October 11, 2021, from <https://biorez.com/>
- Borrelli, M., Joepen, N., Reichl, S., Finis, D., Schoppe, M., Geerling, G., & Schrader, S. (2015). Keratin films for ocular surface reconstruction: Evaluation of biocompatibility in an in-vivo model. *Biomaterials*, 42, 112–120. <https://doi.org/10.1016/j.biomaterials.2014.11.038>
- Brown, A. C., & Barker, T. H. (2014). Fibrin-based biomaterials: Modulation of macroscopic properties through rational design at the molecular level. *Acta Biomaterialia*, 10(4), 1502–1514. <https://doi.org/10.1016/j.actbio.2013.09.008>
- Buckley, P. S., Morris, E. R., Robbins, C., Kemler, B., Frangiamore, S. J., Ciccotti, M. G., Huard, J., LaPrade, R. F., & Hackett, T. R. (2019). Variations in Blood Supply from

- Proximal to Distal in the Ulnar Collateral Ligament of the Elbow: A Qualitative Descriptive Cadaveric Study. *Orthopaedic Journal of Sports Medicine*, 7(7 suppl5), 2325967119S00361. <https://doi.org/10.1177/2325967119S00361>
- Bush, K. A., & Pins, G. D. (2010). Carbodiimide Conjugation of Fibronectin on Collagen Basal Lamina Analogs Enhances Cellular Binding Domains and Epithelialization. *Tissue Engineering Part A*, 16(3), 829–838. <http://dx.doi.org/10.1089/ten.tea.2009.0514>
- Bush-Joseph, C., Romeo, A., Erickson, B., Nwachukwu, B., Rosas, S., Schairer, W., McCormick, F., & Bernard, R. (2015). *Review of a Large Private-Payer Database From 2007 to 2011 Trends in Medial Ulnar Collateral Ligament Reconstruction in the United States: A Retrospective*. <https://www.semanticscholar.org/paper/Review-of-a-Large-Private-Payer-Database-From-2007-Bush-Joseph-Romeo/1b9eebe9c720d708d0a49e36a28d28073694d573>
- Camp, C. L., Conte, S., D'Angelo, J., & Fealy, S. A. (2018). Epidemiology of ulnar collateral ligament reconstruction in Major and Minor League Baseball pitchers: Comprehensive report of 1429 cases. *Journal of Shoulder and Elbow Surgery*, 27(5), 871–878. <https://doi.org/10.1016/j.jse.2018.01.024>
- Camp, C. L., Dines, J. S., Voleti, P. B., James, E. W., & Altchek, D. W. (2016). Ulnar Collateral Ligament Reconstruction of the Elbow: The Docking Technique. *Arthroscopy Techniques*, 5(3), e519–e523. <https://doi.org/10.1016/j.eats.2016.02.013>
- Charalel, R. A., Engberg, K., Noolandi, J., Cochran, J. R., Frank, C., & Ta, C. N. (2012). Diffusion of Protein Through the Human Cornea. *Ophthalmic Research*, 48(1), 50–55. <https://doi.org/10.1159/000329794>
- Chauhan, A., McQueen, P., Chalmers, P. N., Ciccotti, M. G., Camp, C. L., D'Angelo, J., Potter, H. G., Fealy, S. A., Erickson, B. J., Hoenecke, H. R., Keefe, D., McCauley, J., & Fronek, J. (2019). Nonoperative Treatment of Elbow Ulnar Collateral Ligament Injuries With and Without Platelet-Rich Plasma in Professional Baseball Players: A Comparative and Matched Cohort Analysis. *The American Journal of Sports Medicine*, 47(13), 3107–3119. <https://doi.org/10.1177/0363546519876305>
- Chen, J., Xu, J., Wang, A., & Zheng, M. (2009). Scaffolds for tendon and ligament repair: Review of the efficacy of commercial products. *Expert Review of Medical Devices*, 6(1), 61–73. <http://dx.doi.org/10.1586/17434440.6.1.61>
- Cheung, R. C. F., Ng, T. B., Wong, J. H., & Chan, W. Y. (2015). Chitosan: An Update on Potential Biomedical and Pharmaceutical Applications. *Marine Drugs*, 13(8), 5156–5186. <https://doi.org/10.3390/md13085156>
- Cho, C.-H., Lee, S.-M., Lee, Y.-K., & Shin, H.-K. (2014). Mini-Open Suture Bridge Repair with Porcine Dermal Patch Augmentation for Massive Rotator Cuff Tear: Surgical Technique and Preliminary Results. *Clinics in Orthopedic Surgery*, 6(3), 329. <https://doi.org/10.4055/cios.2014.6.3.329>
- Cornwell, K. G., Lei, P., Andreadis, S. T., & Pins, G. D. (2007). Crosslinking of discrete self-assembled collagen threads: Effects on mechanical strength and cell–matrix interactions. *Journal of Biomedical Materials Research Part A*, 80A(2), 362–371. <https://doi.org/10.1002/jbm.a.30893>

- Coughlin, R. P., Lee, Y., Horner, N. S., Simunovic, N., Cadet, E. R., & Ayeni, O. R. (2019). Increased pitch velocity and workload are common risk factors for ulnar collateral ligament injury in baseball players: A systematic review. *Journal of ISAKOS*, 4(1), 41–47. <https://doi.org/10.1136/jisakos-2018-000226>
- De la Riva, B., Sánchez, E., Hernández, A., Reyes, R., Tamimi, F., López-Cabarcos, E., Delgado, A., & Évora, C. (2010). Local controlled release of VEGF and PDGF from a combined brushite–chitosan system enhances bone regeneration. *Journal of Controlled Release*, 143(1), 45–52. <https://doi.org/10.1016/j.jconrel.2009.11.026>
- Deal, J. B., Smith, E., Heard, W., O'Brien, M. J., & Savoie, F. H. (2017). Platelet-Rich Plasma for Primary Treatment of Partial Ulnar Collateral Ligament Tears: MRI Correlation With Results. *Orthopaedic Journal of Sports Medicine*, 5(11), 2325967117738238. <https://doi.org/10.1177/2325967117738238>
- Demir, M., Ramos-Rivera, L., Silva, R., Nazhat, S. N., & Boccaccini, A. R. (2017). Zein-based composites in biomedical applications. *Journal of Biomedical Materials Research Part A*, 105(6), 1656–1665. <https://doi.org/10.1002/jbm.a.36040>
- Dillman, C. J., Fleisig, G. S., & Andrews, J. R. (1993). Biomechanics of Pitching With Emphasis Upon Shoulder Kinematics. *Journal of Orthopaedic & Sports Physical Therapy*, 18(2), 402–408. <https://doi.org/10.2519/jospt.1993.18.2.402>
- Dugas, J. R., Looze, C. A., Jones, C. M., Walters, B. L., Rothermich, M. A., Emblom, B. A., Fleisig, G. S., Aune, K., & Cain, E. L. (2018). Ulnar Collateral Ligament Repair with Internal Brace Augmentation in Amateur Overhead Throwing Athletes. *Orthopaedic Journal of Sports Medicine*, 6(7 suppl4), 2325967118S00084. <https://doi.org/10.1177/2325967118S00084>
- Dustin, A., Geer, E., & Hulburt, T. (2015). A dynamic elbow flexion simulator for cadaveric testing of UCL injury and reconstruction. *2015 41st Annual Northeast Biomedical Engineering Conference (NEBEC)*, 1–2. <https://doi.org/10.1109/NEBEC.2015.7117223>
- Fleisig, G. S., Barrentine, S. W., Zheng, N., Escamilla, R. F., & Andrews, J. R. (1999). Kinematic and kinetic comparison of baseball pitching among various levels of development. *Journal of Biomechanics*, 32(12), 1371–1375. [https://doi.org/10.1016/s0021-9290\(99\)00127-x](https://doi.org/10.1016/s0021-9290(99)00127-x)
- Ford, G. M., Genuario, J., Kinkartz, J., Githens, T., & Noonan, T. (2016). Return-to-Play Outcomes in Professional Baseball Players After Medial Ulnar Collateral Ligament Injuries: Comparison of Operative Versus Nonoperative Treatment Based on Magnetic Resonance Imaging Findings. *The American Journal of Sports Medicine*, 44(3), 723–728. <https://doi.org/10.1177/0363546515621756>
- Frangiamore, S. J., Lynch, T. S., Vaughn, M. D., Soloff, L., Forney, M., Styron, J. F., & Schickendantz, M. S. (2017). Magnetic Resonance Imaging Predictors of Failure in the Nonoperative Management of Ulnar Collateral Ligament Injuries in Professional Baseball Pitchers. *The American Journal of Sports Medicine*, 45(8), 1783–1789. <https://doi.org/10.1177/0363546517699832>
- Friess, W. (1998). Collagen – biomaterial for drug delivery. *European Journal of Pharmaceutics and Biopharmaceutics*, 24.

- Fujioka-Kobayashi, M., Schaller, B., Saulacic, N., Pippenger, B. E., Zhang, Y., & Miron, R. J. (2017, February 9). *Absorbable collagen sponges loaded with recombinant bone morphogenetic protein 9 induces greater osteoblast differentiation when compared to bone morphogenetic protein 2*. <https://onlinelibrary-wiley-com.ezpv7-web-p-u01.wpi.edu/doi/10.1002/cre2.55>
- Ge, Z., Yang, F., Goh, J. C. H., Ramakrishna, S., & Lee, E. H. (2006). Biomaterials and scaffolds for ligament tissue engineering. *Journal of Biomedical Materials Research Part A*, 77A(3), 639–652. <https://doi.org/10.1002/jbm.a.30578>
- Gillespie, R. J., Knapik, D. M., & Akkus, O. (2016). Biologic and Synthetic Grafts in the Reconstruction of Large to Massive Rotator Cuff Tears. *The Journal of the American Academy of Orthopaedic Surgeons*, 24(12), 823–828. <https://doi.org/10.5435/JAAOS-D-15-00229>
- Gilpin, A., & Yang, Y. (2017). Decellularization Strategies for Regenerative Medicine: From Processing Techniques to Applications. *BioMed Research International*, 2017, 9831534. <https://doi.org/10.1155/2017/9831534>
- Glowacki, J., & Mizuno, S. (2008). Collagen scaffolds for tissue engineering. *Biopolymers*, 89(5), 338–344. <https://doi.org/10.1002/bip.20871>
- GRAFTJACKET™ Regenerative Tissue Matrix. (n.d.). *Wright Medical Group*. Retrieved April 27, 2022, from <https://www.wright.com/footandankleproducts/graftjacket>
- Gulotta, L. V., & Rodeo, S. A. (2009). Growth Factors for Rotator Cuff Repair. *Clinics in Sports Medicine*, 28(1), 13–23. <https://doi.org/10.1016/j.csm.2008.09.002>
- Gurbuz, H., Kutoglu, T., Mesut, R., & Gurbuz, H. (2005). Anatomical dimensions of anterior bundle of ulnar collateral ligament and its role in elbow stability. *Folia Medica*, 47(1), 47–52.
- Han, F., Dong, Y., Su, Z., Yin, R., Song, A., & Li, S. (2014). Preparation, characteristics and assessment of a novel gelatin–chitosan sponge scaffold as skin tissue engineering material. *International Journal of Pharmaceutics*, 476(1), 124–133. <https://doi.org/10.1016/j.ijpharm.2014.09.036>
- Hapugoda, S. (n.d.). *Superior ulnar collateral artery | Radiology Reference Article | Radiopaedia.org*. Radiopaedia. Retrieved September 12, 2021, from <https://radiopaedia.org/articles/superior-ulnar-collateral-artery?lang=us>
- Hopkins, A. M., De Laporte, L., Tortelli, F., Spedden, E., Staii, C., Atherton, T. J., Hubbell, J. A., & Kaplan, D. L. (2013, April 18). *Silk Hydrogels as Soft Substrates for Neural Tissue Engineering*. [https://onlinelibrary-wiley-com.ezpv7-web-p-u01.wpi.edu/doi/full/10.1002/adfm.201300435?casa\\_token=254eKCWUACoAAAAA%3AKWMnrCXXBZdUttauHRdL5y0UxqWPxOp9j-5pvT7jovfdvkw1uKQoMKS4GfTaFbZg5NKK-tEhcJn73pAK](https://onlinelibrary-wiley-com.ezpv7-web-p-u01.wpi.edu/doi/full/10.1002/adfm.201300435?casa_token=254eKCWUACoAAAAA%3AKWMnrCXXBZdUttauHRdL5y0UxqWPxOp9j-5pvT7jovfdvkw1uKQoMKS4GfTaFbZg5NKK-tEhcJn73pAK)
- Hurwit, D. J., Garcia, G. H., Liu, J., Altchek, D. W., Romeo, A., & Dines, J. (2017). Management of ulnar collateral ligament injury in throwing athletes: A survey of the American Shoulder and Elbow Surgeons. *Journal of Shoulder and Elbow Surgery*, 26(11), 2023–2028. <https://doi.org/10.1016/j.jse.2017.08.005>
- Jensen, A. R., LaPrade, M. D., Turner, T. W., Dines, J. S., & Camp, C. L. (2020). The History and Evolution of Elbow Medial Ulnar Collateral Ligament Reconstruction: From Tommy

- John to 2020. *Current Reviews in Musculoskeletal Medicine*, 13(3), 349–360.  
<https://doi.org/10.1007/s12178-020-09618-y>
- Jeong Park, Y., Moo Lee, Y., Nae Park, S., Yoon Sheen, S., Pyoung Chung, C., & Lee, S. J. (2000). Platelet derived growth factor releasing chitosan sponge for periodontal bone regeneration. *Biomaterials*, 21(2), 153–159. [https://doi.org/10.1016/S0142-9612\(99\)00143-X](https://doi.org/10.1016/S0142-9612(99)00143-X)
- Ji, W., Sun, Y., Yang, F., van den Beucken, J. J. J. P., Fan, M., Chen, Z., & Jansen, J. A. (2011). Bioactive Electrospun Scaffolds Delivering Growth Factors and Genes for Tissue Engineering Applications. *Pharmaceutical Research*, 28(6), 1259–1272.  
<https://doi.org/10.1007/s11095-010-0320-6>
- Jochems, C. E. A., van der Valk, J. B. F., Stafleu, F. R., & Baumans, V. (2002). The use of fetal bovine serum: Ethical or scientific problem? *Alternatives to Laboratory Animals: ATLA*, 30(2), 219–227. <https://doi.org/10.1177/026119290203000208>
- Joyner, P. W., Bruce, J., Hess, R., Mates, A., Mills, F. B., & Andrews, J. R. (2016). Magnetic resonance imaging–based classification for ulnar collateral ligament injuries of the elbow. *Journal of Shoulder and Elbow Surgery*, 25(10), 1710–1716.  
<https://doi.org/10.1016/j.jse.2016.05.006>
- Kaleshian, G. J., Gaudette, L. W., & Heighton, C. N. (2021, May 6). *Ligament Regeneration System*. Worcester Polytechnic Institute.
- Karuppaiah, K., & Sinha, J. (2019). Scaffolds in the management of massive rotator cuff tears: Current concepts and literature review. *EFORT Open Reviews*, 4(9), 557–566.  
<https://doi.org/10.1302/2058-5241.4.180040>
- Kasoju, N., & Bora, U. (2012). Silk Fibroin in Tissue Engineering. *Advanced Healthcare Materials*, 1(4), 393–412. <https://doi.org/10.1002/adhm.201200097>
- Katoh, K., Shibayama, M., Tanabe, T., & Yamauchi, K. (2004). Preparation and physicochemical properties of compression-molded keratin films. *Biomaterials*, 25(12), 2265–2272. <https://doi.org/10.1016/j.biomaterials.2003.09.021>
- Kieb, M., Sander, F., Prinz, C., Adam, S., Mau-Möller, A., Bader, R., Peters, K., & Tischer, T. (2017). Platelet-Rich Plasma Powder: A New Preparation Method for the Standardization of Growth Factor Concentrations. *The American Journal of Sports Medicine*, 45(4), 954–960. <https://doi.org/10.1177/0363546516674475>
- Kim, J.-H., Kim, T.-H., Kang, M. S., & Kim, H.-W. (2016). Angiogenic Effects of Collagen/Mesoporous Nanoparticle Composite Scaffold Delivering VEGF165. *BioMed Research International*, 2016, e9676934. <https://doi.org/10.1155/2016/9676934>
- Labott, J. R., Aibinder, W. R., Dines, J. S., & Camp, C. L. (2018). Understanding the medial ulnar collateral ligament of the elbow: Review of native ligament anatomy and function. *World Journal of Orthopedics*, 9(6), 78–84. <https://doi.org/10.5312/wjo.v9.i6.78>
- Lee, Y.-M., Park, Y.-J., Lee, S.-J., Ku, Y., Han, S.-B., Klokkevold, P. R., & Chung, C.-P. (2000). The Bone Regenerative Effect of Platelet-Derived Growth Factor-BB Delivered With a Chitosan/Tricalcium Phosphate Sponge Carrier. *Journal of Periodontology*, 71(3), 418–424. <https://doi.org/10.1902/jop.2000.71.3.418>
- Leng, X., Liu, B., Su, B., Liang, M., Shi, L., Li, S., Qu, S., Fu, X., Liu, Y., Yao, M., Kaplan, D. L., Wang, Y., & Wang, X. (2017). In situ ultrasound imaging of silk hydrogel

- degradation and neovascularization. *Journal of Tissue Engineering and Regenerative Medicine*, 11(3), 822–830. <https://doi.org/10.1002/term.1981>
- Ligament Augmentation Device—An overview | *ScienceDirect Topics*. (n.d.). Retrieved April 27, 2022, from <https://www.sciencedirect.com/topics/nursing-and-health-professions/ligament-augmentation-device>
- Lin, J., Li, C., Zhao, Y., Hu, J., & Zhang, L.-M. (2012). Co-electrospun Nanofibrous Membranes of Collagen and Zein for Wound Healing. *ACS Applied Materials & Interfaces*, 4(2), 1050–1057. <https://doi.org/10.1021/am201669z>
- Linsley, C. S., Wu, B. M., & Tawil, B. (2016). Mesenchymal stem cell growth on and mechanical properties of fibrin-based biomimetic bone scaffolds. *Journal of Biomedical Materials Research Part A*, 104(12), 2945–2953. <https://doi.org/10.1002/jbm.a.35840>
- Litvinov, R. I., & Weisel, J. W. (2017). Fibrin mechanical properties and their structural origins. *Matrix Biology : Journal of the International Society for Matrix Biology*, 60–61, 110–123. <https://doi.org/10.1016/j.matbio.2016.08.003>
- Ma, F., Wang, F., Li, R., & Zhu, J. (2018). Application of drug delivery systems for the controlled delivery of growth factors to treat nervous system injury. *Organogenesis*, 14(3), 123–128. <https://doi.org/10.1080/15476278.2018.1491183>
- Maeda, M., Tani, S., Sano, A., & Fujioka, K. (1999). Microstructure and release characteristics of the minipellet, a collagen-based drug delivery system for controlled release of protein drugs. *Journal of Controlled Release*, 62(3), 313–324. [https://doi.org/10.1016/S0168-3659\(99\)00156-X](https://doi.org/10.1016/S0168-3659(99)00156-X)
- Magit, D. (2018). *CORR LECTURE*.
- Magit, D. (2021, September 24). *Objectives Meeting* [Personal communication].
- Marcopoulou, C. E., Vavouraki, H. N., Dereka, X. E., & Vrotsos, I. A. (2003). Proliferative effect of growth factors TGF-beta1, PDGF-BB and rhBMP-2 on human gingival fibroblasts and periodontal ligament cells. *Journal of the International Academy of Periodontology*, 5(3), 63–70.
- Martha Murray, MD | *Boston Children's Hospital*. (n.d.). Retrieved September 27, 2021, from <https://www.childrenshospital.org/directory/physicians/m/martha-murray>
- Mckim, D. M. (2016, October 3). *Why Tendons and Ligaments Heal More Slowly Than Muscle*. Mckimchiropractic. <https://www.mckimchiro.com/single-post/2016/10/03/why-tendons-and-ligaments-heal-more-slowly-than-muscle>
- Meldau, J. E., Srivastava, K., Okoroha, K. R., Ahmad, C. S., Moutzouros, V., & Makhni, E. C. (2020). Cost analysis of Tommy John surgery for Major League Baseball teams. *Journal of Shoulder and Elbow Surgery*, 29(1), 121–125. <https://doi.org/10.1016/j.jse.2019.07.019>
- Min, Q., Tian, D., Zhang, Y., Wang, C., Wan, Y., & Wu, J. (2022). Strong and Elastic Chitosan/Silk Fibroin Hydrogels Incorporated with Growth-Factor-Loaded Microspheres for Cartilage Tissue Engineering. *Biomimetics*, 7(2), 41. <https://doi.org/10.3390/biomimetics7020041>
- Molloy, T., Wang, Y., & Murrell, G. (2003). The roles of growth factors in tendon and ligament healing. *Sports Medicine (Auckland, N.Z.)*, 33(5), 381–394. <https://doi.org/10.2165/00007256-200333050-00004>

- Murray, M. M., Flutie, B. M., Kalish, L. A., Ecklund, K., Fleming, B. C., Proffen, B. L., & Micheli, L. J. (2016). The Bridge-Enhanced Anterior Cruciate Ligament Repair (BEAR) Procedure: An Early Feasibility Cohort Study. *Orthopaedic Journal of Sports Medicine*, 4(11), 2325967116672176. <https://doi.org/10.1177/2325967116672176>
- New Tommy John Surgery Alternative Has Potential to Cut Rehab Time in Half.* (2017, January 30). Stack. <https://www.stack.com/a/new-tommy-john-surgery-promises-to-cut-rehab-time-in-half/>
- Noah, E. M., Chen, J., Jiao, X., Heschel, I., & Pallua, N. (2002). Impact of sterilization on the porous design and cell behavior in collagen sponges prepared for tissue engineering. *Biomaterials*, 23(14), 2855–2861. [https://doi.org/10.1016/S0142-9612\(01\)00412-4](https://doi.org/10.1016/S0142-9612(01)00412-4)
- OrthoADAPT™ Biologic collagen | The Foot and Ankle Online Journal.* (n.d.). Retrieved April 27, 2022, from <http://faoj.org/tag/orthoadapt-biologic-collagen/>
- Oyama, S. (2012). Baseball pitching kinematics, joint loads, and injury prevention. *Journal of Sport and Health Science*, 1(2), 80–91. <https://doi.org/10.1016/j.jshs.2012.06.004>
- Pallotta, I., Kluge, J. A., Moreau, J., Calabrese, R., Kaplan, D. L., & Balduini, A. (2014). Characteristics of platelet gels combined with silk. *Biomaterials*, 35(11), 3678–3687. <https://doi.org/10.1016/j.biomaterials.2013.12.065>
- Patil, V. A., & Masters, K. S. (2020). Engineered Collagen Matrices. *Bioengineering*, 7(4), 163. <https://doi.org/10.3390/bioengineering7040163>
- Pérez-Guzmán, C. J., & Castro-Muñoz, R. (2020). A Review of Zein as a Potential Biopolymer for Tissue Engineering and Nanotechnological Applications. *Processes*, 8(11), 1376. <https://doi.org/10.3390/pr8111376>
- Pins, G. D., & Silver, F. H. (1995). A self-assembled collagen scaffold suitable for use in soft and hard tissue replacement. *Materials Science and Engineering: C*, 3(2), 101–107. [https://doi.org/10.1016/0928-4931\(95\)00109-3](https://doi.org/10.1016/0928-4931(95)00109-3)
- Ratcliffe, A., Butler, D. L., Dymont, N. A., Cagle, P. J., Proctor, C. S., Ratcliffe, S. S., & Flatow, E. L. (2015). Scaffolds for Tendon and Ligament Repair and Regeneration. *Annals of Biomedical Engineering*, 43(3), 819–831. <https://doi.org/10.1007/s10439-015-1263-1>
- Ratcliffe, A., Woo, S. L.-Y., & Mow, V. C. (Eds.). (1990). *Biomechanics of Diarthrodial Joints*. Springer New York. <https://doi.org/10.1007/978-1-4612-3448-7>
- Rebolledo, B. J., Dugas, J. R., Bedi, A., Ciccotti, M. G., Altchek, D. W., & Dines, J. S. (2017). Avoiding Tommy John Surgery: What Are the Alternatives? *The American Journal of Sports Medicine*, 45(13), 3143–3148. <https://doi.org/10.1177/0363546517692548>
- Reddy, M. S. B., Ponnamma, D., Choudhary, R., & Sadasivuni, K. K. (2021). A Comparative Review of Natural and Synthetic Biopolymer Composite Scaffolds. *Polymers*, 13(7), 1105. <https://doi.org/10.3390/polym13071105>
- Roth, T. S., Beason, D. P., Clay, T. B., Cain, E. L., & Dugas, J. R. (2021). The Effect of Ulnar Collateral Ligament Repair With Internal Brace Augmentation on Articular Contact Mechanics: A Cadaveric Study. *Orthopaedic Journal of Sports Medicine*, 9(4), 23259671211001068. <https://doi.org/10.1177/23259671211001069>
- Rouse, J. G., & Van Dyke, M. E. (2010). A Review of Keratin-Based Biomaterials for Biomedical Applications. *Materials*, 3(2), 999–1014. <https://doi.org/10.3390/ma3020999>

- Scarfe, A. W. S. (2019). *Human dermal allograft for massive rotator cuff tears* (No. 117). Vienna: Ludwig Boltzmann Institute for Health Technology Assessment.
- Silva, M., Ferreira, F. N., Alves, N. M., & Paiva, M. C. (2020). Biodegradable polymer nanocomposites for ligament/tendon tissue engineering. *Journal of Nanobiotechnology*, 18(1), 23. <https://doi.org/10.1186/s12951-019-0556-1>
- Smith, M. V. (2013). Ulnar Collateral Ligament Reconstruction with Allograft: Is It a Home Run? *The Journal of Bone and Joint Surgery. American Volume*, 95(12), e87. <https://doi.org/10.2106/JBJS.M.00524>
- Smith, M. V., & Bernholt, D. L. (2020). Ulnar collateral ligament injury in the elbow: Current trends for treatment. *Annals of Joint*, 5(0). <https://doi.org/10.21037/aoj.2020.01.02>
- Stinner, D. J., Noel, S. P., Haggard, W. O., Watson, J. T., & Wenke, J. C. (2010). Local Antibiotic Delivery Using Tailorable Chitosan Sponges: The Future of Infection Control? *Journal of Orthopaedic Trauma*, 24(9), 592–597. <https://doi.org/10.1097/BOT.0b013e3181ed296c>
- Tabata, Y., Miyao, M., Ozeki, M., & Ikada, Y. (2000). Controlled release of vascular endothelial growth factor by use of collagen hydrogels. *Journal of Biomaterials Science, Polymer Edition*, 11(9), 915–930. <https://doi.org/10.1163/156856200744101>
- The Benefits and Risks of Tommy John Surgery*. (2017, August 15). Beacon Orthopaedics & Sports Medicine. <https://www.beaconortho.com/blog/benefits-tommy-john-surgery/>
- The Ligament Injury-Osteoarthritis Connection: The Role of Prolotherapy in Ligament Repair and the Prevention of Osteoarthritis. (2012, March 31). *Journal of Prolotherapy*. <https://journalofprolotherapy.com/the-ligament-injury-osteoarthritis-connection-the-role-of-prolotherapy-in-ligament-repair-and-the-prevention-of-osteoarthritis/>
- The Silk Industry. (n.d.). *PETA UK*. Retrieved April 26, 2022, from <https://www.peta.org.uk/issues/animals-not-wear/silk/>
- Thomas, A. C., Hubbard-Turner, T., Wikstrom, E. A., & Palmieri-Smith, R. M. (2017). Epidemiology of Posttraumatic Osteoarthritis. *Journal of Athletic Training*, 52(6), 491–496. <https://doi.org/10.4085/1062-6050-51.5.08>
- Thomopoulos, S., Das, R., Sakiyama-Elbert, S., Silva, M. J., Charlton, N., & Gelberman, R. H. (2010). bFGF and PDGF-BB for Tendon Repair: Controlled Release and Biologic Activity by Tendon Fibroblasts In Vitro. *Annals of Biomedical Engineering*, 38(2), 225–234. <https://doi.org/10.1007/s10439-009-9844-5>
- Tommy John Surgery In-Depth | Boston Children's Hospital*. (n.d.). Retrieved September 29, 2021, from <https://www.childrenshospital.org/conditions-and-treatments/treatments/tommy-john-surgery/in-depth>
- Tommy John Surgery (Ulnar Collateral Ligament Reconstruction)*. (n.d.). Retrieved September 29, 2021, from <https://www.hopkinsmedicine.org/health/treatment-tests-and-therapies/tommy-john-surgery-ulnar-collateral-ligament-reconstruction>
- Tornier And LifeCell Corporation Initiate Clinical Trial for Conexa(TM) to Repair Rotator Cuff Tears*. (n.d.). BioSpace. Retrieved April 27, 2022, from <https://www.biospace.com/article/tornier-and-lifecell-corporation-initiate-clinical-trial-for-conexa-tm-to-repair-rotator-cuff-tears/>

- Ueda, H., Hong, L., Yamamoto, M., Shigeno, K., Inoue, M., Toba, T., Yoshitani, M., Nakamura, T., Tabata, Y., & Shimizu, Y. (2002). Use of collagen sponge incorporating transforming growth factor- $\beta$ 1 to promote bone repair in skull defects in rabbits. *Biomaterials*, 23(4), 1003–1010. [https://doi.org/10.1016/S0142-9612\(01\)00211-3](https://doi.org/10.1016/S0142-9612(01)00211-3)
- Vasconcelos, A., Freddi, G., & Cavaco-Paulo, A. (2008). Biodegradable Materials Based on Silk Fibroin and Keratin. *Biomacromolecules*, 9(4), 1299–1305. <https://doi.org/10.1021/bm7012789>
- Walton, J. R., Bowman, N. K., Khatib, Y., Linklater, J., & Murrell, G. A. C. (2007). Restore orthobiologic implant: Not recommended for augmentation of rotator cuff repairs. *The Journal of Bone and Joint Surgery. American Volume*, 89(4), 786–791. <https://doi.org/10.2106/JBJS.F.00315>
- Wang, F., Hou, K., Chen, W., Wang, Y., Wang, R., Tian, C., Xu, S., Ji, Y., Yang, Q., Zhao, P., Yu, L., Lu, Z., Zhang, H., Li, F., Wang, H., He, B., Kaplan, D. L., & Xia, Q. (2020). Transgenic PDGF-BB/sericin hydrogel supports for cell proliferation and osteogenic differentiation. *Biomaterials Science*, 8(2), 657–672. <https://doi.org/10.1039/C9BM01478K>
- Wang, H.-J., Gong, S.-J., Lin, Z.-X., Fu, J.-X., Xue, S.-T., Huang, J.-C., & Wang, J.-Y. (2007). In vivo biocompatibility and mechanical properties of porous zein scaffolds. *Biomaterials*, 28(27), 3952–3964. <https://doi.org/10.1016/j.biomaterials.2007.05.017>
- Wang, Y., Cooke, M. J., Sachewsky, N., Morshead, C. M., & Shoichet, M. S. (2013). Bioengineered sequential growth factor delivery stimulates brain tissue regeneration after stroke. *Journal of Controlled Release: Official Journal of the Controlled Release Society*, 172(1), 1–11. <https://doi.org/10.1016/j.jconrel.2013.07.032>
- Wei, G., Jin, Q., Giannobile, W. V., & Ma, P. X. (2006). Nano-fibrous scaffold for controlled delivery of recombinant human PDGF-BB. *Journal of Controlled Release: Official Journal of the Controlled Release Society*, 112(1), 103–110. <https://doi.org/10.1016/j.jconrel.2006.01.011>
- Weisel, J. W., & Litvinov, R. I. (2017). Fibrin Formation, Structure and Properties. *Sub-Cellular Biochemistry*, 82, 405–456. [https://doi.org/10.1007/978-3-319-49674-0\\_13](https://doi.org/10.1007/978-3-319-49674-0_13)
- Wu, H., Lui, J., Wu, J., Wan, Y., & Chen, Y. (2016, April 19). *Controlled delivery of platelet-derived growth factor-BB from injectable microsphere/hydrogel composites | Elsevier Enhanced Reader*. <https://doi.org/10.1016/j.colsurfb.2016.09.005>
- Yamano, S., Haku, K., Yamanaka, T., Dai, J., Takayama, T., Shohara, R., Tachi, K., Ishioka, M., Hanatani, S., Karunakaran, S., Wada, K., & Moursi, A. M. (2014). The effect of a bioactive collagen membrane releasing PDGF or GDF-5 on bone regeneration. *Biomaterials*, 35(8), 2446–2453. <https://doi.org/10.1016/j.biomaterials.2013.12.006>
- Yan, L.-P., Oliveira, J. M., Oliveira, A. L., & Reis, R. L. (2017). Core-shell silk hydrogels with spatially tuned conformations as drug-delivery system. *Journal of Tissue Engineering and Regenerative Medicine*, 11(11), 3168–3177. <https://doi.org/10.1002/term.2226>
- Yang, L., Li, X., Wu, Y., Du, P., Sun, L., Yu, Z., Song, S., Yin, J., Ma, X., Jing, C., Zhao, J., Chen, H., Dong, Y., Zhang, Q., & Zhao, L. (2020). Preparation of PU/Fibrin Vascular Scaffold with Good Biomechanical Properties and Evaluation of Its Performance in vitro

and in vivo. *International Journal of Nanomedicine*, 15, 8697–8715.

<https://doi.org/10.2147/IJN.S274459>

Yao, C., Li, X., Song, T., Li, Y., & Yuepu, P. (2009, January 23). *Biodegradable nanofibrous membrane of zein/silk fibroin by electrospinning*. [https://onlinelibrary-wiley-com.ezpv7-web-p-u01.wpi.edu/doi/full/10.1002/pi.2544?casa\\_token=1bfmOqLkL1gAAAAA%3AQWsXSfM4ZCCMvR0\\_TXB8jTheVXd5A4rEVNLbs4vcqWJBYnZL2WL4nMfN5HTM1C14rAlutWPJ8YUdJrQg](https://onlinelibrary-wiley-com.ezpv7-web-p-u01.wpi.edu/doi/full/10.1002/pi.2544?casa_token=1bfmOqLkL1gAAAAA%3AQWsXSfM4ZCCMvR0_TXB8jTheVXd5A4rEVNLbs4vcqWJBYnZL2WL4nMfN5HTM1C14rAlutWPJ8YUdJrQg)

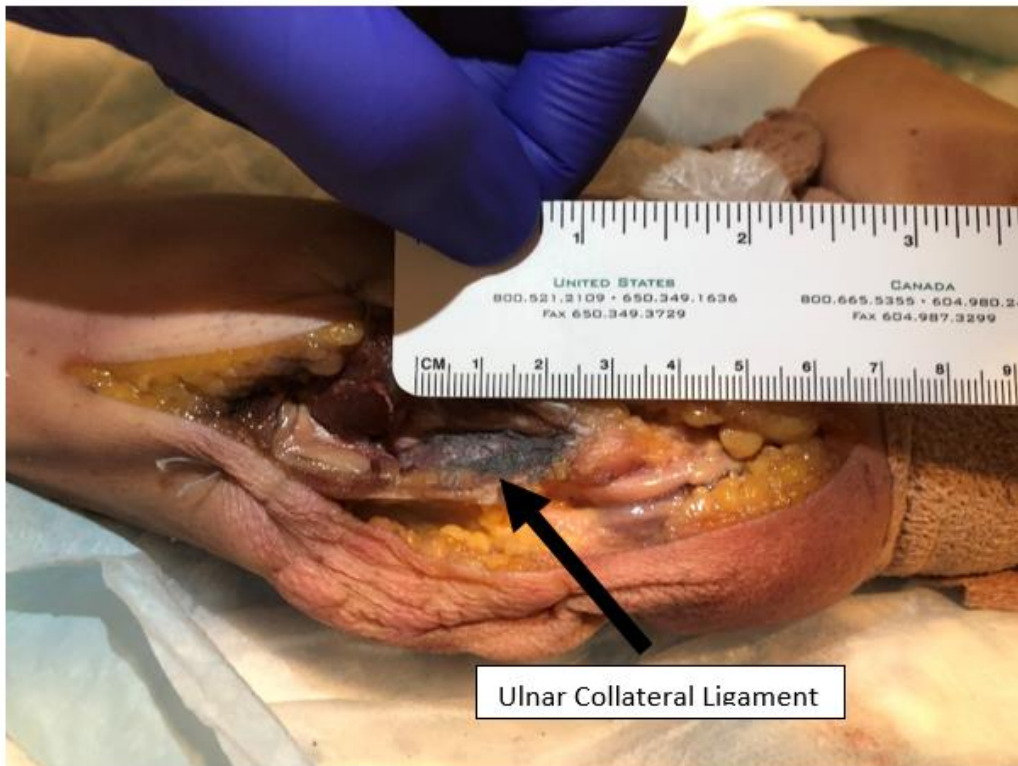
*Zimmer® Collagen Repair Patch Surgical Technique*. (2012). Zimmerbiomet.Com.

<https://www.zimmerbiomet.com/content/dam/zimmer-biomet/medical-professionals/000-surgical-techniques/shoulder/zimmer-collagen-repair-patch-surgical-technique.pdf>

## Appendices

### Appendix A: Images of the Anterior Bundle of the UCL Coated in Silver Particles

Images of the Anterior Bundle of the UCL taken during a cadaver dissection with Dr. Magit. Note that the ligament appears black because of prior testing.



## Appendix B: Pairwise Comparison Charts of the Primary Objectives from Each Individual

Pairwise comparison charts of the primary objectives were completed in order to rank the primary objectives. Note that Dr. Magit's chart was filled out incorrectly and the updated chart has yet to be received.

Dr. Magit	Healing Promotion	Mechanically Sound	Delivers Therapeutic Agent	Surgically Compatible	Reproducible	Cost Effective	Total
Healing Promotion	-	1	0.5	0.5	0.5	0	2.5
Mechanically Sound	0	-	0.5	0.5	0.5	0	1.5
Delivers Therapeutic Agent	0.5	0.5	-	0.5	0.5	1	2.0
Surgically Compatible	0.5	0.5	0.5	-	0.5	1	3.0
Reproducible	0.5	0.5	0.5	0.5	-	1	3.0
Cost Effective	1	1	0	0	0	-	2.0

Professor Pins	Healing Promotion	Mechanically Sound	Delivers Therapeutic Agent	Surgically Compatible	Reproducible	Cost Effective	Total
Healing Promotion	-	0	1	1	0	1	3.0
Mechanically Sound	1	-	1	1	0.5	1	3.5
Delivers Therapeutic Agent	0	0	-	1	0	1	2.0
Surgically Compatible	0	0	0	-	0	1	1.0
Reproducible	1	0.5	1	1	-	1	4.5
Cost Effective	0	0	0	0	0	-	0

Professor Troy	Healing Promotion	Mechanically Sound	Delivers Therapeutic Agent	Surgically Compatible	Reproducible	Cost Effective	Total
Healing Promotion	-	1	0.5	0.5	1	1	4.0
Mechanically Sound	0	-	0	0	0	1	1.0
Delivers Therapeutic Agent	0.5	1	-	1	1	1	4.5
Surgically Compatible	0.5	1	0	-	1	1	3.5
Reproducible	0	1	0	0	-	1	2.0

Cost Effective	0	0	0	0	0	-	0
----------------	---	---	---	---	---	---	---

Maria Decelles	Healing Promotion	Mechanically Sound	Delivers a Therapeutic Agent	Surgically Compatible	Reproducible	Cost Effective	Total
Healing promotion	-	0.5	0.5	1	1	1	4.5
Mechanically Sound	0.5	-	0.5	1	1	1	4.0
Delivers a Therapeutic Agent	0.5	0.5	-	1	1	1	3.5
Surgically Compatible	0	0	0	-	0.5	1	1.5
Reproducible	0	0	0	0.5	-	0.5	1.0
Cost Effective	0	0	0	0	0.5	-	0.5

Evan Hallberg	Healing Promotion	Mechanically Sound	Delivers a Therapeutic Agent	Surgically Compatible	Reproducible	Cost Effective	Total
Healing promotion	-	0.5	0.5	1	1	1	4.0
Mechanically Sound	0.5	-	0.5	1	1	1	3.5
Delivers a Therapeutic Agent	0.5	0.5	-	1	1	1	3.5
Surgically Compatible	0	0	0	-	1	1	2.0
Reproducible	0	0	0	0	-	0.5	0.5
Cost Effective	0	0	0	0	0.5	-	0.5

Brooklyn Paris	Healing promotion	Mechanically Sound	Delivers a Therapeutic Agent	Surgically Compatible	Reproducible	Cost Effective	Total
Healing promotion	-	1	0.5	1	1	1	4.5
Mechanically Sound	0	-	0.5	1	1	1	4
Delivers a Therapeutic Agent	0.5	0.5	-	1	1	1	4
Surgically Compatible	0	0	0	-	1	1	3
Reproducible	0	0	0	0	-	0.5	0.5
Cost Effective	0	0	0	0	0.5	-	0.5

Meagan Smith	Healing promotion	Mechanically Sound	Delivers a Therapeutic Agent	Surgically Compatible	Reproducible	Cost Effective	Total
Healing promotion	-	0.5	1	1	1	1	4.5
Mechanically Sound	0.5	-	1	1	1	1	4.5
Delivers a Therapeutic Agent	0	0	-	1	0.5	1	2.5
Surgically Compatible	0	0	0	-	0	0.5	0.5
Reproducible	0	0	0.5	1	-	1	2.5
Cost Effective	0	0	0	0.5	0	-	0.5

## Appendix C: Pairwise Comparison Charts of the Secondary Objectives from Each Individual

Pairwise comparison charts of the secondary objectives were completed in order to rank the primary objectives.

Professor Pins		Healing Promotion			Mechanically Sound			Delivers a Therapeutic Agent			Reproducible			Total
		Biodegradable	Restores Biomechanical Properties of Ligament	Design Stimulates Healing	Manipulated Safely by Surgeons	Can Withstand Fixation to the Ligament	Scaffold Maintains Structural Integrity throughout the Healing Process	Controlled Release Rate	Therapeutic Agent can be Integrated into Scaffold	Therapeutic Agent Elutes from implantation through repair phase	Precise	Accurate	Manufacturable in High Quantities	
Healing promotion	Biodegradable	-	0	0	0	0	0	0	0	0	0	0	0	0
	Restores Biomechanical Properties of Ligament	1	-	0.5	0.5	1	1	1	1	1	0.5	0.5	1	9
	Design Stimulates Ligament Healing	1	0.5	-	0.5	1	1	1	1	1	0.5	0.5	1	9
Mechanically Sound	Manipulated Safely by Surgeons	1	0.5	0.5	-	1	1	1	1	1	0.5	0.5	1	8.5
	Can Withstand Fixation to the Ligament	1	0	0	0	-	1	0.5	1	1	0	0	1	5.5
	Scaffold Maintains Structural Integrity throughout the Healing Process	0	0	0	0	0	-	0	0	0	0	0	1	1
Deliver	Controlled Release Rate	1	0	0	0	0.5	1	-	1	1	0.5	0.5	1	6.5

	Therapeutic Agent can be Integrated into Scaffold	1	0	0	0	0	1	0	-	0	0	0	1	3
	Therapeutic Agent Elutes from implantation through repair phase	1	0	0	0	0	1	0	1	-	0	0	1	4
Reproducible	Precise	1	0.5	0.5	0.5	1	1	0.5	1	1	-	0	1	8
	Accurate	1	0.5	0.5	0.5	1	1	0.5	1	1	1	-	1	9
	Manufacturable in High Quantities	0	0	0	0	0	0	0	0	0	0	0	-	0

Professor Troy		Healing Promotion			Mechanically Sound			Delivers a Therapeutic Agent			Reproducible			Total
		Biodegradable	Restores Biomechanical Properties of Ligament	Design Stimulates Healing	Manipulated Safely by Surgeons	Can Withstand Fixation to the Ligament	Scaffold Maintains Structural Integrity throughout the Healing Process	Controlled Release Rate	Therapeutic Agent can be Integrated into Scaffold	Therapeutic Agent Elutes from implantation through repair phase	Precise	Accurate	Manufacturable in High Quantities	
Healing promotion	Biodegradable	-	0	0	1	1	1	0	0	0	0	0	0	3
	Restores Biomechanical Properties of Ligament	1	-	1	1	1	1	1	1	1	1	1	1	11
	Design Stimulates Ligament Healing	1	0	-	1	1	1	1	1	1	1	1	1	10
Mech	Manipulated Safely by Surgeons	0	0	0	-	1	1	0	0	0	0	0	0	2

	Can Withstand Fixation to the Ligament	0	0	0	0	-	1	1	1	1	1	1	1	7
	Scaffold Maintains Structural Integrity throughout the Healing Process	0	0	0	0	0	-	0	0	0	0	0	0	0
Delivers Therapeutic Agent	Controlled Release Rate	1	0	0	1	0	1	-	0	1	1	1	1	7
	Therapeutic Agent can be Integrated into Scaffold	1	0	0	1	0	1	1	-	1	1	1	1	8
	Therapeutic Agent Elutes from implantation through repair phase	1	0	0	1	0	1	0	0	-	0	0	1	4
Reproduc	Precise	1	0	0	1	0	1	0	0	1	-	0	1	5
	Accurate	1	0	0	1	0	1	0	0	1	1	-	1	6
	Manufacturable in High Quantities	1	0	0	1	0	1	0	0	0	0	0	-	3

		Healing Promotion			Mechanically Sound			Delivers a Therapeutic Agent			Reproducible			Total
Maria Decelles		Biodegradable	Restores Biomechanical Properties of Ligament	Design Stimulates Healing	Manipulated Safely by Surgeons	Can Withstand Fixation to the Ligament	Scaffold Maintains Structural Integrity throughout the Healing Process	Controlled Release Rate	Therapeutic Agent can be Integrated into Scaffold	Therapeutic Agent Elutes from implantation through repair phase	Precise	Accurate	Manufacturable in High Quantities	
Healin	Biodegradable	-	0.5	0.5	0.5	1	0.5	0.5	1	0.5	0	0	1	6

	Restores Biomechanical Properties of Ligament	0.5	-	0.5	1	1	1	0.5	1	0.5	0.5	0.5	1	8
	Design Stimulates Ligament Healing	0.5	0.5	-	0.5	0.5	1	0.5	1	1	0.5	0.5	1	7.5
Mechanically Sound	Manipulated Safely by Surgeons	0.5	0	0.5	-	0.5	0.5	0	0.5	0	0.5	0.5	1	4.5
	Can Withstand Fixation to the Ligament	0	0	0.5	0.5	-	1	0	0.5	0	0.5	0.5	1	4.5
	Scaffold Maintains Structural Integrity throughout the Healing Process	0.5	0	0	0.5	0	-	0	0.5	0.5	0	0	0.5	2.5
Delivers Therapeutic Agent	Controlled Release Rate	0.5	0.5	0.5	1	1	1	-	0.5	0.5	0.5	0.5	1	7.5
	Therapeutic Agent can be Integrated into Scaffold	0	0	0	0.5	0.5	0.5	0.5	-	1	0	0	1	3
	Therapeutic Agent Elutes from implantation through repair phase	0.5	0.5	0	1	1	0.5	0.5	0	-	1	0.5	1	6.5
Reproducible	Precise	1	0.5	0.5	0.5	0.5	1	0.5	1	0	-	0	1	6.5
	Accurate	1	0.5	0.5	0.5	0.5	1	0.5	1	0.5	1	-	1	8
	Manufacturable in High Quantities	0	0	0	0	0	0.5	0	0	0	0	0	-	0.5

Evan Hallberg	Healing Promotion	Mechanically Sound	Delivers a Therapeutic Agent	Reproducible	Total
---------------	-------------------	--------------------	------------------------------	--------------	-------

		Biodegradable	Restores Biomechanical Properties of Ligament	Design Stimulates Healing	Manipulated Safely by Surgeons	Can Withstand Fixation to the Ligament	Scaffold Maintains Structural Integrity throughout the Healing Process	Controlled Release Rate	Therapeutic Agent can be Integrated into Scaffold	Therapeutic Agent Elutes from implantation through repair phase	Precise	Accurate	Manufacturable in High Quantities	
Healing promotion	Biodegradable	-	0.5	0	1	0	0.5	0	0	0	0.5	0.5	0	3
	Restores Biomechanical Properties of Ligament	0.5	-	0	1	1	1	1	1	0.5	1	1	1	9
	Design Stimulates Ligament Healing	1	1	-	1	1	1	1	1	0.5	1	0	1	9.5
Mechanically Sound	Manipulated Safely by Surgeons	0	0	0	-	1	0	1	1	1	1	1	0.5	6.5
	Can Withstand Fixation to the Ligament	1	0	0	0	-	0	0	1	0	1	0.5	0.5	4
	Scaffold Maintains Structural Integrity throughout the Healing Process	0.5	0	0	1	1	-	1	1	0.5	0	1	0	6
Delivers	Controlled Release Rate	1	0	0	0	1	0	-	1	1	0.5	0.5	0	5
	Therapeutic Agent can be Integrated into Scaffold	1	0	0	0	0	0	0	-	0	1	0	0.5	2.5

	Therapeutic Agent Elutes from implantation through repair phase	1	0.5	0.5	0	1	0.5	0	1	-	1	0	1	6.5
Reproducible	Precise	0.5	0	0	0	0	1	0.5	0	0	-	0	0	2
	Accurate	0.5	0	1	0	0.5	0	0.5	1	1	1	-	0.5	6
	Manufacturable in High Quantities	1	0	0	0.5	0.5	1	1	0.5	0	1	0.5	-	6

Brooklyn Paris		Healing Promotion			Mechanically Sound			Delivers a Therapeutic Agent			Reproducible			Total
		Biodegradable	Restores Biomechanical Properties of Ligament	Design Stimulates Healing	Manipulated Safely by Surgeons	Can Withstand Fixation to the Ligament	Scaffold Maintains Structural Integrity throughout the Healing Process	Controlled Release Rate	Therapeutic Agent can be Integrated into Scaffold	Therapeutic Agent Elutes from implantation through repair phase	Precise	Accurate	Manufacturable in High Quantities	
Healing promotion	Biodegradable	-	0	0	0.5	0.5	1	0.5	1	0.5	1	1	0.5	6.5
	Restores Biomechanical Properties of Ligament	1	-	0.5	1	0.5	0.5	1	1	1	0.5	0.5	1	8.5
	Design Stimulates Ligament Healing	1	0.5	-	1	0.5	0.5	1	1	1	0.5	0.5	1	8.5
Mech	Manipulated Safely by Surgeons	0.5	0	0	-	0.5	0.5	1	1	1	0.5	0.5	1	6.5

	Can Withstand Fixation to the Ligament	0.5	0.5	0.5	0.5	-	0.5	1	1	1	0.5	0.5	1	7.5
	Scaffold Maintains Structural Integrity throughout the Healing Process	0	0.5	0.5	0.5	0.5	-	1	1	0	1	1	0.5	6.5
Delivers Therapeutic Agent	Controlled Release Rate	0.5	0	0	0	0	0	-	0	0	0	0	0.5	1
	Therapeutic Agent can be Integrated into Scaffold	0	0	0	0	0	0	1	-	1	0	0	0.5	2.5
	Therapeutic Agent Elutes from implantation through repair phase	0.5	0	0	0	0	1	1	0	-	0	0	1	3.5
Reproducible	Precise	0	0.5	0.5	0.5	0.5	0	1	1	1	-	0.5	0.5	6
	Accurate	0	0.5	0.5	0.5	0.5	0	1	1	1	0.5	-	1	6.5
	Manufacturable in High Quantities	0.5	0	0	0	0	0.5	0.5	0.5	0	0.5	0	-	2.5

Meagan Smith	Healing Promotion	Mechanically Sound	Delivers a Therapeutic Agent	Reproducible	Total
--------------	-------------------	--------------------	------------------------------	--------------	-------

			Biodegradable	Restores Biomechanical Properties of Ligament	Design Stimulates Healing	Manipulated Safely by Surgeons	Can Withstand Fixation to the Ligament	Scaffold Maintains Structural Integrity throughout the Healing Process	Controlled Release Rate	Therapeutic Agent can be Integrated into Scaffold	Therapeutic Agent Elutes from implantation through repair phase	Precise	Accurate	Manufacturable in High Quantities	
Healing promotion	Biodegradable	-	0	0	0.5	0	0.5	0	0	0	0	0	0	0	1
	Restores Biomechanical Properties of Ligament	1	-	0.5	0.5	0.5	1	1	0.5	1	0.5	0.5	0.5	1	8
	Design Stimulates Ligament Healing	1	0.5	-	1	0.5	1	1	0.5	1	0.5	0.5	0.5	1	8.5
Mechanically Sound	Manipulated Safely by Surgeons	0.5	0.5	0	-	0	0.5	0.5	0.5	0.5	0	0	0.5	0.5	3.5
	Can Withstand Fixation to the Ligament	1	0.5	0.5	1	-	0.5	1	0.5	1	0.5	0.5	0.5	1	8

	Scaffold Maintains Structural Integrity throughout the Healing Process	0.5	0	0	0.5	0.5	-	1	0.5	0.5	0.5	0.5	1	5.5
Delivers Therapeutic Agent	Controlled Release Rate	1	0	0	0.5	0	0	-	0	0	0	0	0.5	2
	Therapeutic Agent can be Integrated into Scaffold	1	0.5	0.5	0.5	0.5	0.5	1	-	1	0.5	0.5	1	6.5
	Therapeutic agent elutes throughout the repair phase of healing	1	0	0	0.5	0	0.5	1	0	-	0	0	1	4
Reproducible	Precise	1	0.5	0.5	1	0.5	0.5	1	0.5	1	-	0.5	1	7
	Accurate	1	0.5	0.5	1	0.5	0.5	1	0.5	1	0.5	-	1	8
	Manufacturable in High Quantities	1	0	0	0.5	0	0	0.5	0	0	0	0	-	2

# Appendix D: Design Team Gantt Chart

Gantt Charts for A, B, C and D-Term.

TASK TITLE	OWNER	A TERM																								
		8/30 - 9/3		9/6 - 9/10		9/13 - 9/17		9/20 - 9/24		9/27 - 10/1		10/4 - 10/8		10/11 - 10/15												
		M	T	W	R	F	M	T	W	R	F	M	T	W	R	F	M	T	W	R	F	M	T	W	R	F
<b>A Term</b>																										
Write Introduction (chp 1)	All																									
Peer Review Introduction Chapter	All																									
Write Literature Review Draft (chp 2)	All																									
Peer Review Literature Review Chapter	All																									
Define Project Strategy (chp 3)	All																									
Peer Review Project Strategy Chapter	All																									

TASK TITLE	OWNER	B Term																								
		10/25 - 10/29		11/1 - 11/5		11/8 - 11/12		11/15 - 11/19		11/22 - 11/26		11/29 - 12/3		12/6 - 12/10		12/13 - 12/16										
		M	T	W	R	F	M	T	W	R	F	M	T	W	R	F	M	T	W	R	F	M	T	W	R	F
<b>B term</b>																										
Finalize Objectives	All																									
Design Background	All																									
Identify wants and needs	All																									
Identify Functions and Specifications	All																									
Alternative Design Development	All																									
Prep for group brainstorming session	All																									
Group brain storming session	All																									
Develop Conceptual Designs	All																									
Filter out Designs	All																									
Detail Alternative Designs in Solidworks/other Modeling	All																									
Alternative Design Testing	All																									
Develop Testing Protocols	All																									
Design mechanical test system to evaluate Device (Instron)	All																									
Conduct Feasibility Studies/ Experiments to Collect and Analyze Preliminary Data	All																									
Create Final Design Procedure	All																									
Develop analytical techniques to characterize system	All																									
Finalize B Term Report	All																									

TASK TITLE	OWNER	C Term																								
		1/10 - 1/14		1/17 - 1/21		1/24 - 1/28		1/31 - 2/4		2/7 - 2/11		2/14 - 2/18		2/21 - 2/25		2/28 - 3/4										
		M	T	W	R	F	M	T	W	R	F	M	T	W	R	F	M	T	W	R	F	M	T	W	R	F
<b>C term</b>																										
Meet with Prof. Coburn	All																									
Meet with Biosurfaces	All																									
Learn how to make silks	All																									
Practice for Mechanical Testing of Zien and Analysis	Brooklynn & Maria																									
Create Silk BSA loaded Silk Hydrogels and BSA loaded Sponge Reinforced Hydrogels	All																									
Drug Elution Testing of Alternative BSA Designs	Meagan & Evan																									
Analyze Drug Elution Data	All																									
Mechanical Testing of Zien Samples and Analysis	Maria, Evan, Meagan																									
Final Report	All																									
Determine Final Design Construct and Materials	All																									
Order any materials needed for final design	All																									
Request Silk solution from Kate	All																									
Measure Volumes Gels Absorb	Evan & Maria																									
Calculate final numbers needed for all testing	Brooklynn & Meagan																									
Make molds for Final Design Size	Brooklynn & Meagan																									
C term Presentation	All																									
Finish C term Report	All																									



## **Appendix E: Pugh Analysis Weighting Criteria**

For the Pugh analyses, design considerations (top row) were ranked against the design criteria (first column). A weight was determined for each design criteria, either 1, 2, 3, 4, or 5. Where 5 signified the design must meet the criteria and a 1 meant it would be nice if the design did meet that criterion. Then each design criterion was ranked either -1, 0, or 1 against the design being considered. If a design consideration was ranked 0 it means the design met the criteria, if it ranked 1 it went above and beyond the baseline, and finally if it ranked -1 it did not meet the baseline. These ranks were then multiplied by the weight of the criterion, which led us to the total score for each design. The high the score, the better the design.

## Appendix F: Materials with Growth Factors Research

Table with materials of interest, what growth factors they have been used with in literature, and how long the drug release period was.

<b>Material</b>	<b>Structure</b>	<b>Which GF?</b>	<b>How long did it release (days)?</b>	<b>Source</b>
Collagen Sponge	Membrane	PDGF, GDF-5	3	(Yamano et al., 2014)
	sponge with NP	VEGF	28	(Kim et al., 2016)
	Sponge/Matrix	BMP-2/BMP-9	10	(Fujioka-Kobayashi et al., 2017)
Silk Hydrogel	Silk Hydrogel	VEGF, PDGF-AB and TGF- $\beta$ 1	21	(Pallotta et al., 2014)
	Silk Hydrogel	PDGF-BB	42	(F. Wang et al., 2020)
	Silk Hydrogel	PDGF-BB and KGN	7	(Min et al., 2022)
Zein Electrospun Mats	--	--	--	--
Chitosan Sponges		PDGF-BB	6	(Jeong Park et al., 2000)
	brushite-chitosan scaffold	PDGF/VEGF	14-36	(De la Riva et al., 2010)
	Chitosan/tricalcium phosphate	PDGF-BB	14	(Lee et al., 2000)
Keratin Films	--	--	--	--

**Appendix G: Table of Strength and Modulus Values of Materials Researched**

<b>Materi</b>	<b>Polymer</b>	<b>Structure</b>	<b>Modulus (MPa)</b>	<b>Fracture Strength (MPa)</b>	<b>Source</b>
Collagen	Collagen Thread	Uncrosslinked	4.0 +/- 1.2	1.5 +/- 0.2	(Cornwell et al., 2007)
	Collagen Thread	Carbodimiide	68 +/- 31	11 +/- 4	(Cornwell et al., 2007)
	Collagen	Freeze-drying (98.8% porous)	0.24		(Reddy et al., 2021)
	Collagan Fiber	Rat tail tendon (wet)	498.8 +/- 44.0 (high)	53.5 +/- 11.1	(Pins & Silver, 1995)
	Collagan Fiber	Insoluable Collagen I (wet)	204 +/- 51.7 (high)	26.6 +/- 3.83	(Pins & Silver, 1995)
	Collagan Fiber	Soluble collagen (wet)	378 +/- 141.5 (high)	37.2 +/- 15.2	(Pins & Silver, 1995)
Silk	Silk Fibroin	Solvent casting	310 +/- 90	22.8 +/- 13.7	(Reddy et al., 2021)
	Silk Fibroin	Freeze-drying	70 +/- 0.00101	14 +/- 0.002	(Reddy et al., 2021)
	B. mori Silk	Single brins	16000	650 +/- 40	(Pérez-Guzmán & Castro-Muñoz, 2020)
Zein	Zein	Electrospun nanofiborous matrix	35.31 +/- 5.53	0.79 +/- 0.12	(Pérez-Guzmán & Castro-Muñoz, 2020)
	Zein 3D Scaffold	Lyophilization	751.63 +/- 58.85	3.91 +/- 0.86	(H.-J. Wang et al., 2007)
Chitosan	Chitosan	Lyophilization	6.8 +/- 0.5	4.7 +/- 0.4	(Reddy et al., 2021)
Keratin	S-sulfo Keratin Films	Compression Molded - 70 deg	697 +/- 80	11.5 +/- 2.3	(Kato et al., 2004)
	S-sulfo Keratin Films	Compression Molded - 80 deg	879 +/- 88	7.9 +/- 2.7	(Kato et al., 2004)
	S-sulfo Keratin Films	Compression Molded - 140 deg	946 +/- 27	21.8 +/- 2.7	(Kato et al., 2004)
	S-sulfo Keratin Films	Compression Molded - 160 deg	710 +/- 82	17.7 +/- 1.7	(Kato et al., 2004)
	70% keratin/30% PEO	nanofibers	7 +/- 2	1.6 +/- 0.3	(Aluigi et al., 2008)
Fib	Fibrin Fiber	Uncrosslinked	1.7 +/- 1.3	-	(Litvinov & Weisel, 2017)

	Fibrin Fiber	Crosslinked	14.5 +/- 3.5	-	(Litvinov & Weisel, 2017)
	Fibrin	Electrospun	11	3.5	(Yang et al., 2020)
	Fibrin	25 mg/mL	0.00974 +/- 0.00254		(Linsley et al., 2016)
PLLA	PLLA	Electrospun nanofibers - 3 aligned	55.0 +/- 2.8	7.62 +/- 0.2	(Silva et al., 2020)
	PLLA	Square braided	354.4 +/- 68.5	52.3 +/- 7.7	(Silva et al., 2020)
	PLLA	Aligned electrospun fiber	22.76 +/- 5.63		(Silva et al., 2020)
	PLLA	Electrospun random nanofibers	0.63 +/- 0.56		(Silva et al., 2020)

## Appendix H: MATLAB Code for Mathematically Modeling Diffusion Across a Semi-Permeable

```

%% Diffusion Across a Permeable Membrane Mathematical Modeling
% BSA
clc;clear
%  $C1(i,:) = -N/V * (\exp((-D(1)/h) * (t(i)/\tau)) - 1)$ ;
%  $\tau = ((V1 + A * h/2) * (V2 + A * h/2)) / A * V$ 
% N = total solute mass in system (6.8 mg)
% V = total volume
% h = thickness
% A = surface Area = .709cm2
% V1 = 3.4 mL
% V2 = 3.4 mL minus 100 microL each iteration
% N value for BSA:
% N Value for PDGF: 0.000297

N = 6.8; % mg
V = 6.8; % mL
h = 0.04; % cm
A = .709; % cm2
V1 = 3.4; % mL
V2 = 3.4; % mL
tau = ((V1 + (A * h) / 2) * (V2 + (A * h) / 2)) / (A * V);

D = [0:.001:.021]; % cm2/day
% to convert cm2/day to cm2/sec: D*86,400
t = [0:1:28]; % days

% Ideal range is D(7).006 and D(11).01

for i = 1:length(t)
    C3(i,:) = (-N/V * (exp((( -D(3))/h) * (t(i)/tau)) - 1)) * V/N;
    C5(i,:) = (-N/V * (exp((( -D(5))/h) * (t(i)/tau)) - 1)) * V/N;
    C7(i,:) = (-N/V * (exp((( -D(7))/h) * (t(i)/tau)) - 1)) * V/N; %% .006
    C9(i,:) = (-N/V * (exp((( -D(9))/h) * (t(i)/tau)) - 1)) * V/N;
    C11(i,:) = (-N/V * (exp((( -D(11))/h) * (t(i)/tau)) - 1)) * V/N; %% .01
    C15(i,:) = (-N/V * (exp((( -D(15))/h) * (t(i)/tau)) - 1)) * V/N;

    % These are the experimental values we got to compare to theoretical D
    % values
    Dexp = (7.84 * 10-3); % cm2/ day or 9.07 * 10-8 cm2/s
    Cexp(i,:) = (-N/V * (exp((-Dexp/h) * (t(i)/tau)) - 1)) * V/N;
end
figure
plot(t, C3, 'b', 'linewidth', 2) % D = .002
hold on

```

```

plot(t, C5,'b', 'linewidth', 2) %D = .004
hold on
plot(t, C7, 'k--', 'linewidth', 2) %D = .006
hold on
plot(t, C9, 'k--', 'linewidth', 2) %%D = .008
hold on
plot(t, C11 , 'r', 'linewidth', 2) %D = .01
hold on
plot(t, C15,'r', 'linewidth', 2) %D = .014
hold on
plot(t, Cexp,'m*', 'linewidth', 5)

xlim([0 28]);
ylim([0 1.2]);
set(gca, 'FontName', 'source sans pro');
set(gcf,'color','w');
leg = legend('Slow Diffusion Profile', 'Ideal Diffusion Profile', 'Fast Diffusion Profile', 'BSA
Diffusion Profile' );
%title(leg,'Diffusion Coefficient (cm^2/day)');
xlabel('Time (days)', 'fontsize',20);
ax = gca;
ax.FontSize = 15;
ylabel({'Mass Ratio (eluded protein (mg)); / total protein loaded(mg)'}), 'fontsize', 20);

%% Diffusion Across a Permeable Membrane Mathematical Modeling
% PDGF-BB
clc;clear
%  $C1(i,:) = -N/V * (\exp((-D(1)/h) * (t(i)/\tau)) - 1);$ 
%  $\tau = ((V1 + A * h / 2) * (V2 + A * h / 2)) / (A * V)$ 

% N = total solute mass in system (6.8 mg)
% V = total volume
% h = thickness
% A = surface Area = .709cm^2
% V1 = 3.4 mL
% V2 = 3.4 mL minus 100 microL each iteration
% N value for BSA:
% N Value for PDGF: 0.000297

N = 6.8; % mg
V = 6.8; % mL
h = 0.04; % cm
A = .709; % cm^2
V1 = 3.4; % mL
V2 = 3.4; % mL
tau = ((V1 + (A * h) / 2) * (V2 + (A * h) / 2)) / (A * V);

```

```

D = [0:.001:.021]; % cm^2/day
% to convert cm^2/day to cm^2/sec: D*86,400
t = [0:1:28]; % days

% Ideal range is D(7).006 and D(11).01

for i = 1:length(t)
    C3(i,:) = (-N/V*(exp((-D(3)/h)*(t(i)/tau))-1))*V/N;
    C5(i,:) = (-N/V*(exp((-D(5)/h)*(t(i)/tau))-1))*V/N;
    C7(i,:) = (-N/V*(exp((-D(7)/h)*(t(i)/tau))-1))*V/N;%%.006
    C9(i,:) = (-N/V*(exp((-D(9)/h)*(t(i)/tau))-1))*V/N;
    C11(i,:) = (-N/V*(exp((-D(11)/h)*(t(i)/tau))-1))*V/N;%%.01
    C15(i,:) = (-N/V*(exp((-D(15)/h)*(t(i)/tau))-1))*V/N;

    % These are the experimental values we got to compare to theoretical D
    % values
    Dexp = (7.9*10^-3); % cm^2/ day or 9.07*10^-8 cm^2/s
    Cexp(i,:) = (-N/V*(exp((-Dexp/h)*(t(i)/tau))-1))*V/N;

end

figure
plot(t, C3,'b', 'linewidth', 2) %D = .002
hold on
plot(t, C5,'b', 'linewidth', 2) %D = .004
hold on
plot(t, C7, 'k--', 'linewidth', 2) %D = .006
hold on
plot(t, C9, 'k--', 'linewidth', 2) %%D = .008
hold on
plot(t, C11, 'r', 'linewidth', 2) %D = .01
hold on
plot(t, C15,'r', 'linewidth', 2) %D = .014
hold on
plot(t, Cexp,'m*', 'linewidth', 5)

xlim([0 28]);
ylim([0 1.2]);
set(gca, 'FontName', 'source sans pro');
set(gcf,'color','w');
leg = legend('Slow Diffusion Profile', 'Ideal Diffusion Profile', 'Fast Diffusion Profile', 'PDGF-
BB Diffusion Profile' );
%title(leg,'Diffusion Coefficient (cm^2/day)');
xlabel('Time (days)', 'fontsize',20);
ax = gca;

```

```
ax.FontSize = 15;  
ylabel({'Mass Ratio (eluded protein (mg)); / total protein loaded(mg)'}), 'fontsize', 20);
```

## Appendix I: Bill of Materials

Materials	Company	Catalog #	Cost
PDGF-BB	ProSpec	CYT-501	\$130 per 10 micrograms
PDGF ELISA KIT	ThermoFisher Scientific	BMS 2071	\$637
Collagen	Professor Pins Lab	N/A	No cost
Silk	Professor Coburn Lab	N/A	No cost
Bovine Serum Albumin (BSA)			N/A
PDMS Base	Corning Silgard 182		N/A
PDMS Curing Agent			N/A
DPBS (-) and (+)	Corning	20721009	N/A
Chicken Skin	N/A	N/A	\$15
Dihydroxyl-L-Phenylalanine			\$63 per 5 grams
12-well, 24-well plates	Celltreat Scientific Products	229112, 229124	N/A
Pipette tips (1-10 $\mu$ L, 20-200 $\mu$ L, 100-1000 $\mu$ L)	VWR Universal	76322-134, 76322-150, 76322-154	N/A
Micropipettes (0.5-10 $\mu$ L, 20-200 $\mu$ L, 100-1000 $\mu$ L)	Accumax	VAP-100, VAP-800, VAP-600	N/A
Orbital Shaker Plate			N/A
Zeiss Inverted Microscope			N/A
Moo Gloo TI Transglutaminase	Modernist Pantry	1203-50	N/A
Microplate Reader	Thermo Scientific Mulitskan FC	N07710	N/A
Fluorescent microscope			N/A
Microcentrifuge	Spinplus	?	
WPI Lab Fees	N/A	N/A	\$200

## Appendix J: Silk Hydrogel Fabrication Protocol

**Purpose:** Outline the steps to fabricate a BSA or PDGF-BB loaded silk hydrogel

Note: It is recommended to practice with your solution the day or two before making gels to find the ideal sonification times.

1. Dilute or concentrate silk solution to desired exact % concentration (aqueous solution)
2. Fill a bin with ice
3. Put on gloves
4. Gather and label 2 mL micropipette tubes in a holder and place in the ice
5. Pipet 1.5 mL silk solution into micropipette (it is recommended to use no less than 1.5 mL)
6. At the sonicator, put the micropipette into the holder and put the probe into the micropipette as much as you can without overflowing the solution
7. Sonication settings
  - a. Duty cycle: constant
  - b. Timer: N/A
  - c. Output control: 1
8. Turn on sonification by turning the timer and record how long it was sonicated for
9. Remove micropipette tube and wipe down prob
10. Use a positive displacement pipet to make a 300-microliter gel (prime the pipet to get rid of bubbles) in another micropipette tube

### Adding Albumin or Growth Factor Solution to Silk Hydrogel

1. Make sure the albumin or growth factor solution is pre-aloquated
  - a. 20 microliter of 65 mg/mL BSA, or 15 microliter of 100 microgram/mL PDGF-BB
2. Add silk Pregel soliton to the loading solution and pipet up and down to mix

### Creating a Sponge Reinforced Hydrogel

1. Allocate half of the sonicated solution into the mold and add a cut and measured collagen sponge sample
2. Fill the rest of the mold well with the remaining solution
3. Degass with a vacuum pump for 20 minutes, releasing excess gas by twisting the valve every 4 minutes
11. Store at room temperature

### Additional Notes:

- Older silk sonicates faster
- Adding other non-gel solutions causes gelation to happen later
- If you want a reproducible product, under the same conditions, sonicate together
- It is recommended to avoid sonicating silk directly after solution production

## **Appendix K: Sterilization Protocols for Final Design**

Purpose: Sterilize necessary materials, tools, solutions and machinery that are involved in the process of constructing the final design to ensure quality cell proliferation results and to prove the design is sterilizable in accordance with our project goals.

### **Sterilization Protocol for PDGF-BB loaded Silk Solution:**

#### **Materials:**

- Desired volume of 5% non-sterile silk solution
- Sterile 10 mL centrifuge tube

#### **Protocol:**

1. Ensure that proper attire is being worn while sterilizing materials and working in the BSC. This includes wearing goggles, gloves, and garments/lab coats.
2. Ensure all materials entering the BSC are sterile by wiping them down with 70% ethanol. If an item is transferred into the BSC ensure that the autoclave bag is wiped down and opened in the BSC.
3. Sterilize desired volume of silk solution by filtering the non-sterile water through a 20-micrometer impurity filter attached to a 50 mL lore lock syringe and dispense into the sterile 10 mL centrifuge tubes

### **Sterilization Protocol for Collagen Sponges:**

#### **Materials:**

- Ten 7.5 mm by 20 mm UV cross linked collagen sponge samples in a \_\_ size petri dish
- Two 10 mL centrifuge tubes filled with water
- 70% Ethanol (ETOOH)
- Micrometer filters
- Two 10 mL Autoclaved centrifuge tubes
- Sterile Petri Dishes
- 10 mL centrifuge tubes

#### **Protocol:**

1. Ensure that proper attire is being worn while sterilizing materials and working in the BSC. This includes wearing goggles, gloves, and garments/lab coats.
2. Ensure all materials entering the BSC are sterile by wiping them down with 70% ethanol. If an item is transferred into the BSC ensure that the autoclave bag is wiped down and opened in the BSC.
3. Pour 70% ETOOH into a sterile petri dish and place all collagen sponge samples into the ETOOH solution and leave to soak for one hour
4. Take 2 10 mL centrifuge tubes of water and thoroughly wipe the

5. Sterilize 10 mL of water by filtering the non-sterile water through a 20-micrometer impurity filter attached to a 50 mL lore lock syringe and dispense into the sterile 10 mL centrifuge tubes
6. After the sponges are done soaking in ETOOH, aspirate the ETOOH ensuring not to disturb the collagen sponges
7. Rinse the collagen sponges with sterile water for 5 minutes. Repeat this 3 times to ensure that all residual ETOOH is removed from the collagen sponges.
8. Aspirate the residual water in the petri dish.
9. Carefully blot the perimeter of the collagen sponges with filter paper to remove any extra residual water.
10. Leave sponges uncovered for 25 minutes to evaporate even more residual water but ensuring that the samples are not dehydrated as that will transform the sponges into unusable films.

### **Sterilization Protocol for PDMS Molds**

#### **Materials:**

- PDMS molds
- UV sterilizer
- Timer

#### **Protocol:**

1. Place PDMS molds in sterile petri dishes.
2. Sterilize the PDMS Molds by placing them in a UV sterilizer set to top and bottom for 30 minutes.

### **Sterilization Protocol for Additional Machinery and Materials:**

#### **Materials:**

- Sonicator
- Vacuum Chamber
- Ring Stand
- Ring Stand Clip

#### **Protocol:**

1. It is essential that any machinery and tools must be properly sterilized prior to entering the BSC.
2. Ensure that proper attire is being worn while sterilizing materials and working in the BSC. This includes wearing goggles, gloves, and garments/lab coats.
3. Thoroughly wipe the sonicator, vacuum chamber ring stand and ring stand clip with 70% ETOOH and place in the BSC.

### **Sterilization Protocol for Acellular Dermal Matrix (ADM)**

The ADM were sterilized upon arrival and were shipped and stored in air sealed bags. No further sterilization protocol is required.

## **Appendix L: Cell Proliferation Testing and Bioactivity Testing**

### **Step 1: PDGF-BB Bioactivity Testing at Differing Concentrations**

The purpose of this test was to verify the bioactivity of the PDGF-BB at different concentrations on the proliferation of NIH 3T3 mouse fibroblastic cells in comparison to the positive control, 10% FBS cell culture media, and determine which is optimal for the final design.

#### **Materials and Equipment:**

- Culture Media
  - 88% DMEM
  - 1% Glutamax
  - 1% Pennstrep
  - 10% FBS
- PDGF-BB at a concentration of 1µg/10µl
- 12-well plate (4)
- Laboratory tape and marker to label
- 37°C, 95-100% humidity, 5% CO<sub>2</sub> incubator
- Micropipettes and micropipette tips
- Serological pipettes and pipette tips
- DPBS (-)
- Trypsin
- Hemocytometer
- Zeiss inverted microscope with Zen software

#### **Procedure:**

1. Formulate 10% FBS cell culture media using above concentrations.
2. Make a suspension of known cell concentration (1000 cells/uL) using NIH 3T3 mouse fibroblastic cells.
3. Add 1 mL of 10% FBS cell culture media into each well.
4. Dispense 30 uL of the suspension (30,000 cells) into each well of the four 12-well plates
5. Label two plates as day three and two plates as day five. On each set of plates, label triplicate wells with two concentrations of growth factor and a control, and mark X on the remaining wells. An example of a set of plates can be seen below.

20K cells/well	1	2	3	4	Day 3
<b>A</b>	0.167	0.167	0.167	X	BP 3T3 Date
<b>B</b>	0.417	0.417	0.417	X	
<b>C</b>	0	0	0	X	

20K cells/well	1	2	3	4	Day 3
<b>A</b>	0.667	0.667	0.667	X	BP 3T3 Date
<b>B</b>	1.00	1.00	1.00	X	
<b>C</b>	0	0	0	X	

- Add each concentration of growth factor (of 1 $\mu$ g/10 $\mu$ l stock). For three of the wells with cells, 0 ug of growth factor will be used to serve as a negative control.
- After 3, remove one plate from the incubator and image all wells.
- After imaging, aspirate the media in each of the wells.
- Add 1 mL of DPBS (-) to each well, swirl to mix, and then aspirate.
- Add 0.5 mL of trypsin to each well and place it in the incubator for 5-10 minutes.
- Take the plate out of the incubator, and check to ensure that the cells are rounded and detached through the microscope. Once this is confirmed, add 0.5 mL of culture media to each well. Pipette up and down to evenly suspend the cells and to remove them from the surface of the plate.
- After ensuring an even cell suspension, take a 7  $\mu$ L sample and load it into a hemocytometer.
- Count the cells in each corner of the hemocytometer and take the average. Multiply this number by 10,000 to determine the number of cells in 1mL.
- Repeat steps 8-13 on days 3 and 5.
- Based on the most significant increase in proliferation of the cells, determine the best concentration of PDGF-BB for the final scaffold design.

## **Step 2: Scaffold Bioactivity testing**

The purpose of this test was to determine the effects of the final concentration of PDGF-BB on the proliferation of CRL 2097 human fibroblastic cells in comparison to the positive control, 10% FBS cell culture media.

### **Proof of Concept:**

- To confirm the BrdU protocol, a practice assay was run. This was done before setting up the final cell proliferation experiment and uses the Cell Proliferation Assay protocol with BrdU below
- Formulate 10% FBS cell culture media using above concentrations.
- Make a suspension of known cell concentration (1,000 cells/ $\mu$ L) using CRL 2097 human fibroblastic cells.

4. Dispense 25  $\mu\text{L}$  of the suspension (20,000 cells) into each well of a 4-well plate. Add 500  $\mu\text{L}$  of 10% FBS cell culture media into each well. Label the plate with the type of cells, cells per well, initials, and date they were seeded.
5. After the cells have incubated for 16 hours, begin the BrdU assay protocol. Cells will be assessed about 22 hrs after seeding.

### **Procedure:**

1. Set up a drug elution study as described in Appendix N.
2. Formulate 10% FBS cell culture media using above concentrations.
3. Make a suspension of known cell concentration (1,000 cells/ $\mu\text{L}$ ) using CRL 2097 human fibroblastic cells.
4. Dispense 20  $\mu\text{L}$  of the suspension (20,000 cells) into each well of a 24-well plate. Add 1 mL of 10% FBS cell culture media into each well. Label the wells according to the diagram below.
5. Place the cells into the incubator.
6. After 1 day, remove the 12-well plate from incubation, check for health of the cells under the microscope, and image representative wells of cells on 10X.
7. Thaw drug elution samples from days 1, 2, 3, 4, 7 and 10. Remove 150  $\mu\text{L}$  of this supernatant and add it to each well of the plate. Label the plates according to the diagram below in two sets – one for three days after adding the supernatant and one for five days adding supernatant. Four different scaffolds will be analyzed for each day of drug elution testing.
8. After the cells have been incubating with the supernatant for three days, remove those two 24-well plates and complete the BrdU assay, which is described below.
9. Repeat this assay after the cells have been incubating with the supernatant for five days.

### **Cell Proliferation Assay using Bromo-deoxyuridine (BrdU)**

This assay measures the proliferation of cells through BrdU. An antibody attaches to BrdU, which takes the place of part of the DNA of the cell. A fluorescent secondary antibody attaches, and then the nucleus and cytoplasm can be seen through a fluorescent microscope. Images can be taken that show the cells with a nucleus that has proliferated in the presence of BrdU.

### **Materials:**

- Culture medium as described earlier in this protocol
- BrdU Labeling Reagent (ThermoFisher, Cat # 000103, 10mM in DMSO, stored at  $-4^{\circ}\text{C}$ )
- DPBS (+) (Dulbecco's phosphate buffered saline with  $\text{Ca}^{++}/\text{Mg}^{++}$ , MediaTech Cat # 21-030-CV, VWR, Cat # 4500-430)
- 1% BSA or 5% FBS prepared in DPBS (+)
- Alexaflour-488 conjugated anti-mouse IgG1 or IgG (ThermoFisher Cat # A-1101)
- Ice cold methanol (JT Bater, Cat 9070-13, VWR Cat # JT9070-13, 250 ml aliquot stored at  $-20^{\circ}\text{C}$ )
- 0.05% Tween-20 prepared in DPBS (+) (10% Tween-20 solution, VWR Cat # 95059248)
- Cells grown in 24-well plates

- 1.5 N HCl (diluted from 6.0 N in distilled H<sub>2</sub>O, EMD, Cat # HX0603M/6, VWR Cat # EM-HX0603M-6)
- DAPI 10 mg/mL solution in H<sub>2</sub>O (VWR Cat # 89139-118) or Hoechst 33342 stock solution prepared at 0.5 mg/mL in H<sub>2</sub>O (EMD Cat # 382065-100MG, VWR Cat # 80056-706)

**Procedure:**

1. Add 1.0  $\mu$ L of BrdU stock solution per mL of culture medium to cells being assayed and incubate for four hours. (0.7  $\mu$ L of BrdU in 700  $\mu$ L of medium)
2. Aspirate cell culture medium and briefly rinse cells 2X in DPBS (+)
3. Aspirate DPBS (+). Add ice cold (-20°C) methanol (500  $\mu$ L well for 24-well plate). Incubate for 10 min at room temp (RT)
4. Aspirate methanol and wash two times with 500  $\mu$ L DPBS (+). Plates can be stored at 4°C with PBS in wells if analysis is not to be done right away
5. Aspirate DPBS (+) and add 1.5 N HCl (add 500  $\mu$ L/well for 24-well plate) and incubate at RT for 20 min
6. Aspirate HCl and rinse three times with 500  $\mu$ L/well of DPBS (+)
7. If cells were cultured with serum, blocking is not necessary. If cultured in a serum free system, block at RT for at least 15 min with 1% FBS in BSA prepared in DPBS (+).
8. Dilute anti-BrdU antibody 1:50 in DPBS (+)/0.05% Tween-20
9. Add antibody solution at 150  $\mu$ L/well for 24-wellplate and incubate at RT for 30 min
10. Aspirate antibody solution and rinse 2-3X with DPBS (+)
11. Dilute fluorescence conjugated secondary antibody 1:500 in DPBS (+)/0.05% Tween-20. Add 200  $\mu$ L/well for 24-well plate. Incubate at RT for 30 min.
12. Rinse 3X with DPBS (+) (without Tween)
13. Add 0.2  $\mu$ g/mL DAPI prepared in DPBS (+) and incubate at RT for 10 min.
14. Aspirate stain solution, and rinse 2X with 500  $\mu$ L DPBS (+) and add DPBS (+) (1.0 mL/well for 24-well plate)
15. Cells are ready for observation by fluorescence microscopy. Plates can be stored at 4°C wrapped in foil to protect from light.
16. Take images using 10X on a fluorescence microscope with FITC, DAPI, and Brightfield settings. Add scale bar to images and image each well on each mode.

Total time: 2.5-3.5 hrs

## **Appendix M: Acellular Dermal Matrix (ADM) Tensile Testing Protocol**

**Purpose:** Measure the stiffness and failure load of ADM

### **Materials:**

- ADM hydrated in DPBS (-)
- Instron E1000

Scaffold Sample Needed: 5 to be tested in one direction and 5 to be tested in other direction (anisotropic samples)

1. Soak samples in a DPBS (-) bath for one hour
2. Acquire graph paper or engineering paper and add lines to your specified dimensions using calipers or a ruler
3. Tape sample down against graph or engineering paper
4. Use the lines that you made on the graph paper as reference and use a meat cleaver to cut the sample that is taped onto the graph paper to your desired width
  - a. Width: 0.15mm (150 microns)
5. Confirm that the load cell installed on the Instron is appropriate for the Force value acquired with the samples specified dimensions
6. Begin uniaxial Vertical Tensile Test.

### **Tensile Test:**

1. Receive training for the Instron E 1000 machine and book the instrument
2. Sign into Instron logbook with date and username
3. If not already on, turn on Instron and wait 15 minutes
4. Turn off the air
5. With the help of at least one other person, put the Instron in the horizontal position
6. Turn on air
7. In the pink tab select commission and select the commission in use (horizontal or vertical)
8. Unarm position and load limits
9. Put the Instron in channel I
10. Move the body to be within the black line
11. Load the 2000N load cell or other needed for testing
12. Calibrate the load/load wizard
13. Confirm on the Bluehill Software that the load cell value is read.
14. Lock calibration and save calibration (date.loadcell.initials)
15. Load fixtures

16. Open the Bluehill Universal Program Tensile Method (test control: 25%/minute as determined by previous understanding of viscoelastic tissue, end of test criteria: 40% force and 1900 N force)
17. Load the sample and record dimensions
18. Clamp in sample in between two pieces of PMS as to secure the ends of the sample
  - a. Ensure that the very ends of the sample are clamped as to ensure that the sample will yield towards the middle and not near the clamps
19. Put in channel II
20. Turn on position and load limits
21. With channel 1 on, move the actuator to apply a tare load if desired
22. Zero extension and force
23. Go to channel 2 and begin test
24. Un-enable load and position limits
25. Unload the sample
26. Put in channel 0
27. Close the Instron program. Do not power off the Instron

## **Appendix N: Drug Elution Testing**

**Purpose** To quantify the release profile of protein from the scaffold design.

### **Materials and Equipment**

- dPBS (-)
- 820 mg/mL BSA stock solution
  - 820 mg of Bovine serum albumin (BSA), solid
  - 1 mL dPBS(-)
- MicroBCA reagent
- 1.5 mL Microcentrifuge tubes
- 12-well culture plates
- Orbital shaker
- Microcentrifuge tube storage box
- Laboratory tape and marker to label boxes and tubes
- spectrophotometer
- 96 well plates
- 37°C incubator
- Micropipettes and micropipette tips

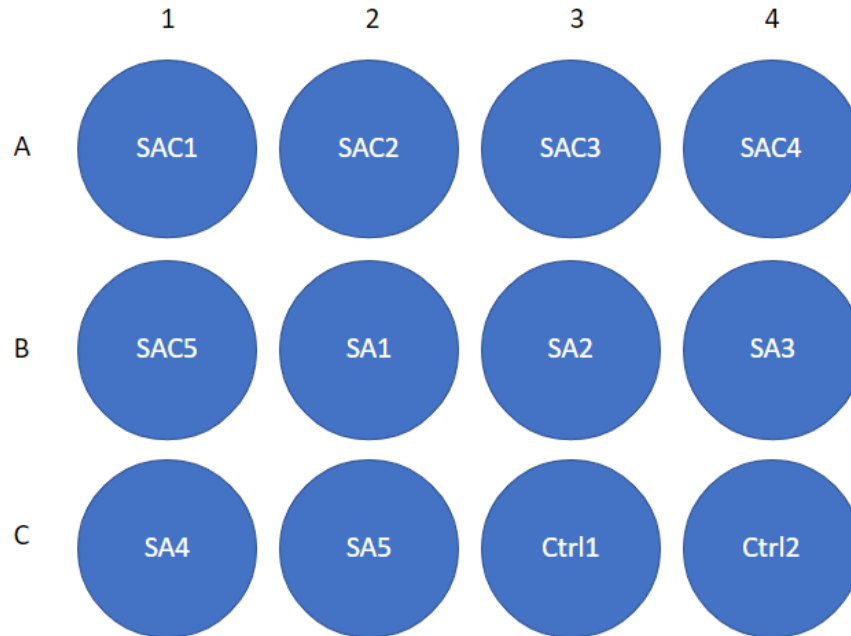
### **Step One: Protein Standard Curve Preparation**

- 1) Label a microcentrifuge with the date, your team number and the solution: “2 mg/mL BSA”.
- 2) Create the 2 mg/mL BSA solution by diluting the 20 mg/mL stock solution 1:10 in dPBS(-) in a 1.5 mL microcentrifuge tube (final volume = 1 mL).
- 3) Label 8 microcentrifuge tubes with the date, initials and each of the following BSA concentrations:
  - a. 0, 31.25, 62.5, 125, 250, 500, 1000, 2000  $\mu\text{g/mL}$
- 4) Generate samples at the concentrations listed above by serial dilution of the 2 **mg/mL BSA** working solution.
- 5) In the tube labeled 500  $\mu\text{g/mL}$  pipet 500  $\mu\text{l}$  of the 1mg/mL solution you just made and mix it with 500  $\mu\text{l}$  dPBS(-), to dilute the solution in half.
- 6) For each subsequent dilution, take 500  $\mu\text{l}$  of the previous solution and dilute it 1:1 with dPBS(-) for a final volume of 1 mL; For the 0  $\mu\text{g/mL}$  sample, use dPBS(-) without protein.

### **Step Two: Compiling a Release Profile**

6. Set up the 5 testing conditions
  - a. Add each of the 5 unloaded silk hydrogel into individual wells in the first 12 well plate.
  - b. Add each of the 5 BSA loaded silk hydrogel into individual wells in the first 12 well plate.

- c. Add each of the 5 collagen sponges into individual wells in the second 12 well plate.
- d. Add each of the 5 collagen sponge reinforced BSA loaded silk hydrogel into individual wells in the second 12 well plate. See example plate below



7. Add 1 mL of dPBS(-) to each well place them in a revolver inside an incubator at 37°C
8. Pull samples by removing all of the supernatant at time points 0 hours (1), 24 hours (2), 48 hours (3), 72 hours (4), 96 hours (5), 7 days (6), 10 days (7), and 14 days (8).
9. Place samples in labeled microcentrifuge tubes with the test condition, trial number and time point. Store samples in a box at -80°C.
10. Add 1 mL of fresh dPBS(-) back into the sample wells and place the well plate into the rotating incubator after each time sample is collected.
11. Repeat steps 4 and 5 for each time point for each sample.

### **Step Three: Measure Protein Concentrations in Standards and Supernatant Samples**

1. Make the BCA working reagent
  - a. Need 200  $\mu$ L for each sample
  - b. 8 parts of Reagent A
  - c. 1 part of Reagent B
2. Label a 96 well plate with known standard concentrations and unknown supernatant samples collected into separate wells in this plate.
3. Add 25  $\mu$ L of each of your BSA standard curve samples IN DUPLICATE to the 96 well plate.
4. Add 25  $\mu$ L of each supernatant samples to the same 96 well plate. See sample labeled plate below.

	<b>1</b>	<b>2</b>	<b>3</b>	<b>4</b>	<b>5</b>	<b>6</b>	<b>7</b>	<b>8</b>	<b>9</b>	<b>10</b>	<b>11</b>	<b>12</b>
<b>a</b>	C1 t=0	C2 t=0	C3 t=0	C4 t=0	C5 t=0	SAC1 t=0	SAC2 t=0	SAC3 t=0	SAC4 t=0	SAC5 t=0	Std1	Std1
<b>b</b>	C1 t=1	C2 t=1	C3 t=1	C4 t=1	C5 t=1	SAC1 t=1	SAC2 t=1	SAC3 t=1	SAC4 t=1	SAC5 t=1	Std2	Std2
<b>c</b>	C1 t=2	C2 t=2	C3 t=2	C4 t=2	C5 t=2	SAC1 t=2	SAC2 t=2	SAC3 t=2	SAC4 t=2	SAC5 t=2	Std3	Std3
<b>d</b>	C1 t=3	C2 t=3	C3 t=3	C4 t=3	C5 t=3	SAC1 t=3	SAC2 t=3	SAC3 t=3	SAC4 t=3	SAC5 t=3	Std4	Std4
<b>e</b>	C1 t=4	C2 t=4	C3 t=4	C4 t=4	C5 t=4	SAC1 t=4	SAC2 t=4	SAC3 t=4	SAC4 t=4	SAC5 t=4	Std5	Std5
<b>f</b>	C1 t=7	C2 t=7	C3 t=7	C4 t=7	C5 t=7	SAC1 t=7	SAC2 t=7	SAC3 t=7	SAC4 t=7	SAC5 t=7	Std6	Std6
<b>g</b>	C1 t=10	C2 t=10	C3 t=10	C4 t=10	C5 t=10	SAC1 t=10	SAC2 t=10	SAC3 t=10	SAC4 t=10	SAC5 t=10	Std7	Std7
<b>h</b>	C1 t=14	C2 t=14	C3 t=14	C4 t=14	C5 t=14	SAC1 t=14	SAC2 t=14	SAC3 t=14	SAC4 t=14	SAC5 t=14	Blank	Blank

5. Add 200  $\mu$ L of the BCA working reagent to each well/protein sample.
6. Gently swirl the plate to mix.
7. Cover the plate; label the time on the lid of the plate and place in the oven (37°C) for 30 minutes.
8. Read the absorbance on a spectrophotometer (plate reader) set at 570 nm.
9. Dispose of any leftover BCA reagent as hazardous waste.

## Appendix O: Diffusivity Across Casing Material Protocol

Purpose: Identify the diffusion coefficient of BSA or PDGF-BB through ADM casing to evaluate its ability to mitigate immediate drug elution from the scaffold design.

### Materials:

- Ussing Chamber with two 3.4mL reservoirs connected via press fitting with a decellularized film membrane bridging the two chambers.
- Acellular Dermal Matrix (ADM)
- 2mg/mL BSA concentration of fabricated scaffold
- Mixing plate
- Timer

### Protocol:

1. Cut a 1 cm by 1 cm square of ADM under the sterilization hood to ensure sterility and that there is minimal contamination to the sample
2. Measure the width of the ADM sample length and diameter of opening of the Ussing chamber bridging the two chambers
3. Place a film of ADM at the joint in the tubing between the two reservoirs and lightly tighten the knob, press fitting the two chambers and sample together
4. Prepare a growth factor solution of known concentration for one reservoir (2mg/mL)
5. Using a syringe dispense 3.4 mL of BSA solution into Chamber 1
6. Using a different syringe dispense 3.4 mL of DPBS (-) into Chamber 2
7. Record the time at which both chambers are filled with solutions.
8. Extract a 100 microliter sample by using a syringe to remove fluid from Chamber 2 every 24 hours for 7 days.
9. Perform a BCA or ELISA reading of collected sample to molar quantify concentration
10. Determine the diffusion coefficient of growth factor through ADM using Ficks Law of Diffusion below. Assume the system is isothermal and isobaric relative to molar average velocity. The boundary conditions are equal volumes in the reservoirs and mass transport is independent of convection.

$$D = -\ln\left(1 - \left(\frac{C_2(t)}{\left(\frac{N}{V}\right)}\right)\right) \cdot h \cdot \frac{t}{\tau}$$
$$\tau = \frac{\left(V_1 + \frac{Ah}{2}\right)\left(V_2 + \frac{Ah}{2}\right)}{AV}$$

Where N is the total solute mass in system (6.8mg), V is the total volume (6.8μL), D is the diffusion coefficient in cm<sup>2</sup>/s, C<sub>2</sub> is the protein concentration in the acceptor chamber at a given time in mg/mL, h is thickness of the barrier known to be 400 μm, t is time in hours, A is surface area of the barrier in mm<sup>2</sup>, and τ is the scaling factor.